Title
Signal Transduction Mechanisms in Caulobacter crescentus

Author
Zik, Justin Joseph

Publication Date
2019

Peer reviewed|Thesis/dissertation

Signal Transduction Mechanisms in *Caulobacter crescentus*

By

Justin Joseph Zik

A dissertation submitted in partial satisfaction of the

requirements for the degree of

Doctor of Philosophy

in

Microbiology

in the

Graduate Division

of the

University of California, Berkeley

Committee in charge:

Professor Kathleen R. Ryan, Chair
Professor Arash Komeili
Professor Michiko E. Taga
Professor Nicholas T. Ingolia

Spring 2019

Abstract

Signal Transduction Mechanisms in *Caulobacter crescentus*

by

Justin Joseph Zik

Doctor of Philosophy in Microbiology

University of California, Berkeley

Professor Kathleen R. Ryan, Chair

Bacteria must be able to respond to a multitude of unanticipated environmental insults in order to survive and ensure the production of subsequent generations. Appropriate responses are dictated via the coordination of intricate signal transduction pathways that transmit circumstantial information into a physical cellular output. Many of these processes integrate into regulation of the cell cycle to control growth and development with environmental status. Here, I start by summarizing the current literature pertaining to cell cycle regulation of the model alpha-proteobacterium *Caulobacter crescentus*. I discuss how the *Caulobacter* cell cycle is governed by a complex network of two-component signal transduction proteins; adaptor-mediated, regulated proteolysis of critical cell cycle-regulators; and the interplay of these proteins with an assortment of second messenger molecules, all of which involve both canonical and non-canonical interactions of which *Caulobacter* has played an integral role towards their understanding. This summary is followed by my own research into the regulation and interaction of a selection of these signal transduction proteins, and how these processes may affect *Caulobacter*'s physiology. Namely, I define a non-canonical, second messenger-mediated interaction by two response regulator proteins. In the last section, I elucidate the role of an essential tyrosine phosphatase homolog as being required for maintaining wild-type levels of lipid A, a molecule comprising the outer leaflet of the outer membrane of Gram-negative bacteria. Lipid A is generally thought to be an essential structure stabilizing the lipid bilayer of the outer membrane. Through suppressor analysis, I discover mutations that allow *Caulobacter* to survive in the absence of this tyrosine phosphatase homolog, and extend these results to known players in lipid A biosynthesis, generating strains devoid of lipid A and demonstrating the conditionally-essential nature of lipid A in *Caulobacter*.

Table of Contents

Acknowledgements

First and foremost, I would like to thank my labmates and PI, as most of my time in graduate school was spent surrounding myself by these people, and they helped create an island of sanity amongst tumultuous waters. They were the focal point of intense and intellectual discussions that facilitated bringing my project to an appropriate stopping-point and providing me with the expertise I needed to succeed. Specifically, I would like to name Kathleen Ryan, Charlie Huang, Stephen Smith, and Sneha Jani as the people most impactful during my time in the laboratory, not to mention the slew of undergraduates who are too numerous to name. This work would not have been possible without them all.

I would also like to thank my committee members, Kathleen Ryan (again), Arash Komeili, Michi Taga, and Nicholas Ingolia. Their helpful interactions and constant support were paramount towards pushing me towards the completion of my project, and they never doubted my ability to be a successful scientist (that I am aware of).

I am incredibly appreciative of the people who have directly contributed to the work presented in this thesis. I would first like to thank Stephen Smith, who was my first mentor in the lab and who allowed me to assist him in working towards his publication, from which part of chapter 2 is derived. I would also like to thank both Kamal Joshi and Peter Chien, our collaborators who helped make the project possible. For the work in chapter 3, I thank Karen Davies and her colleagues at Lawrence Berkeley National Laboratory for their extraordinary work in collecting the cryo-electron tomography images, and thank both Sung Hwan Yoon and David Goodlett for their incredible work in collecting and analyzing the mass spectrometry data.

My parents have been especially helpful in listening and providing support as they've watched me go through the perils of graduate school, and I would like to extend an extreme thank you to them as well.

My perseverance would have been impossible had it not been for the friends I've made through this especially trying experience, so I'd like to offer them my thanks as well. Namely (in no particular order), Johan Jaenisch, Kristen LeGault, Aniket Kesari, Thomas Rembert, Ricardo Milos, Carly Straus, Carly Weiss, Mark Patana, Zachary Barth, Amelia McKitterick, Tyler Helmann, Sophia Ewens, Hector Trujillo, Sneha Jani, and the few others who've made this ordeal endurable.

Lastly, I'd like to thank the establishment of Cornerstone and their selection of delicious beverages for providing solace and making this place that much more bearable.

Preface

The focus of this dissertation is the culmination of my work investigating diverse processes in *Caulobacter crescentus* encompassing a broad range of topics that can be summed under the theme of signal transduction mechanisms that govern critical cellular functions. The first chapter is dedicated to a comprehensive summary of the current state of knowledge of important processes regulated via two-component signal transduction proteins, regulated proteolysis, and second-messenger signaling in *Caulobacter*, and is adapted from the currently-unreleased publication:

- Zik J.J., and Ryan K.R. The *Caulobacter crescentus* cell cycle control network: an integrated system of two-component signaling proteins, cyclic di-GMP-dependent processes, and regulated proteolysis. In *Cell Cycle Regulation and Development in Alphaproteobacteria*, ed. E. Biondi. Springer Nature, *in press*.

Chapter 2 focuses on my initial work in the Ryan Laboratory, including my contribution towards the following publication. The introduction will present from a historical perspective of the state of the field when I began this work, along with a relevant excerpt from the preceding publication regarding subsequent studies that have made significant strides towards the understanding of the mechanism governing proteolysis of the addressed cell cycle-regulatory protein.

- Smith S.C., *Joshi K.K., *Zik J.J., Kamajaya A., Trinh K., Chien P., and Ryan K.R. Cell cycle-dependent adaptor complex for ClpXP-mediated proteolysis directly integrates phosphorylation and second messenger signals. *PNAS* (2014) 111(39): 14229-14234 (*contributed equally to this work)

Lastly, chapter 3 represents my final and primary project in the laboratory, and is a reproduction from the following, currently-unpublished manuscript:

- Zik J.J., Yoon S.H., Gudoor R., Davis K.M., Goodlett D.R., and Ryan K.R. Iron limitation renders lipopolysaccharide nonessential in *Caulobacter crescentus*. (*Submitted*)

All materials have been reproduced with permissions from the authors, with individual contributions described in the acknowledgements section.

Chapter 1

Cell cycle signal transduction and proteolysis govern the *Caulobacter crescentus* asymmetric cell cycle – A review

1.1 Introduction

Caulobacter cell division is asymmetric, producing one motile swarmer cell and one sessile stalked cell (Fig. 1a) (1). The stalked progeny immediately begins a new round of chromosome replication (S-phase) and cell division, while the swarmer progeny is temporarily suspended in a nonreplicating state (G1). When the appropriate environmental conditions are present, the swarmer cell differentiates into a stalked cell by remodeling its polar organelles. The polar flagellum is ejected and is replaced by the stalk, a narrow extension of the cell envelope bearing adhesive holdfast material at the tip. At the same time, the cell gains the ability initiate chromosome replication, so that entry into the cell cycle is associated with a motile-to-sessile lifestyle decision. The cell division cycle and its associated morphological changes are orchestrated by a core network of two-component signaling proteins and proteins that make, degrade, and respond to the signaling molecule cyclic-di-GMP. Here we provide brief descriptions of these systems to serve as background for their specific functions in *Caulobacter*.

The two-component signaling paradigm

Two-component signaling systems are ubiquitous in bacteria, where they mediate responses to both intracellular and extracellular cues (2). Histidine kinases possess a variety of sensory domains, but all share the conserved dimerization and histidine phosphotransfer (DHp) domain and the ATP-binding catalytic domain (CA). In a canonical two-component signaling pathway, the histidine kinase senses a specific signal and autophosphorylates on a conserved histidine residue within the DHp domain, using the terminal phosphoryl group of a bound ATP molecule. The histidine kinase then serves as a phosphodonor for its cognate response regulator, the output component of the system. Response regulators contain a conserved receiver domain (RD) which catalyzes transfer of the phosphoryl group to a conserved aspartate residue within the RD. Phosphorylation of the conserved aspartate triggers conformational changes in the RD, which lead to downstream responses. Most response regulators exert their effects through additional domains whose activity is regulated by receiver domain phosphorylation (3). For example, response regulators with sequence-specific DNA-binding domains alter gene expression in response to upstream signals, and those with attached diguanylate cyclase or phosphodiesterase domains function by synthesizing or breaking down cyclic-di-GMP,

respectively. Response regulators consisting of an isolated RD work via phosphorylation-induced changes in protein-protein interactions.

Signal shut-off in two-component systems occurs via several mechanisms. Purified response regulator proteins have different degrees of auto-phosphatase activity, with some phosphorylated species persisting only for seconds, while others are stable for minutes to hours (4). Some signaling pathways include dedicated phosphatases that dephosphorylate specific response regulators (5). Finally, histidine kinases of the HisKA family are often bifunctional, mediating either phosphorylation or dephosphorylation of the cognate response regulator (6). The output of a HisKA protein therefore depends upon factors that modulate its signaling state.

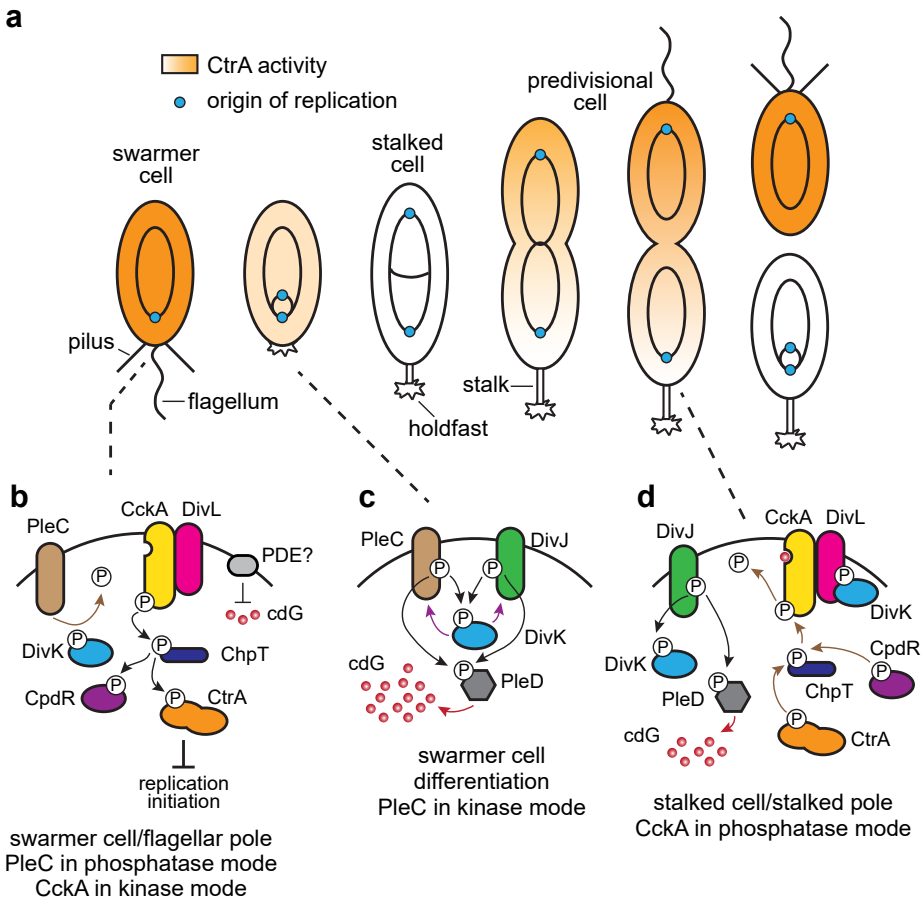

Figure 1. a, Schematic of the *Caulobacter* cell cycle. *Internal ovals*, chromosomes in various stages of replication **b-d**, Activities of signaling proteins at the indicated poles in the indicated cells. *Black arrows*, phosphorylation events; *brown arrows*, dephosphorylation events; *red arrows*, cdG synthesis; *purple arrows*, allosteric stimulation of DivJ and PleC kinase activity by DivK~P; *black bars*, upstream element inhibits downstream element

Cyclic-di-GMP-dependent signaling

Cyclic-di-GMP (cdG) is a second messenger found throughout the *Bacteria* that functions as a key regulator of lifestyle decisions (7). Low intracellular levels of cdG typically favor a motile, planktonic lifestyle, while higher concentrations trigger surface attachment and

biofilm formation. cdG is synthesized by diguanylate cyclases (DGCs) and degraded by phosphodiesterases (PDEs). These enzymes often contain additional signaling domains such as RD and Per-Arnt-Sim (PAS), which regulate DGC or PDE activity in response to upstream signals. cdG exerts its effects by binding to proteins and allosterically regulating their activity (8). PilZ domain-containing proteins are common cdG effectors, as are catalytically inactive DGC domains repurposed to serve as cdG sensors. Because some DGC and PDE enzymes are themselves response regulators, and because cdG can directly or indirectly affect the activity of histidine kinases (9, 10), cdG-based signaling systems and two-component systems can be intimately interconnected.

1.2 Two core phosphorylation pathways regulate the *Caulobacter* cell cycle and development

DivJ-PleC-DivK. *Caulobacter* development and cell cycle progression are orchestrated by a pair of two-component signaling pathways that are interconnected by the small molecule c-di-GMP and by non-canonical interactions among histidine kinases and response regulators. One pathway consists of the membrane-bound histidine kinase DivJ, the bifunctional, membrane-bound kinase PleC, and the single-domain response regulator DivK. In predivisional cells, DivJ is located at the stalked pole and functions as a DivK kinase (Fig. 1d) (11). PleC is located at the flagellar pole opposite the stalk (11), where it dephosphorylates DivK (Fig. 1b) (11, 12). When cell division is under way, and the cytoplasm of the predivisional cell becomes separated in to stalked and swarmer compartments, phosphorylated DivK (DivK~P) accumulates in the stalked compartment, while unphosphorylated DivK accumulates in the swarmer compartment (13). In *Caulobacter* progeny, high levels of DivK~P are associated with the replicative stalked cell fate, whereas unphosphorylated DivK is associated with the motile, non-replicating swarmer state.

CckA-ChpT-CtrA. The second core two-component system is composed of the bifunctional histidine kinase CckA, the histidine phosphotransferase ChpT, and the two response regulators CtrA and CpdR (14-17). All are essential for viability except CpdR, which is dispensable. When CckA is in kinase mode, the phosphoryl group from ATP is transferred from the conserved histidine residue in the DHp domain to a conserved aspartate residue within a contiguous receiver domain. From there, it is passed to the histidine phosphotransferase protein ChpT, which in turn phosphorylates either CtrA or CpdR (16). CckA resides at both poles of the *Caulobacter* predivisional cell, but it acts primarily as a phosphatase at the stalked pole (Fig. 1d) and as a kinase at the pole opposite the stalk (Fig. 1a) (18-20). Thus, when cell division occurs, the stalked progeny inherits unphosphorylated CtrA and CpdR, while the swarmer progeny inherits phosphorylated CtrA and CpdR.

CtrA contains an N-terminal receiver domain and a C-terminal DNA-binding domain. When phosphorylated, CtrA directly promotes or represses the expression of ~100 *Caulobacter* genes (21), and its indirect regulon includes one third of the transcripts whose levels vary during the *Caulobacter* cell cycle (22). CtrA modulates the expression of genes for flagellar motility, pilus production, DNA methylation, and cell division, among other processes. Although CtrA is

essential for cell cycle progression, it also represses the initiation of DNA replication by binding to sites within the chromosomal replication origin (*C*ori) (23). To satisfy these conflicting requirements, levels of CtrA protein and CtrA phosphorylation oscillate during the cell cycle, with high levels of CtrA~P in swarmer and predivisional cells, and low levels in stalked cells that are initiating chromosome replication (Fig. 1a) (24, 25).

CpdR is a single-domain response regulator that is active when unphosphorylated (see section 1.6). In this state, CpdR promotes the degradation of some substrates by the ATP-dependent protease ClpXP (17, 26, 27). Importantly, CpdR is required for the regulated degradation of CtrA that occurs during swarmer cell differentiation and in the stalked compartment of the predivisional cell (17, 28). Thus, when CckA is in kinase mode, both CtrA and CpdR are phosphorylated, generating active, stable CtrA (Fig. 1b). When CckA functions as a phosphatase, CtrA is both dephosphorylated (Fig. 1d) and subject to proteolysis by ClpXP (Fig. 2d,e) assisted by CpdR and other factors discussed in section 1.6 below.

Caulobacter swarmer cells are characterized by high levels of CtrA~P and low levels of DivK~P, while the reverse is true of stalked cells (13, 24, 25, 29). The absence of CtrA~P allows the newly born stalked cell to initiate chromosome replication immediately (Fig. 1a). In contrast, the swarmer cell is incapable of beginning chromosome replication until CtrA~P has been eliminated. The CtrA protein is rapidly degraded by ClpXP during swarmer cell differentiation (24, 30). This reaction requires unphosphorylated CpdR, as well as two additional adaptor proteins that deliver CtrA to the protease (17, 31, 32). However, even when amino acid substitutions are made which render CtrA immune to proteolysis, the existing CtrA protein becomes dephosphorylated during the SW-ST transition (24). Thus, cell cycle-regulated deactivation of CtrA is initiated by CckA acting in phosphatase mode.

1.3 Non-canonical interactions between the DivJ-PleC-DivK and CckA-ChpT-CtrA pathways control polarity and development

The differentiation of a non-replicating, motile swarmer cell into a sessile, replicating stalked cell requires a complete change in the signaling status of the regulatory network. As described above, CckA must be converted from a kinase, phosphorylating CtrA and CpdR, to a phosphatase, dephosphorylating both targets. Changes in the activity of the DivJ-PleC-DivK pathway drive this developmental transition.

DivK is an essential protein, and mutants harboring conditional alleles of *divK* arrest in the G1 phase of the cell cycle, unable to initiate chromosome replication (12, 33). This phenotype provided the first clue that DivK is responsible for deactivating CtrA, and DivK~P is now known to switch CckA from its kinase to its phosphatase signaling mode (34). During SW-ST differentiation, DivJ becomes localized at the flagellated pole, and PleC is subsequently released (11, 35). DivJ localization requires the polar organizing protein PopZ and the localization factor SpmX, which also stimulates DivJ's kinase activity (36-38). Although PleC usually functions as a DivK~P phosphatase, the transient colocalization of DivJ and PleC

initiates a positive feedback loop, in which DivK~P phosphorylated by DivJ allosterically stimulates the kinase activity of both DivJ and PleC (Fig. 1c) (35). The resulting increase in DivK~P levels toggles CckA from the kinase to the phosphatase mode, which leads to the elimination of CtrA~P and the commencement of S-phase (34, 39).

The effects of DivK upon CckA are mediated by another two-component signaling protein, the atypical histidine kinase homolog DivL. Also essential for *Caulobacter* viability, DivL resembles histidine kinase proteins, but has a tyrosine residue in place of the conserved, phosphorylated histidine (40). Cells with conditional mutations in *divL* have the opposite phenotype of those lacking DivK; they fail to divide, contain many chromosomes per cell, and have have less CtrA~P than wild-type cells (41, 42), indicating that DivL is important for the activation of CtrA. However, rather than functioning as a kinase itself, DivL is required for CckA localization at the pole opposite the stalk and for the kinase activity of CckA (Fig. 1b) (19, 34, 39, 41). DivL can be co-immunoprecipitated with CckA from *Caulobacter* lysates, but it is unknown whether DivL interacts directly with CckA, or if it interacts through intermediary proteins (19). In either case, the activation of a *bona fide* histidine kinase by a pseudokinase is a novel, non-canonical interaction between two-component proteins, and it may point to a function for pseudokinases encoded in other bacterial genomes.

DivK~P toggles CckA from kinase to phosphatase mode by interacting directly with DivL (Fig. 1d) (34). The binding site for DivK~P on DivL includes the region where a cognate response regulator would normally dock during phosphotransfer, but specific binding to the phosphorylated form of DivK also requires three PAS domains that lie N-terminal to the DHp domain in DivL (34, 39). The PAS domains are not thought to interact directly with DivK~P, but to influence the positioning of the catalytic CA domain, thereby impacting the DivK~P binding site. In the current model (Fig. 1d), an interaction between DivL and CckA promotes CckA kinase activity, whereas a ternary complex including DivK~P as well favors CckA phosphatase activity (34, 39). However, it is also formally possible that DivK~P binding causes DivL to release CckA, causing it to revert to phosphatase mode. Thus, DivL functions as sensor for a cytoplasmic response regulator, DivK~P, using the DHp and CA domains that are traditionally involved in histidine kinase output. In an interaction that awaits further dissection, DivL transmits the information of its interaction with DivK~P to CckA, linking the activity of the DivJ-PleC-DivK pathway to the CckA-ChpT-CtrA pathway.

1.4 cdG signaling regulates the *Caulobacter* cell cycle and polar development

The cell cycle signaling network both generates and is modulated by cdG oscillations

Measurement of cdG levels in individual *Caulobacter* cells using a fluorescent biosensor demonstrated that the swarmer progeny contains <100 nM cdG, while the stalked progeny contains ~500 nM cdG (43). Measurement of cdG by LC-MS in *Caulobacter* cultures undergoing synchronous passage through the cell cycle also revealed a transient increase in cdG

levels from <100 nM to ~275 nM during swarmer cell differentiation, followed by a slow decay back to ~100 nM in predivisional cells (44). Here we describe the signaling pathways that produce oscillations in the level of cdG, as well as mechanisms by which cdG impacts cell cycle progression and polar morphogenesis.

DivJ and PleC each interact with a second response regulator, PleD, which possesses two tandem receiver domains followed by a DGC domain (45). Phosphorylation of the first receiver domain causes PleD to dimerize and activates the production of cdG (46). During swarmer cell differentiation, when DivJ and PleC are temporarily co-localized at the developing flagellar pole, phosphorylation of DivK by DivJ initiates a positive feedback loop, in which DivK~P stimulates the kinase activity of DivJ and also causes PleC to enter kinase mode. Both DivJ and PleC then act as kinases for PleD, leading to a surge in cdG production by PleD~P (Fig. 1c) (35, 47). Switching PleC from phosphatase to kinase mode is an important step in polar morphogenesis, as cells expressing a variant of PleC lacking kinase activity (13) do not experience an increase in cdG levels are are impaired in holdfast and stalk biogenesis (35).

Increased production of cdG by PleD contributes to, but is not sufficient for, the increase in [cdG] during swarmer cell development. A second diguanylate cyclase, DgcB, produces cdG throughout the cell cycle, and its effects are counteracted specifically in swarmer cells by the phosphodiesterase PdeA (47). Importantly, PdeA is proteolyzed by ClpXP during swarmer cell differentiation (Fig. 2e), so that cdG synthesis by PleD and DgcB is temporarily unopposed. In addition to ClpXP, PdeA degradation requires the unphosphorylated form of CpdR, so toggling CckA into phosphatase mode is important for the surge in cdG that occurs during swarmer cell development (26, 47).

cdG produced by the action of cell cycle-regulated DGC and PDE enzymes feeds back to modulate key steps in the cell cycle network. First, cdG binds directly to CckA and promotes its phosphatase activity (Figs. 1d, 2e) (9, 10, 48), thereby playing an important role, along with DivK~P, in switching CckA to phosphatase mode. CckA is the second histidine kinase demonstrated to respond directly to cdG, after SgmT, which regulates the expression of extracellular matrix proteins in *Myxococcus xanthus* (49). Reinforcing its effects on the CckA-ChpT-CtrA pathway, cdG is also necessary for regulated proteolysis of CtrA by ClpXP during swarmer cell differentiation (Figs. 2d, e). cdG binds directly to an adaptor protein, PopA, that functions in the temporally regulated degradation of CtrA and other substrates (32). Together these effects promote the initiation of chromosome replication and entry into the cell division cycle.

cdG signaling is required for polar morphogenesis

By generating a *Caulobacter* mutant lacking all DGC enzymes (cdG^0), Abel *et al*. (44) demonstrated that cdG is necessary for the proper construction of all polar organelles; the mutant strain is stalkless and lacks the flagellum, pili, and the adhesive holdfast. Synthesis of the stalk and holdfast are initiated during swarmer cell differentiation, when [cdG] is at its peak, while synthesis of the flagellum and pili occur in predivisional cells, when the level of cdG is lower (43, 44, 50-54). The different steps in polar morphogenesis may occur at different threshold

levels of cdG, an inference that was generally supported by examining polar structures in cdG^0 mutants containing various levels of cdG produced by a heterologous DGC enzyme (44). However, in *Caulobacter* mutants with cdG produced only by a constitutively active heterologous enzyme, each cellular process that was measured occurred at a higher [cdG] concentration than it did in wild-type cells (44). These findings suggest that measurements of [cdG] in wild-type *Caulobacter* underestimate the true concentrations, or possibly that cdG produced by native enzymes that are temporally regulated or spatially localized is more efficient at promoting downstream effects. Although cdG is a rapidly diffusing small molecule, and there is no direct evidence of anisotropy in its distribution (43), we cannot entirely rule out the possibility that localized production, degradation, and sensing of cdG is involved in some aspects of *Caulobacter* cell polarity.

cdG has not yet been mechanistically linked to every polar structure, in part because it is still easier to identify proteins that synthesize and degrade cdG than to identify cdG-binding effectors. However, great progress in this area has been achieved using affinity binding techniques (55), and the *Caulobacter* proteins revealed by this method include cdG effectors that modulate flagellar motor function and participate in holdfast biosynthesis (56-58). Here we focus on cdG-regulated polar morphogenesis events that occur at distinct times in the *Caulobacter* cell cycle and development.

Predivisional cells of the cdG^0 mutant fail to synthesize even the earliest sub-structures in flagellar biogenesis, the MS-ring and switch complex (44). Flagellar construction is initiated when the assembly factor TipF binds cdG using an enzymatically inactive PDE domain (59). Upon cdG binding, TipF localizes to the pole opposite the stalk and there recruits the flagellar placement factor PflI and FliG of the switch complex, which attract additional flagellar proteins. cdG is also thought to stimulate the expression of flagellar genes later in the transcriptional hierarchy by a mechanism unrelated to TipF, but the effector(s) responsible are unknown (59).

The flagellum is built in predivisional cells and begins to rotate shortly before cell separation. The Δ*pleC* mutant is nonmotile because the the polar flagellum is paralyzed (60). A possible linkage between PleC and flagellar rotation is the cdG sensor DgrA. DgrA binds cdG via a PilZ domain, and in the cdG-bound state inhibits flagellar motility (61). One hypothesis is that PleC acting in phosphatase mode deactivates PleD or activates a PDE enzyme at the flagellar pole of the predivisional cell. This process would cause the observed drop in [cdG] in the swarmer compartment (43), preventing DgrA from inhibiting flagellar rotation and yielding motile swarmer progeny.

When swarmer cells differentiate, they eject the flagellum and synthesize an adhesive holdfast at the same pole. The Δ*pleD* mutant fails to eject the flagellum because the MS-ring protein FliF is not proteolyzed by ClpAP (62, 63). This relationship suggests that there may be a cdG-dependent adaptor for ClpAP-mediated proteolysis, analogous to PopA.

The swarmer cell begins to synthesize holdfast even before the flagellum is ejected, because optimal surface attachment requires both flagellar motility and the holdfast (53, 54). After synchronization, when swarmer cells are released into dilute liquid culture, holdfast synthesis begins after about 20 minutes. In contrast, isolated swarmer cells begin expressing the

holdfast only 1-2 minutes after exposure to a surface (64). These results suggested that holdfast production is under cell cycle control, but can be accelerated by surface contact. A recent study found that the inhibition of flagellar rotation by a nearby surface is sensed by the cdG synthase DgcB. DgcB interacts directly or indirectly with the flagellar stator component MotA, and a change in motor function or in some property of the cytoplasmic membrane is thought to stimulate its activity (56). The same study identified HfsJ, a glycosyltransferase essential for holdfast production, as a cdG-dependent effector protein. Therefore, surface sensing via the flagellum and DgcB is thought to generate a local increase in cdG, which stimulates HfsJ activity and triggers holdfast production in advance of when it would begin in a planktonic swarmer cell.

Together, these studies demonstrate the wide range of mechanisms by which cdG can modulate bacterial behavior. Although we do not yet know how cdG is connected to *Caulobacter* pilus or stalk synthesis, we are likely to encounter the same level of complexity in their relationship to cdG.

1.5 Spatial regulation of CckA activity

Caulobacter CckA was the first histidine kinase shown to be located at a distinct position within a bacterial cell (15), other than CheA within the chemoreceptor complex (65). Prior to these observations, it had been assumed that signaling proteins performed their functions while diffusing throughout the cytoplasm or cytoplasmic membrane. The importance of protein localization for the correct signaling output is clear for enzymes such as DivJ and PleC, whose activities need to be at opposite poles of the cell to generate progeny with asymmetric replicative fates and polar organelles (13, 66, 67). PleC switches its activity temporally, from a phosphatase to a kinase, during swarmer cell differentiation (Fig. 1c). The positive feedback mechanism responsible for the switch is described in section 4.3. Here we consider several mechanisms proposed to account for distinct CckA kinase and phosphatase activities at the two poles of the *Caulobacter* predivisional cell.

Swarmer cells contain high levels of CtrA~P (Fig. 1a) and low levels of DivK~P, while the reverse is true in stalked cells (24, 29). The stimulation of CckA phosphatase activity by by DivK~P would seem to enforce this inverse relationship, yet *Caulobacter* predivisional cells contain high levels of both CtrA~P and DivK~P (24, 29). Therefore, some fraction of the CckA protein in predivisional cells must be protected from the effects of DivK~P. Studies using *Caulobacter* cells treated with the division inhibitor cephalexin showed that, when an elongated cell contains two chromosomes, DNA replication is five times more likely to commence at the chromosomal origin near the stalked pole than at the origin near the flagellar pole (20). Using mutants in which CckA kinase or phosphatase activity was selectively impaired, it was demonstrated that replicative asymmetry required both activities. The model that emerged is that CckA acts as a kinase at the flagellar pole (Fig. 1b) and as a phosphatase at the stalked pole (Fig. 1d), generating a gradient of CtrA activity along the length of the cell (Fig. 1a) (20). At the flagellar pole, where [CtrA~P] is highest, replication initiation is blocked, but at the stalked pole, where [CtrA~P] is lowest, replication can commence even in the absence of cell division.

Several processes have been proposed to explain how CckA performs different functions at the two poles. DivL accumulates at the flagellar pole, which suggests that it may specifically promote CckA kinase activity at this site (19). However, DivL is also distributed around the cell membrane, and the swarmer and stalked progeny inherit roughly equal amounts of DivL (68). Therefore, it can't be assumed that DivL only interacts with CckA at the flagellar pole.

Features intrinsic to CckA could spatially regulate its activity. Reconstitution of CckA in liposomes showed that, in the absence of other factors, CckA is more likely to work as a kinase when it is present at higher densities in a membrane (10). This property could bias CckA that is diffusely located around the cytoplasmic membrane toward the phosphatase state, but it does not easily explain how CckA can have opposing activities at the two cell poles. Although foci of fluorescently labeled CckA proteins are often brighter at the flagellar pole than at the stalked pole (15, 69), we do not know if this corresponds to a higher local density of CckA at the flagellar pole.

CckA may be biased towards the kinase state at the flagellar pole because there, it is protected from cdG and DivK~P, which promote the switch to phosphatase mode. With respect to cdG, this possibility was investigated using a truncated variant of CckA lacking only its cytoplasmic membrane anchor, *cckAΔTM*, which diffuses throughout the cytoplasm. *cckAΔTM* cannot compensate for a deletion of the native *cckA* gene, and when expressed in a wild-type strain, it causes over-replication of chromosomal DNA, suggesting that it functions as a phosphatase to deactivate CtrA (15, 18). In confirmation, a double *cckA* mutant lacking the transmembrane domain and also lacking phosphatase activity, has no effect when overexpressed in wild-type cells (18). Importantly, a double *cckA* mutant lacking the membrane anchor and unable to bind cdG (or *cckAΔTM* expressed in the cdG^0 background) leads to a strong G1 arrest, indicating that the cytoplasmic pool of cdG prevents kinase activity in CckA molecules that are delocalized from the flagellar pole (48). These results suggest that the flagellar pole may be depleted of cdG by an unknown, localized phosphodiesterase (Fig. 1b).

The localized phosphatase activity of PleC is thought to protect CckA at the flagellar pole from DivK~P (Fig. 1b). A temperature-sensitive *pleC* mutant contained only 18% of the wild-type amount of CckA~P after a short incubation at the nonpermissive temperature, indicating that PleC inactivation rapidly and profoundly reduces CckA kinase activity (34). A single-domain PAS protein called MopJ is also partially responsible for maintaining CckA kinase activity in the face of DivK~P. The Δ*mopJ* strain has moderately reduced CtrA activity in exponentially growing cells, and it is far more sensitive than a wild-type strain to DivK overexpression, suggesting that MopJ counteracts DivK activity (70). Overexpression of MopJ increases DivK localization to both poles but does not affect the cellular level of DivK~P. In contrast, DivL is delocalized from the flagellar pole in the Δ*mopJ* strain (70). Together, these results suggest that MopJ promotes CckA kinase activity by promoting the flagellar pole localization of DivL and by reducing the impact of DivK~P through an uncharacterized mechanism (Fig. 3b).

1.6 Proteolytic regulation of the *Caulobacter* cell cycle

Regulated degradation of select protein substrates is a crucial process in maintaining proper cell physiology and homeostasis in all organisms. In bacteria, regulated proteolysis is important for numerous processes, including the response to envelope stress (71), spore formation (72), and the clearance of misfolded and prematurely-terminated proteins (73, 74). Studies in *Caulobacter* in particular have underscored the importance of regulated proteolysis in cell cycle progression and differentiation.

AAA+ proteases and adaptor-mediated proteolysis

The ubiquitous AAA+ (ATPases associated with diverse cellular activities) family of proteases mediates the degradation of proteins in a highly-controlled manner. AAA+ proteases consist of a barrel-shaped peptidase chamber, the entry of which is gated by an oligomeric unfoldase component that contains the AAA+ domain. The unfoldase uses successive rounds of ATP hydrolysis to unfold the substrate into a linear peptide chain and translocate it through a central axial pore into the peptidase chamber, where the substrate is subsequently cleaved into short peptide fragments (75). ClpXP is the best-characterized AAA+ protease, in which a hexamer of the unfoldase component, ClpX, binds to a tetradecamer of the ClpP peptidase (Fig. 2b) (76, 77). ClpX is responsible for substrate recognition, either on its own or with the assistance of dedicated adaptor proteins. The first example of adaptor-mediated proteolysis came from studies of degradation of ssrA-tagged substrates in *E. coli*. The ssrA tag is covalently added to the C-terminus of a polypeptide on a stalled ribosome by transfer-messenger RNA (tmRNA) in a process termed trans-translation, which releases the polypeptide and frees the ribosome for productive engagements (78, 79). Since the polypeptide is prematurely terminated, the ssrA-tag directs the unfinished product to ClpXP for degradation (80, 81). Two alanine residues and the α-carboxylate at the C-terminus of the ssrA tag are directly recognized by ClpX (82-84). Once engaged, ATP hydrolysis induces conformational changes in ClpX that drive substrate translocation and unfolding.

Although ClpXP alone can recognize and degrade ssrA-tagged substrates, degradation is accelerated by the SspB adaptor protein (80, 81). SspB acts as a tether, binding to both ClpX and the ssrA tag to increase the local substrate concentration exposed to ClpXP (81, 82, 85). The N-terminus of SspB contains a dimerization domain that binds to the ssrA tag, and this is connected through an unstructured linker to a short C-terminal motif that binds to the N-terminal domain of ClpX (NTD_{ClpX}) (86-88). Substrate tethering effectively reduces the K_m of catalysis while negligibly affecting the V_{max} (81). Although SspB was first shown to facilitate proteolysis of ssrA-tagged substrates, it is also an adaptor for other distinct proteins (89). A simple tethering of substrate to protease is not the only way for an adaptor to stimulate proteolysis. An alternative mechanism is used by the RssB response regulator in *E. coli*, which, which activated by phosphorylation, binds to the stationary phase sigma factor σ^S to induce conformational changes that allow σ^S to be recognized by ClpX (90). In this case, RssB does not contact ClpX directly. Instances of adaptor-mediated proteolysis important for the *Caulobacter* cell cycle and development are explored below.

The *Caulobacter* genome encodes five AAA+ proteases: ClpXP, ClpAP, HslUV, FtsH, and Lon (91) . ClpXP, ClpAP, and HslUV are bipartite enzymes, with ATPase and peptidase components encoded by separate genes, while FtsH and Lon contain both domains on a single polypeptide (92). The peptidase ClpP associates with either ClpX or ClpA independently, and these complexes proteolyze distinct substrates (93, 94). So far, ClpXP, ClpAP, and Lon are known to mediate cell cycle-regulated proteolysis in *Caulobacter* (30, 95, 96). ClpX, ClpP, and Lon are present at constant levels throughout the cell cycle (30, 97), but the concentrations of their substrates fluctuate dramatically due to temporal control mechanisms regulating both protein synthesis and degradation (Fig. 2a).

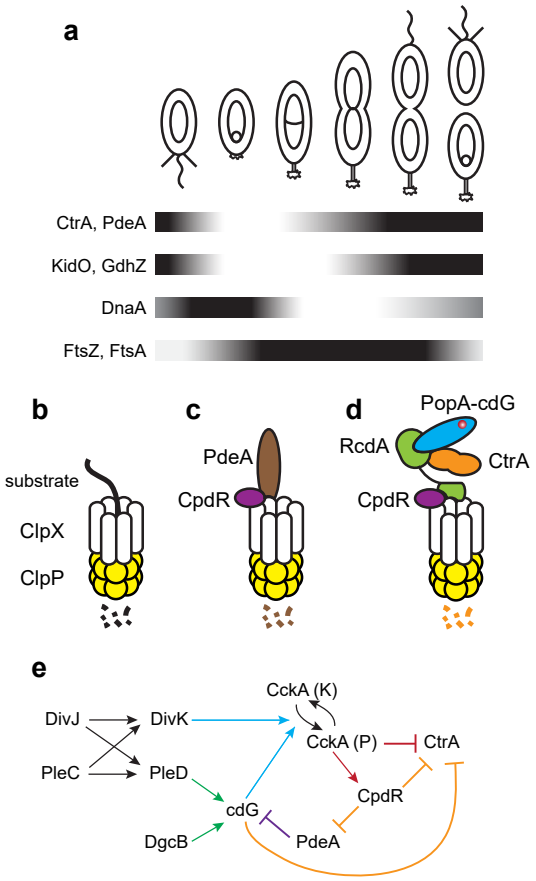

Figure 2. a, Relative abundances of proteins whose levels and/or stability change during the cell cycle **b**, ClpXP proteolysis unassisted by adaptors **c**, ClpXP degrades PdeA with the assistance of the priming factor CpdR d ClpXP degrades CtrA with the assistance of a multi-component adaptor comprising CpdR, RcdA, and cdG-bound PopA e Signaling events leading to the degradation of PdeA and CtrA during swarmer cell differentiation. Dashed arrows, phosphorylation events; CckA (K), CckA in kinase mode; CckA (P), CckA in phosphatase mode; blue arrows, DivK~P and cdG promote the phosphatase activity of CckA; red arrow, CckA activates CpdR via dephosphorylation; red bar, CckA deactivates CtrA via dephosphorylation; green arrows, cdG synthesis; purple bar, cdG hydrolysis; brown bars, upstream components stimulate ClpXP-mediated proteolysis of downstream components.

Cell cycle regulation of CtrA proteolysis

The CtrA response regulator is both dephosphorylated and proteolyzed during swarmer cell differentiation and in the stalked compartment of predivisional cells to license the initiation of DNA replication by DnaA (24, 98, 99). CtrA and DnaA bind to overlapping sites in the *Caulobacter* origin of replication (*Cori*), and CtrA has been shown to displace DnaA from its binding sites *in vitro* (23, 100). CtrA degradation in these two cell types is accomplished by ClpXP in association with a highly-regulated adaptor complex which binds to ClpX (Fig. 2d) (28, 101). The details of the CtrA degradation complex are the focus of chapter 2 and will be discussed therein.

Regulated proteolysis of proteins that modulate CtrA activity

The PdeA phosphodiesterase contains an N-terminal PAS domain, followed by an inactive DGC domain and a C-terminal EAL domain that hydrolyzes cdG (26, 47, 102). As described above, PdeA opposes the activity of DgcB in SW cells and prevents a premature increase in cdG levels. Degradation of PdeA during the SW-ST transition triggers the increase in [cdG] that is important both for polar morphogenesis and for the efficient degradation of CtrA.

PdeA is degraded by ClpXP in concert with the adaptor CpdR (Fig. 2c) (47). The C-terminal amino acids of PdeA (RG) comprise a weak degradation signal for ClpXP (26). Mutation of these residues to DD or addition of a FLAG epitope tag blocks PdeA degradation *in vitro* and *in vivo* (26, 47) . Underscoring the importance of cdG for swarmer cell development, holdfast production and CtrA proteolysis are delayed in a *pdeA-FLAG* strain, and these effects are exacerbated by simultaneous deletions of either *pleD* or *dgcB* (47). Deletion of the PdeA PAS domain blocks degradation. But surprisingly, although the truncated ΔPAS-PdeA variant has PDE activity, it does not produce the same phenotype *in vivo* as another stable variant with an altered C-terminus, PdeA-DD (26). The PAS domain is therefore likely to perform an unknown signaling role in addition to regulating PdeA stability. CpdR reduces the K_M for PdeA degradation 3-fold, consistent with a tethering function, but it also increases v_{max} by ~30-fold, suggesting that CpdR can also improve the turnover rate of substrates with intrinsically weak degradation tags (26).

As described above, SciP associates with CtrA and DNA in swarmer cells and prevents the inappropriate expression of CtrA-regulated genes that are specifically transcribed in predivisional cells. SciP is itself subject to regulated proteolysis during swarmer cell differentiation, and this process is important for proper cell cycle progression (95). Accordingly, expression of a stabilized SciP-M2 variant down-regulates the transcription of CtrA-activated genes and inhibits cell division. SciP is degraded by the Lon protease *in vivo* and *in vitro*, and, like CtrA, it is protected from degradation *in vitro* within the CtrA-SciP-DNA ternary complex (95).

Proteolysis of substrates that regulate DNA replication and methylation

As in nearly all bacteria, DNA replication in *Caulobacter* is initiated by the highly-conserved AAA+ protein DnaA (98). When in its active, ATP-bound state, DnaA binds to specific sites within the origin of replication, oligomerizes, and promotes local unwinding of the DNA (103). These steps permit the subsequent assembly of the replisome and the beginning of new DNA synthesis. A primary mechanism that prevents further, premature replication initiation events is replicatory inactivation of DnaA (RIDA). When bound to the sliding clamp of the replisome on newly synthesized DNA, Hda (homolog of DnaA). contacts DnaA and stimulates its ATP hydrolysis activity to produce the inactive, ADP-bound form of DnaA (104). Unlike *E. coli*, *Caulobacter* replicates its chromosome once and only once per cell division (105). This periodicity of DNA replication depends upon the essential *Caulobacter* Hda homolog, HdaA, which operates similarly to its *E. coli* counterpart (106-109).

Although HdaA is critical for the timing of replication initiation (106), steady-state levels of DnaA also fluctuate somewhat during the *Caulobacter* cell cycle (Fig. 2a) (110). DnaA levels increase in swarmer cells and decrease in stalked cells after replication has begun. DnaA is degraded with a half-life of 45-60 minutes in unstressed conditions (111, 112), and overexpression of *dnaA* causes overinitiation of DNA replication and ultimately death (107). DnaA is chiefly degraded by the Lon protease *in vivo* (112). In *E. coli*, Lon is known to recognize and degrade unfolded proteins generated by stress or DnaK depletion (113). Consistent with this cellular role, Lon-mediated proteolysis of *Caulobacter* DnaA is stimulated *in vitro* by the addition of unfolded substrates (112). The allosteric stimulation of Lon activity may only apply to certain substrates, since degradation of SciP is not enhanced by unfolded substrates. The stimulation of DnaA proteolysis by unfolded proteins has physiological consequences in cells exposed to proteotoxic stress. In response to heat shock or loss of the conserved chaperone DnaK, elevated levels of unfolded proteins stimulate Lon to degrade DnaA and consequently inhibit the initiation of chromosome replication (112).

While Lon is the primary protease for DnaA degradation in *Caulobacter* during log phase, ClpAP is required for the complete removal of DnaA observed during stationary phase (114). *In vitro*, ClpAP degrades DnaA, but at a slower rate than Lon. DnaAR357A, a variant that cannot hydrolyze ATP, is degraded much more slowly than wild-type DnaA by Lon, but both substrates are degraded at similar rates by ClpAP (109, 114) . These results suggest that ClpAP may contribute significantly to the degradation of active, ATP-bound DnaA when its levels are inappropriately elevated *in vivo*. Indeed, expression of *dnaAR357A* is much more detrimental to Δ*clpA* cells than to wild-type cells (114), indicating that ClpAP-mediated degradation serves as a mechanism to protect *Caulobacter* from an excess of activated DnaA. ClpAP has therefore been designated an auxiliary protease that may help fine-tune the levels of DnaA in the cell or aid in degradation when Lon become saturated.

The Lon protease plays a critical role near the end of the cell cycle, when it is responsible for degrading the essential DNA methyltransferase CcrM (97, 115). CcrM is restricted to PD cells and catalyzes N^6-methylation of adenine at GAnTC sequences to convert chromosome from a hemimethylated to a fully methylated state near the end of S-phase (115, 116). Expression of many cell cycle-regulated genes is directly influenced by the methylation state of GAnTC sequences within their promoters (117, 118). Genes nearer the origin of replication become hemimethylated earlier during S-phase and remain so for a longer time than genes nearer the terminus. Thus, genes whose transcription depends upon hemimethylation of promoter sequences are transcribed at different times, depending upon their distance from the origin of replication (119). This system of transcriptional regulation does not function correctly if CcrM is present and active throughout S-phase, rapidly methylating all newly synthesized strands of DNA. Thus, constitutive overexpression of *ccrM* or deletion of *lon* nearly eliminates hemimethylated DNA and causes cell morphology defects (97, 116). The increase in CcrM abundance at the end of the cell cycle, followed by its rapid degradation, is not believed to be driven by regulated proteolysis. Instead, Lon is thought to degrade CcrM at a constant rate, and a burst of CcrM synthesis late in the cell cycle temporarily overcomes Lon-mediated proteolysis (97, 116).

Degradation of proteins involved in cell division

The proteolysis of two key regulators of FtsZ dynamics is important for proper assembly of the Z-ring at the midcell prior to division. KidO and GdhZ promote disassembly of the Z-ring in predivisional cells, which facilitates cell division, and in swarmer cells, which prevents premature Z-ring assembly (120, 121). GdhZ, an NAD-dependent glutamate dehydrogenase that converts glutamate to alpha-ketoglutarate, acts synergistically with KidO to regulate FtsZ (121). Consistent with these activities, KidO and GdhZ are present in G1-phase swarmer cells and in late predivisional cells but are absent during S-phase (Fig. 2a) (120, 121). *In vivo*, ClpXP, CpdR, RcdA, and PopA are each required for the cell cycle-regulated degradation of KidO and GdhZ during swarmer cell differentiation, but it is unknown if these proteins are sufficient for KidO or GdhZ proteolysis *in vitro* (120, 121). Constitutive expression of the stabilized variant *kidO-DD* from the *Caulobacter* chromosome inhibits cell division, and overexpression of wild-type *kidO* also disperses FtsZ from Z-rings (120). Stabilization of GdhZ also results in mild cell elongation, whereas the simultaneous stabilization of GdhZ and the constitutive expression of KidO-DD causes more severe cell filamentation (121). Collectively, these data indicate that temporally regulated degradation of KidO and GdhZ is important for proper cell division. We discuss below (section 1.8) the possibility that KidO, by binding NADH, could be regulated by changes in the redox status of the *Caulobacter* cytoplasm.

Some components of the divisome itself are proteolyzed during or after septation, including FtsZ, FtsA, and FtsQ (Fig. 2a) (122, 123). While these proteins are regulated at the level of transcription, constitutive expression throughout the cell cycle still yields oscillations in abundance, consistent with temporally controlled degradation (122-124) . FtsZ is degraded by both ClpXP and ClpAP *in vivo*, and either protease can degrade FtsZ *in vitro* without any additional proteins (96). ClpAP is the primary protease for FtsA degradation *in vivo*, but the poor solubility of FtsA has precluded a thorough analysis of its degradation *in vitro* (96). Both FtsZ and FtsA are degraded more rapidly in swarmer cells than in stalked cells. Constitutive expression of FtsZ in a Δ*clpA* mutant background results in slightly longer cells with mis-positioned Z-rings, as compared to either mutant individually (96), and overexpression of either FtsZ or FtsA results in cell division defects and a decrease in viability (123, 124). However, the physiological consequences of blocking the degradation of divisome components, as opposed to overexpressing them, remain to be characterized. Although unassisted ClpXP or ClpAP can degrade FtsZ *in vitro*, it is unknown if other factors *in vivo* govern the cell type-specific degradation of divisome proteins. Further studies are needed to determine if proteolytic clearance of divisome proteins plays a role in cell constriction or in preventing premature divisome assembly in daughter cells.

1.7 Nutrient cues affecting the *Caulobacter* cell cycle

The previous sections have described the core network regulating the *Caulobacter* cell cycle and development. These systems have chiefly been studied and described in well-fed, unstressed, exponentially growing cells, but equally important are the ways in which the network

is modulated by environmental cues to maximize fitness in changing conditions. In this section, we focus on molecular mechanisms that connect nutrient and redox signals to the core network described above.

(p)ppGpp is produced in response to starvation in E. coli

When *E. coli* cells are starved for various nutrients, they synthesize the "alarmone" signaling molecules guanosine tetraphosphate and guanosine pentaphosphate (here collectively called (p)ppGpp), which trigger the downregulation of macromolecular syntheses (125, 126). RelA responds to amino acid starvation by associating with ribosomes and producing (p)ppGpp when an uncharged tRNA molecule enters the A-site of the ribosome (127). SpoT, which can both synthesize and hydrolyze (p)ppGpp, has been suggested to respond to starvation for several nutrients, including carbon (128), fatty acids (129), and iron (130). However, only fatty acid starvation has been mechanistically linked to SpoT activation, via the binding of SpoT to holo-acyl carrier protein (126). Increased (p)ppGpp levels directly or indirectly inhibit the synthesis of DNA, RNA, and proteins. For example, by binding to RNAP, (p)ppGpp interferes with the transcription of a subset of RNAs, most importantly rRNAs and tRNAs, which in turn reduces translation (131). (p)ppGpp also inhibits the initiation of chromosome replication in *E. coli* by inhibiting *dnaA* transcription (132).

(p)ppGpp is a key mediator of Caulobacter starvation responses

It is well established that starvation for carbon or nitrogen blocks the *Caulobacter* cell cycle in the G1 swarmer phase (111, 133-135). Isolated swarmer cells that are released into minimal medium lacking either a carbon or nitrogen source remain motile and do not initiate chromosome replication. In laboratory conditions, synchronized stalked cells that have already initiated chromosome replication are able to complete replication when their nitrogen source is withdrawn (135). However, cells that complete chromosome replication during carbon or nitrogen starvation may sustain damage that reduces competitive fitness. In addition, it is believed that prolonging the motile phase in response to starvation gives swarmer cells the chance to locate a more favorable environment before committing to a sessile, replicative lifestyle.

At the molecular level, in carbon- or nitrogen-limited swarmer cells, the CtrA protein is stabilized, rather than being degraded during swarmer cell development, and the abundance of DnaA is greatly reduced (111, 133, 136). The flagellum is maintained at the pole, and the remodeling of polar signaling proteins is also disrupted. In particular, DivJ does not accumulate at the presumptive stalked pole (136). As in *E. coli*, carbon or nitrogen starvation triggers an increase in intracellular levels of (p)ppGpp (136).

Caulobacter has only one protein capable of synthesizing (p)ppGpp, the bifunctional enzyme SpoT (91). Swarmer cells lacking SpoT do not arrest their cell cycle appropriately when released into medium lacking carbon or nitrogen, suggesting that (p)ppGpp is an important signal of starvation (133, 136, 137). To uncover the cellular effects of (p)ppGpp in the absence of

actual starvation, Gonzalez and Collier (138) expressed a hyperactive (p)ppGpp synthase (RelA′) using an inducible promoter in wild-type *Caulobacter* under nutrient-replete conditions (138). These experiments showed that (p)ppGpp synthesis is sufficient to slow growth, stabilize the CtrA protein, and delay the initiation of chromosome replication and the successive localization of DivJ and release of PleC from the flagellar pole. Given that (p)ppGpp is both necessary and sufficient for these phenotypic effects of starvation, work is ongoing to determine both how different types of starvation are sensed by SpoT and how (p)ppGpp modulates cell cycle progression.

Linkages between ammonium deprivation and (p)ppGpp synthesis

In contrast to *E. coli*, *Caulobacter* cells do not experience an increase in (p)ppGpp levels during fatty acid starvation (139), so *Caulobacter* SpoT is not likely to be regulated in the exact same ways as its homolog in *E. coli*. Recent work, however, has uncovered the mechanism by which *Caulobacter* SpoT senses and responds to ammonium limitation (Fig. 3a) (135). *Caulobacter* assimilates ammonium exclusively via the glutamine synthetase GlnA, whose transcription and activity are promoted by the general nitrogen sensor GlnD (140). As expected, the *Caulobacter* Δ*glnD* and Δ*glnA* mutants are auxotrophic for glutamine. Interestingly, however, both mutants grow slowly and accumulate G1-phase swarmer cells when cultivated in complex PYE medium, which contains a mixture of amino acids (141). These growth and cell cycle defects are relieved by adding glutamine to the PYE medium, indicating that low glutamine levels specifically trigger a G1-phase cell cycle delay (135).

Additional work demonstrated that cellular glutamine levels are communicated to SpoT by a nitrogen-related phosphoenolpyruvate (PEP) phosphotransferase system (PTS^{Ntr}). In canonical PTS systems, which sense and respond to carbon availability, an EI enzyme autophosphorylates using PEP, and the phosphoryl group is transferred sequentially to the HPr and EII proteins, which regulate the uptake of carbohydrates (142). PTS^{Ntr} systems are comprised of similar components, but respond instead to nitrogen availability. Similar to a PTS^{Ntr} system in *Sinorhizobium meliloti* (143), glutamine binding inhibits EI^{Ntr} phosphorylation in *Caulobacter* (135). Thus, when glutamine is limiting, due to an inability to assimilate ammonium, phosphorylated forms of HPr^{Ntr} and EII^{Ntr} accumulate. Ronneau et al. (135) found that EII^{Ntr}~P binds SpoT directly and inhibits its (p)ppGpp hydrolase activity, while HPr^{Ntr}~P indirectly stimulates the (p)ppGpp synthetase activity of SpoT (Fig. 3a). These interactions connect nitrogen limitation with a rise in intracellular (p)ppGpp. Consistent with these findings, deletion of *Caulobacter pstP*, encoding EI^{Ntr}, blocks (p)ppGpp accumulation and G1-phase swarmer cell accumulation during nitrogen starvation (135).

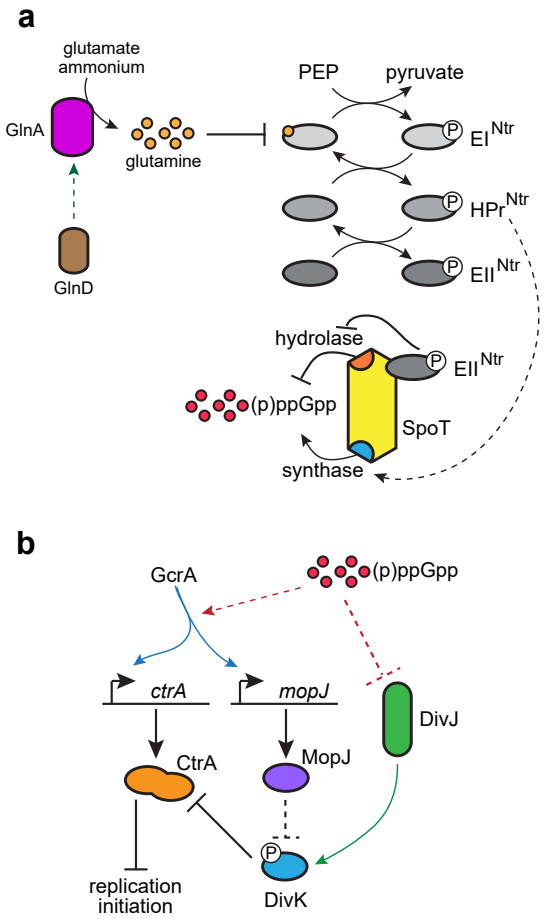

Figure 3. a, Ammonium limitation stimulates (p)ppGpp synthesis by SpoT via the PTSNtr system. Green dashed arrow, GlnD indirectly stimulates glnA transcription and GlnA activity; black bars, upstream element inhibits downstream element or process; black dashed arrow, HPrNtr stimulates the (p)ppGpp synthase activity of SpoT by an unknown, indirect mechanism. **b**, Proposed mechanisms linking (p)ppGpp to CtrA stabilization during ammonium limitation and/or prolonged stationary phase. Blue arrows, GcrA-activated transcription; green arrow, DivJ phosphorylates DivK; black bars, upstream element inhibits downstream element or process; dashed black bar, MopJ inhibits DivK~P activity by an unknown mechanism; dashed black arrow, MopJ stimulates CtrA activity indirectly via polar localization of DivL; dashed red arrow, (p)ppGpp stimulates GcrA-dependent transcription by an unknown mechanism; dashed red bar, (p)ppGpp inhibits polar localization of DivJ by an unknown mechanism.

Effects of (p)ppGpp in Caulobacter

(p)ppGpp appears to affect the function of the CckA-ChpT-CtrA phosphorelay in at least two ways, but no molecular mechanisms have yet been described. Mutants lacking either *ptsP* or *spoT* have reduced transcription of *ctrA* and *mopJ*, along with two additional targets of the transcriptional regulator GcrA (144). GcrA recognizes a specific, methylated DNA motif and binds to the σ^{70} subunit and RNAP core enzyme (118, 145). GcrA is normally essential for *Caulobacter* viability (146) , but a Δ*gcrA* mutation can be made in a strain that overproduces (p)ppGpp (118). Together, these results suggest that (p)ppGpp participates in the regulation of GcrA-dependent genes, possibly by binding directly to RNAP, or through an indirect mechanism (Fig. 3b). Binding of (p)ppGpp to *Caulobacter* RNAP has not yet been examined, but the amino acid residues that mediate (p)ppGpp binding in *E. coli* are conserved in the respective *Caulobacter* subunits (147, 148).

During abrupt nitrogen or carbon starvation (111, 133) or during glucose exhaustion (136, 149), CtrA is maintained at a moderate level, while DnaA levels fall dramatically. The maintenance of CtrA levels during glucose exhaustion requires SpoT (136, 149), and (p)ppGpp synthesis by RelA′ in well-fed cells is sufficient to decrease the rate of CtrA proteolysis (138). Together, these results indicate that CtrA is stabilized during nutrient limitation by a process that

requires (p)ppGpp. Although it is tempting to speculate that a (p)ppGpp-binding protein directly interferes with CtrA proteolysis, it is perhaps more likely that (p)ppGpp acts upstream in the regulatory network to maintain both CtrA phosphorylation and stability. In support of this idea, glucose exhaustion decreases the fraction of wild-type cells with a polar focus of DivJ, consistent with a delay in swarmer cell differentiation, but glucose exhaustion does not prevent DivJ localization in a Δ*spoT* mutant (136). Further, (p)ppGpp synthesis by RelA′ in well-fed cells delays the localization of DivJ and the delocalization of PleC in developing swarmer cells (138). These results suggest a model in which (p)ppGpp directly or indirectly inhibits the localization of DivJ at the developing flagellar pole, thereby blocking the increases in DivK~P, PleD~P, and cdG levels that would normally occur during differentiation (Fig. 3b). In consequence, CckA remains in kinase mode to activate and stabilize CtrA. If this model is correct, then CckA, CtrA, and CpdR should remain phosphorylated in starved cells, and further studies should reveal a factor involved in or upstream of DivJ localization (36-38) whose activity is sensitive to (p)ppGpp.

The DNA replication delay observed in starved *Caulobacter* cells could be attributed to CtrA blocking the initiation of chromosome replication, to the rapid clearance of the replication initiation protein DnaA, or to a combination of both. DnaA clearance during nitrogen or carbon starvation was initially attributed to an increase in the rate of DnaA proteolysis (111, 133). However, a subsequent study showed that, while Lon-mediated proteolysis is required to clear DnaA, the rate of DnaA degradation does not increase after exhaustion of the carbon source (149). Instead, the starvation-induced drop in DnaA abundance depends on reduced translation of the *dnaA* message, mediated by an element in its 5′ untranslated region (149). In another discrepancy, one study found SpoT necessary for DnaA clearance during carbon starvation (133), while a different study found that Δ*spoT* cells eliminate DnaA normally upon glucose exhaustion (149). Abrupt withdrawal of glucose from isolated swarmer cells (133) is not identical to the more gradual exhaustion of glucose by an unsynchronized population of cells (149), and it is possible that these subtle differences in experimental design are revealing important nuances in *Caulobacter* responses to nutrient stress.

Yet another similar stress is encountered when a batch culture growing exponentially in rich medium exhausts one or more nutrients, accumulates waste products, slows growth, and enters stationary phase. During the stationary phase transition in *Caulobacter*, CtrA is stabilized, and DnaA is eliminated through a decrease in translation (149). Interestingly, although the Δ*spoT* mutant properly modulates CtrA and DnaA levels during the initial transition into stationary phase (149), SpoT, PtsP, and MopJ are each required to maintain wild-type levels of CtrA after several hours in stationary phase (Fig. 3b) (70, 144). *Caulobacter* may therefore use distinct signaling pathways to modulate the cell cycle network in early and prolonged stationary phase. In addition, mutations that cause overproduction of (p)ppGpp increase the transcription of CtrA-dependent genes during prolonged stationary phase (144). This indicates that (p)ppGpp can upregulate both the abundance and activity of CtrA, in agreement with a model in which it impacts the cell cycle regulatory network at or upstream of CckA.

1.8 Oscillations in cellular redox status and their effects

Bacteria are well known to sense sharp changes in external redox-active compounds and mount appropriate responses to enhance survival (150). However, more subtle variations in intracellular redox conditions can also function as signals affecting developmental processes such as sporulation and biofilm formation (151). Here we consider current research into the possibility that variations in redox state regulate the *Caulobacter* cell cycle.

Using a derivative of GFP (roGFP2) whose fluorescence is modulated by an intramolecular disulfide bond (152, 153), Narayanan, et al. (154) were the first to observe cell cycle-dependent variation in the thiol-redox status of the bacterial cytoplasm. *Caulobacter* G1- and early S-phase cells are in a relatively reduced state, followed by a peak of oxidation during S-phase and a slow return to the reduced state in predivisional cells. The causes underlying the redox cycle are presently unknown, but one hypothesis is that increased activity of ribonucleotide reductase during S-phase could temporarily oxidize the cytoplasm, since this enzyme depends on reduced thiol carrier proteins for regeneration (151). To date, two systems have emerged as possible links between the cytoplasmic redox status and cell cycle progression.

Redox-sensitive NstA regulates topoisomerase IV

Topoisomerase IV (topo IV) is an essential enzyme responsible for decatenating linked circular chromosomes just prior to cell division (155). The small protein NstA binds to topo IV and inhibits its decatenating activity, and constitutive expression of NstA blocks *Caulobacter* chromosome segregation and cell division (154). The active form of NstA, a disulfide-linked dimer, is present during S-phase, when the cytoplasm is relatively oxidized, but is absent during G1-phase, when the cytoplasm is relatively reduced. Redox-sensitive disulfide bond formation may thereby limit the inhibitory activity of NstA to S-phase, which would release topo IV from inhibition when it is needed late in the cell cycle (156). It remains to be demonstrated, however, that the inhibitory NstA dimer is absent from late predivisional cells (154). The deletion of *nstA* causes no reported phenotypic consequences in *Caulobacter* (154), indicating either that a redundant mechanism inhibits topo IV activity in S-phase cells, or that temporary inhibition of topo IV is not critical for cell cycle progression in laboratory conditions.

NADH-producing and NADH-binding proteins regulate Z-ring assembly

The divisome is a potential target of the cytoplasmic redox state, because two modulators of the Z-ring, KidO and GdhZ, both interact with NAD(H) (120, 121). KidO is similar to NAD(P)H-dependent oxidoreductases and binds NAD(H), but it lacks critical catalytic residues (120). When bound to NADH, KidO inhibits Z-ring formation by preventing FtsZ filament bundling (121). GdhZ is an NAD-dependent glutamate dehydrogenase that oxidizes glutamate, yielding α-ketoglutarate and NADH (121). This reaction is required for the catabolism of specific amino acids, such as glutamate and glutamine, but not for the catabolism of sugars such as glucose and xylose (157). GdhZ stimulates the GTPase activity of FtsZ, which inhibits filament polymerization (121). GdhZ may also indirectly inhibit Z-ring formation by

colocalizing with KidO on Z-rings and providing the NADH cofactor for KidO activity (120, 121).

Because it is specifically the NADH-bound form of KidO that inhibits Z-rings, and because the cytoplasm is relatively reduced in swarmer and predivisional cells, an attractive hypothesis is that the ratio of NADH to NAD^+ in the cytoplasm controls KidO activity. However, if cytoplasmic redox status is involved, it is not the only regulator of KidO. As described above (section 1.6), KidO and GdhZ are both regulated by proteolysis, such that their levels are high in swarmer and late predivisional cells but low during S-phase (Fig. 2a). Expression of a stabilized variant of KidO during S-phase results in FtsZ mislocalization and cell elongation (120), indicating that the relatively oxidized state of the cytoplasm during S-phase is not sufficient to inhibit KidO activity and preserve Z-rings.

During growth on complex PYE medium, where GdhZ is necessary for the catabolism of amino acids (141), KidO and GdhZ interact with each other and with the Z-ring (120, 121). In contrast, GdhZ is delocalized from the Z-ring when glucose is added to the medium, suggesting that it doesn't regulate FtsZ in this growth condition (121). Mutants lacking either KidO or GdhZ have irregular cell sizes and altered Z-ring dynamics when grown in PYE medium, but addition of glucose to the medium suppresses these defects in the *ΔgdhZ* mutant (120, 121). Taken together, these results suggest that during growth on glucose, either GdhZ's direct inhibition of the Z-ring is unnecessary, or GdhZ is not an important source of the NADH cofactor for KidO, or both. Mutants in which the catalytic activity of GdhZ (producing NADH) is separated from its ability to stimulate the GTPase activity of FtsZ would help to distinguish between these models. Furthermore, the redox status of the *Caulobacter* cytoplasm may be different during growth on amino acids, which is unknown, than on glucose (154). If the cytoplasmic pool of NAD(H) is more reduced during growth on glucose than on amino acids, then KidO may be able to obtain NADH and regulate Z-ring assembly without the need for GdhZ. It is also possible, however, that an unknown division regulator cooperates with KidO during growth on glucose.

1.9 Outlook

Although the *Caulobacter* cell cycle signaling machinery has been intensively studied, fundamental questions continue to arise. Several non-canonical interactions between two-component proteins have been uncovered in the *Caulobacter* cell cycle network, and we expect that future work will continue to describe the molecular details of signal transduction in these novel systems. *Caulobacter* was one of the first bacteria in which signaling proteins, proteases, and proteolytic adaptors were found to be dynamically, subcellularly localized. We expect that future studies in *Caulobacter* will continue to tackle the challenging problems of observing and explaining at a molecular level cases where a protein performs distinct activities in different subcellular locations. Studies of cdG-dependent processes in *Caulobacter* have revealed new classes of proteins that bind cdG, and additional effector proteins are likely to be discovered during efforts to link cdG to stalk and pilus biosynthesis. Studies in other systems suggest that protein-protein interactions between a DGC or PDE enzyme and a cdG-dependent effector can

generate spatially regulated signals, where the cdG produced (or degraded) by an enzyme only affects one or a small number of cellular processes (158, 159). Such regulatory mechanisms may underlie the specific effects of particular DGC enzymes on cell motility and attachment (44) or the flagellar-pole specific protection of CckA from cdG (48). With respect to proteolysis, we expect that additional recognition mechanisms and adaptor proteins will be discovered that target substrates to proteases other than ClpXP. It will also be important to reconcile *in vitro* and *in vivo* approaches to determine how substrates that are degraded in an unregulated manner *in vitro* are proteolyzed under rigorous cell cycle control *in vivo*. Finally, although the unstressed, exponential-phase cell cycle has been the main focus of the field in the past, there is now keen interest in understanding exactly how (p)ppGpp modulates the cell cycle network during nutrient stress and stationary phase.

Chapter 2

Temporal degradation of the master transcriptional regulator CtrA requires a ClpXP-associated complex

2.1 Introduction

Regulated proteolysis is crucial in coordinating diverse cellular processes across all domains of life. Misfolded or truncated proteins may interfere with essential cellular functions and are actively cleared by targeting them for degradation. Additionally, many responses to internal and external signals rely on regulated proteolysis of key components. For instance, the heat shock response in *Escherichia coli* requires stabilization of σ^{32}, which is constitutively synthesized and degraded under normal conditions (160). Eukaryotic cell cycle progression relies on regulated proteolysis of a class of proteins known as cyclins, which accumulate during G2 to permit entry into mitosis and which are subsequently degraded to commit cells to this stage (161). Proteolysis represents an irreversible and robust response, and therefore must be carefully regulated to prevent indiscriminate protein degradation.

Caulobacter crescentus is an alphaproteobacterium that provides an excellent model system to study regulated proteolysis in the coordination of cell cycle events. Each *Caulobacter* division yields a motile, flagellated swarmer cell and a sessile stalked cell, the latter of which adheres to surfaces via the holdfast, an adhesive extracellular polysaccharide located at the distal end of the stalk (162). The swarmer cells must transition to stalked cells before undergoing division, and this process is facilitated by the coordinated activity of an assortment of non-canonical two-component proteins and a ClpXP-based proteolytic complex (1, 163). The morphology and cell cycle of *Caulobacter* is well-adapted to its lifestyle in primarily oligotrophic, freshwater streams. The characteristic curvature of *Caulobacter* is imparted by the intermediate filament-like crescentin, which associates with the membrane on the concave side of the cell and is thought to locally decrease the rate of nascent peptidoglycan (PG) synthesis (164, 165). Curvature would thus follow by allowing PG synthesis to proceed at a higher rate on the convex side of the cell. Stalked cells attached to surfaces in a constantly-flowing environment are oriented via curvature to deposit daughter cells near the downstream surface, allowing greater local colonization (166). Nutrient scarcity results in a cell cycle block at the swarmer phase, biasing daughter cells to seek out and colonize more nutrient-rich locales (134, 167).

Central to the progression of the *Caulobacter* cell cycle is the temporal activation and deactivation of the essential protein CtrA, a two-domain response regulator with an N-terminal receiver domain and a C-terminal DNA binding domain (14, 24, 168, 169). CtrA

transcriptionally regulates about 100 genes required for cell division, DNA methylation, and polar development, while also binding to sites in the chromosomal origin of replication (*Cori*) to prevent the initiation of DNA replication (21, 23, 170) . Active, phosphorylated CtrA binds to its consensus sites TTAA-N7-TTAA in *Cori* in both swarmer and late predivisional cells to prevent the initiation of DNA replication (14, 23). CtrA activity is controlled by two redundant mechanisms: phosphorylation and proteolysis. The phosphorylation state of CtrA is directly regulated by the reversible action of the CckA/ChpT phosphorelay (15, 16, 18, 25). During the swarmer-to-stalked cell transition, CtrA is both desphosphorylated and degraded to permit DNA replication (24, 30). CtrA is resynthesized and phosphorylated in early predivisional cells for the activation of target genes to resume growth and prepare for division (14, 21, 24).

The AAA+ protease ClpXP is responsible for degrading CtrA at appropriate times in the cell cycle (30, 171). CtrA proteolysis is accomplished with the help of three proteins—CpdR, RcdA, and PopA—collectively referred to as the "accessory factors" (17, 31, 32). The accessory factors form a complex with CtrA and ClpXP *in vivo* (17, 31, 32). CpdR is a single-domain response regulator that, when phosphorylated, is incompetent to stimulate CtrA proteolysis (17). Phosphorylation of CpdR occurs via the same CckA/ChpT phosphorelay that mediates CtrA phosphorylation, and dephosphorylation of both CpdR and CtrA is thought to occur when this phosphorelay reverses (16). Thus, CckA/ChpT would ensure CtrA inactivation both by directly dephosphorylating CtrA and by indirectly stimulating its proteolysis via CpdR. CtrA degradation also depends on PopA binding to the bacterial second messenger cyclic diguanylate (cdG) (32). cdG levels are low in swarmer cells but increase during the swarmer-to-stalked cell transition by two cellular events: degradation of a cdG hydrolyzing enzyme, PdeA, and activation of the diguanylate cyclase (DGC) PleD, which synthesizes cdG from two molecules of GTP (45-47). PleD DGC activity resides in an active site in its GGDEF domain which is regulated by a negative feedback loop involving cdG binding to a separate allosteric site, also within the GGDEF domain (45, 172, 173). PopA is a paralog of PleD with a conserved allosteric site but degenerate active site, and thus cannot synthesize cdG (32). PopA stimulation of CtrA proteolysis depends on cdG binding to its allosteric site. RcdA's precise function cannot be predicted from its amino acid sequence or structure (174).

ClpXP alone readily degrades CtrA *in vitro* with ATP (171), so the biochemical functions of the accessory factors have thus far been a mystery. Insight into the mechanism of CtrA proteolysis may be informed by studies of other well-characterized ClpXP substrates. ClpXP consists of a ClpX hexamer ($ClpX_6$) that gates entry of proteins to a proteolytic chamber formed by two stacked ClpP heptamers (175, 176). Substrates are unfolded as ClpX ATPase activity drives peptide translocation through a central pore in $ClpX_6$ to the ClpP cavity (84, 177-179) . Many proteolytic mechanisms employ so-called "adaptor proteins" that tether the substrate to the protease, effectively increasing local substrate concentration (160). Some adaptor proteins bind to the N-terminal zinc-binding domain (ZBD) of ClpX that resides on the periphery of the hexamer (180, 181). The extensively-studied *E. coli* ssrA tag targets truncated proteins to ClpXP for degradation, a process which is sped up by the adaptor SspB (80, 81, 85, 86). Incomplete peptide chains at stalled ribosomes are released by addition of an eleven amino acid ssrA tag to the C-terminus (79). The attached ssrA tag has two conserved C-terminal alanine residues (A10 and A11) that are critical for making initial contacts with the $ClpX_6$ pore, and mutations A10D or A11D in ssrA abolish recognition by $ClpX_6$ (82, 84). Significantly, the C-terminus of CtrA also

consists of two adjacent alanines, and mutation of these to aspartates (CtrA-DD) abolishes degradation by ClpXP (24). Like CtrA, ssrA-tagged substrates can be degraded by ClpXP alone (*i.e.* without SspB) (80). The accessory factors may be functioning as an adaptor to bring CtrA to ClpXP for degradation.

Considering that ClpXP rapidly degrades CtrA *in vitro* in the absence of the accessory factors, and that ClpXP is present throughout the cell cycle, it is unclear what prevents CtrA proteolysis in swarmer and early predivisional cells. DNA binding prevents CtrA proteolysis by ClpX *in vitro* (95), but this cannot solely account for the lack of degradation *in vivo*, as there are an estimated 9,000 molecules of CtrA in *Caulobacter* swarmer cells (182) but only about 400 putative CtrA binding sites on the chromosome (21). Furthermore, a CtrA mutant lacking the DNA-binding domain but retaining 15 C-terminal amino acids for ClpX recognition (CtrA-RD+15), appears to be stable in swarmer cells and late predivisional cells (99). SciP, a swarmer cell-specific protein that forms a ternary complex with DNA-bound CtrA to prevent activation of specific genes, enhances the binding of CtrA to DNA in EMSA experiments (183, 184), but the contribution of SciP to CtrA stability *in vivo* has not been determined.

Here, we analyze direct pairwise interactions between a set of accessory factors using an *in vitro* pulldown system to help determine the role and structural makeup of a putative ClpXP-degradation machine. Additionally, we asses the contribution of DNA-binding to CtrA stability *in vivo* by comparing the rate of degradation of CtrA RD+15 to full-length CtrA in cells in which regulated CtrA proteolysis has been inactivated. Finally, although CtrA has been shown to be protected from degradation in swarmer cells, we assess the stability of newly-synthesized CtrA in predivisional cells to confirm that the perceived stability is not due to *de novo* synthesis outpacing proteolysis.

2.2 Methods

Bacterial Strains, Plasmids, and Culture Conditions. Table 1 lists the strains and plasmids used in this work. All experiments were performed with derivatives of *Caulobacter crescentus* strain CB15N (185) grown to midexponential phase. Plasmids were mobilized from *Escherichia coli* to *C. crescentus* by conjugation using *E. coli* strain S17-1 (141). CB15N strains were grown in peptone yeast extract (PYE) medium or minimal glucose (M2G) medium at 30 °C (2). Where indicated, growth media were supplemented with glucose (0.02%) or xylose (0.03%) to repress or induce, respectively, expression from the *xylX* promoter (186). *E. coli* cloning strains were grown in Luria broth at 37 °C, and solid and liquid media were supplemented with antibiotics as described (41). PCR products were cloned into the pGEMT-Easy vector (Promega) and sequenced before being subcloned into destination vectors. Site-directed mutagenesis was performed by using the QuikChange protocol (Stratagene). Sequences of primers used for amplification or sequence modification are available upon request.

Protein Purification. The proteins His_6-CtrA, His_6-CtrA3, His_6-CtrA-DD, His_6-RcdA, His_6-PopA, and His_6-EnvZ HK were expressed from the pET vectors indicated in Table 2. All proteins were overexpressed in *E. coli* Tuner cells grown to an OD600 = 0.6 at 37°C in Terrific

Broth (187). Isopropylthiogalatoside was added to a final concentration of 0.4 mM, and cells were incubated overnight at 18 °C. Cells were harvested by centrifugation at 6,000 × g for 5 min, and pellets were frozen in liquid nitrogen and stored at -80 °C until use. Proteins were purified by the following protocol with modifications where indicated. Cell pellets were thawed and resuspended in Standard Lysis Buffer (SLB; 50 mM Tris-HCl, pH 8.2, 100 mM KCl, 1 mM $MgCl_2$, 10% glycerol, 2 mM 2-mercaptoethanol). CtrA variants were purified by using SLB containing only 50 mM KCl and no $MgCl_2$. Cells were lysed by 1 hr treatment with 1 mg/mL lysozyme and 40 units of Benzonase nuclease (Novagen) on ice, followed by sonication. Lysates were cleared by three rounds of centrifugation at 20,000 × g. Imidazole was added to a concentration of 15 mM, and cleared lysates were incubated with 1 mL of Ni-nitrilotriacetic acid (Ni-NTA) agarose (Qiagen) that had been pre-equilibrated with the lysis buffer specific for the protein to be purified. The agarose was applied to a gravity column and washed three times with the appropriate lysis buffer. In all cases, the second of the three washes was supplemented with 300 mM NaCl to remove nonspecifically bound proteins.

Unless otherwise indicated, the desired protein was eluted from Ni-NTA agarose by using the appropriate lysis buffer supplemented with 300 mM imidazole. RcdA was removed from Ni-NTA by overnight cleavage with 20 units of thrombin (EMD/Novagen). All proteins were further purified by ion-exchange chromatography using HiTrap Q HP columns (GE). Elution was achieved with a gradient of increasing KCl concentration in SLB supplemented with 1 mM DTT. All proteins were exchanged into PD buffer [25 mM Hepes–KOH, pH 7.6, 5 mM $MgCl_2$, 15 mM NaCl, 10% (vol/vol) glycerol] supplemented with 100 mM KCl and 1 mM DTT before freezing in liquid nitrogen and storage at –80 °C.

CtrA Clearance in Mixed Culture. Strains KR3596, KR3656, and KR3601, which are Δ*popA* with a plasmid-encoded, xylose-inducible copy of N-terminally YFP-fused CtrA RD+15, CtrA, or CtrA RD+15-DD, or their Δ*rcdA* counterparts, KR903, KR3594, or KR3599, were grown in PYE with either kanamycin or oxytetracycline. Log phase cells were diluted to OD660 = 0.2 in the same medium, induced with 0.03% xylose, and allowed to grow for three hours. Cells were spun down, washed twice with M2 salts, and released into PYE with 0.02% dextrose with either kanamycin or oxytetracycline at an OD660 of 0.05. Timepoints were taken every 30 minutes by removing 1 mL of cells, spinning down, removing the supernatant, and freezing immediately in liquid nitrogen. Samples were normalized by volume and analyzed by SDS/PAGE and Western blotting with α-GFP Living Colors A.v. Monoclonal Antibody (JL-8) (Clontech) (1:5,000). Bands were quanitified as amount remaining compared to timepoint = 0 minutes using Image Lab (Bio-rad).

Coaffinity Purification. His_6-CtrA, His_6-CtrA3, His_6-CtrA-DD, His_6-PopA, and His_6-EnvZ-HK (0.5 mL at 1.8 μM protein) were incubated with 20 μL of Ni–nitrilotriacetic acid (Ni-NTA) agarose beads (Qiagen) at 4 °C for 1 h in PD buffer/10 mM imidazole/30 mM KCl. After washing with 0.5 mL of PD buffer/10 mM imidazole, resin was resuspended using 0.25 mL of PD buffer/25 mM imidazole/30 mM KCl containing 0.6 μM prey protein. Assays included 20 μM cdG where indicated. After incubating 1 h, the beads were washed with PD buffer/25 mM imidazole supplemented with 20 μM cdG, if it was present in the binding stage. Bound proteins were eluted with PD buffer/500 mM imidazole. Eluted proteins were analyzed by SDS/PAGE and staining with Lumitein fluorescent protein dye (Biotium).

CtrA Degradation Rates in Swarmer and Predivisional Cells. Swarmer cells of wild-type *Caulobacter* NA1000 were harvested and released into M2G at OD660 = 0.3 as described previously (14). 10 μCi/mL of [35S]methionine was added at either 10 min for swarmer cells or 85 minutes for predivisional cells. After 5 minutes, cells were chased with 1 mM unlabeled methionine and 0.3% casamino acids. 1 mL of culture was removed at 5 minute intervals starting immediately after chasing. Samples were spun down and the supernatant was removed before freezing in liquid nitrogen. Cells were thawed, resuspended in 50 μL of SDS buffer (10mM Tris pH 8.2, 1% SDS, 1mM EDTA), and boiled for 2 minutes. 800 μL of chilled IP Wash Buffer (50mM Tris pH 8.2, 150mM NaCl, 0.5% Triton X-100) was added, followed by 25 μL of Pansorbin that had been washed with IP Wash Buffer. Samples were inverted and incubated on ice for 10 minutes. Samples were gently spun down for 2 minutes, and the supernatant was transferred to fresh tubes. 1.5 μL of CtrA antiserum (14) was added to each tube, and samples were rocked on a nutator for 2 hours at 4°C. The entire sample volume was transferred to fresh tubes containing 30 μL of washed Protein A Agarose Beads (Cell Signaling Technology) and rocked on a nutator for an additional 1 hours at 4°C. Samples were gently spun down and washed 3x with IP Wash Buffer. The supernatant was removed, 15 μL of 2x SDS-loading buffer was added to the beads, and samples were boiled for 5 minutes. Samples were run on 12% polyacrylamide gels and imaged using a Typhoon phosphorimager. Bands were quanitifed using ImageJ.

Table 1. Strains used in this study

Strain Number	Description	Reference
KR4000	Wild-type Caulobacter NA1000/CB15N	(185)
KR3596	Δ*popA::tetAR* pAK08	This study
KR3656	Δ*popA::tetAR* pKW1	This study
KR3601	Δ*popA::tetAR* pKR166A	This study
KR3594	Δ*rcdA::hyg* pKR173	This study
KR903	Δ*rcdA::hyg* pEJ146	This study
KR3599	Δ*rcdA::hyg* pKR166A	This study

Table 2. Plasmids used in this study

Plasmid	Description	Reference
pMR10	Broad-host-range, low-copy vector, kan^R	(188)
pMR20	Broad-host-range, low-copy vector, tet^R	(188)
pJT31	pET28a-His_6-PopA	This study
pES53	pET28a-His_6-RcdA	(174)
pES118	pET28a-His_6-EnvZ HK	This study
pSS39	pET33b-His_6-CtrA	This study
pSS44	pET33b-His_6-CtrA-DD	This study
pKZ13b	pET42-His_6-CtrA3	This study
pAK08	pMR10-Pxyl-YFP-CtrA RD+15	This study
pKW1	pMR10-Pxyl-YFP-CtrA	This study

pKR166A	pMR10-Pxyl-YFP-RD+15-DD	This study
pKR173	pMR20-Pxyl-YFP-CtrA	This study
pEJ146	pMR10-Pxyl-YFP-RD+15	This study

2.3 Results

PopA directly interacts with both CtrA and RcdA

Temporal requlation of CtrA proteolysis requires two signals encoded within the CtrA polypeptide. The first signal comprises two alanine residues at the C-terminus, analogous to those of the ssrA peptide, which are recognized by the $ClpX_6$ central pore. The second signal resides in the first 56 amino acids of the CtrA receiver domain. Since *rcdA* and *cpdR* are required for temporally-regulated proteolysis of CtrA, α-proteobacteria with homologs of these genes should contain co-conserved residues in the CtrA receiver domain that are required for its degradation. Aligning 26 CtrA protein sequences from various α-proteobacteria grouped by the presence or absence of *rcdA* and *cpdR* allowed us to identify candidate residues which were subsequently mapped onto a model of the CtrA receiver domained based off of another response regulator, Spo0F (Fig. 4a, b; Protein Data Bank ID code 1NAT; (189)). Six residues were predicted to lie on the exposed surface of the first alpha-helix (α1) of CtrA, and we determined that substitution of three of these residues (A11T, Q14K, and K21A) yielded a CtrA variant (CtrA3) that was both functional and degraded more slowly that wild-type CtrA *in vivo* (data not shown, (28)).

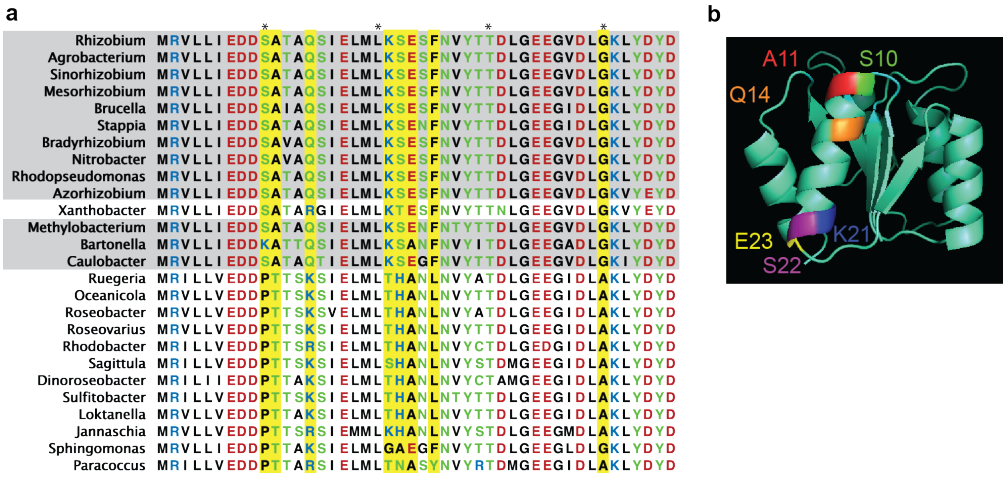

Figure 4: Residues in α1 of the CtrA receiver domain are needed for efficient proteolysis. a, Bioinformatic search for the receiver domain degradation signal in CtrA. Amino-terminal regions of CtrA receiver domains from each of 26 genera in the α-proteobacteria were aligned by using Clustal Omega. Organisms whose genomes encode homologs of RcdA and CpdR are shaded light gray, and organisms whose genomes lack these genes are unshaded. CtrA residues highly conserved in bacteria with homologs of *rcdA* and *cpdR*, but divergent in species lacking these genes, are highlighted in yellow. Asterisks mark intervals of 10 residues. Species and National Center for Biotechnology Information genome accession numbers associated with the CtrA receiver domain sequences can be found in Appendix Table 1. **b**, Model of the CtrA receiver domain highlighting surface-exposed residues that co-occur in α-proteobacterial genomes with *rcdA* and *cpdR*.

The accessory factors are part of a complex that includes ClpXP and CtrA, but the nature of their interactions and their ability to facilitate CtrA proteolysis remains undetermined. We sought to dissect binary interactions between various combinations of proteins in this complex. Bacterial two-hybrid (BACTH) studies have demonstrated a direct interaction between PopA and RcdA and between CpdR and ClpX (32, 47), but no studies have demonstrated a direct interaction between CtrA and any of these other proteins. It is assumed, however, that ClpX must interact with CtrA, because ClpXP alone can degrade CtrA.

We performed coaffinity purification assays using His_6-tagged CtrA variants to identify a member of the putative proteolytic complex that directly recognizes CtrA. His_6-CtrA3 contains the A11T, Q14K, and K21A substitutions, whereas His_6-CtrA-DD replaces the two alanines at the C terminus of CtrA with aspartic acids, resulting in a nondegradable protein (24). We used the unrelated His_6-tagged EnvZ histidine kinase domain (EnvZ HK) as a negative control bait protein. PopA bound directly to His_6-CtrA and His_6-CtrA-DD, but only in the presence of cdG. In contrast, His_6-CtrA3 bound PopA poorly with background levels similar to His_6-EnvZ HK, even when cdG was included (Fig. 5a). Using His_6-PopA or -EnvZ HK as bait, we confirmed that RcdA and PopA interact directly (32), but this interaction was independent of cdG (Fig. 5b). These results suggest that efficient proteolysis of CtrA by ClpXP during the swarmer-to-stalked cell transition, when cdG levels rise, requires a direct interaction of CtrA through α1 to cdG-bound PopA, and that RcdA may directly affect the localization or activity of PopA to facilitate this process.

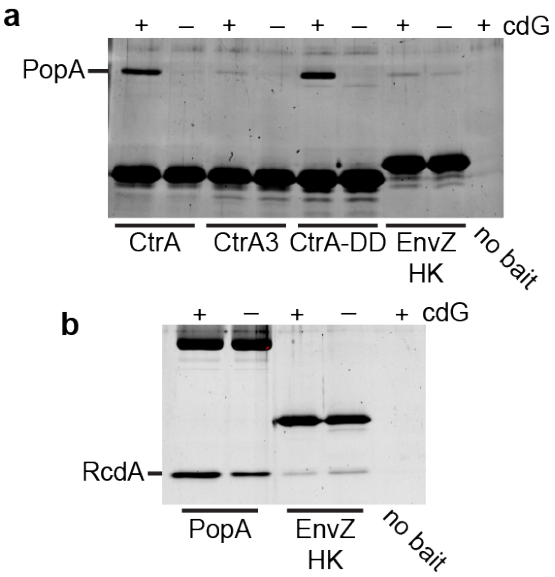

Figure 5: Direct interactions between CtrA, PopA, and RcdA. a, His_6-tagged bait proteins were incubated with Ni-NTA resin, PopA, and 20 μM cdG where indicated. Stable complexes were eluted and analyzed by SDS/PAGE and Lumitein staining. **b**, The indicated His_6-tagged bait proteins (PopA and EnvZ HK) were incubated with Ni-NTA resin, RcdA, and 20 μM cdG where indicated. Protein complexes were visualized as in *A*.

DNA-binding does not significantly protect CtrA from degradation in vivo

Since DNA-binding inhibits CtrA degradation by ClpXP *in vitro* (95), we decided to assess the physiological significance of this phenomenon to protecting CtrA from degradation during inappropriate intervals. We used the truncated CtrA variant RD+15, which is degraded with the cell cycle (99) but unable to bind DNA due to the absence of the DNA-binding domain,

and compared the degradation rate to wild-type CtrA in whole cells after inducing their expression using a xylose-driven promoter for three hours. CtrA synthesis was inhibited by removing xylose and incubating with dextrose, and the rate of clearance was measured by Western blot. These experiments were performed in either a Δ*rcdA* or Δ*popA* background to prevent regulated proteolysis from obscuring an unassisted basal rate of degradation by ClpXP (31, 32). We observed a negligible difference in the rate of clearance of CtrA and RD+15 in Δ*rcdA* cells, and a slight increase in the stability of full-length CtrA compared to RD+15 in Δ*popA* cells. Neither CtrA or RD+15 was as stable as the non-degradable variant CtrA-DD (24), which remained completely stable after 5 hours. These results demonstrate that DNA-binding, in the absence of regulated CtrA proteolysis, does not fully contribute to the stability of CtrA to levels expected of a non-degradable variant.

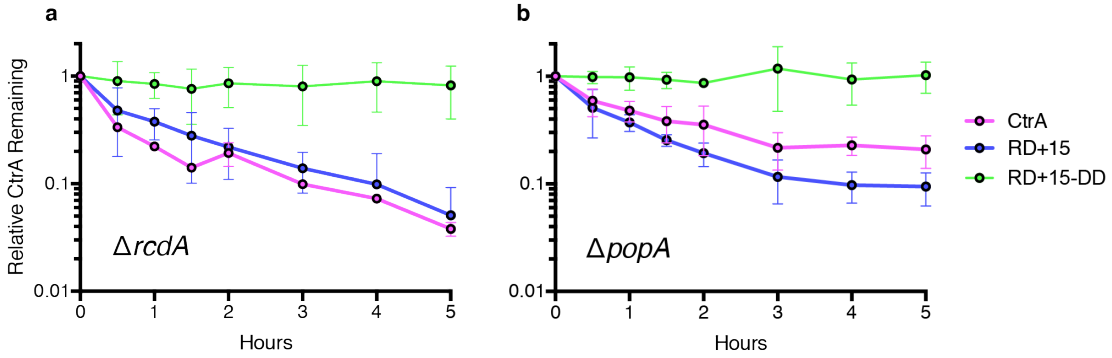

Figure 6: Contribution of DNA-binding activity to CtrA stability *in vivo*. Graphs showing the relative amount of CtrA variants remaining after five hours post-induction in either **a**, Δ*rcdA* or **b**, Δ*popA* mutants (mean ± s.d., N=3). CtrA variants were plasmid-encoded and under control of a xylose-driven promoter. Cells were grown in PYE with either kanamycin or oxytetracycline, and synthesis of plasmid-borne CtrA variants was induced for 3 hours with 0.03% xylose in log phase. Cells were washed 2x with M2 salts, then released into PYE with antibiotic and 0.02% dextrose. Samples were collected for Western blot analysis at the indicated timepoints.

CtrA is protected from degradation by ClpXP in early predivisional cells

ClpXP can degrade CtrA *in vitro* at a rate that rivals its rate of clearance during the swarmer-to-stalked cell transition (171). In swarmer cells, CtrA remains stable despite the presence of ClpXP (24, 30), indicating that it is protected from degradation via an undetermined mechanism. After accessory factor-stimulated degradation at the swarmer-to-stalked cell transition (17, 31, 32), CtrA is rapidly resynthesized in predivisional cells (24). While CtrA is required to continue cell cycle progression at this stage (21), it is unknown if CtrA is similarly protected from degradation in early predivisional cells. CtrA synthesis could outpace proteolysis, resulting in sufficient CtrA activity for continuation of the cell cycle before its stabilization in swarmer cells after division. We decided to assess the stability of CtrA synthesized *de novo* in early predivisional cells.

CtrA is degraded during the swarmer-to-stalked cell transition at around 15 minutes in synchronized swamer cells, and is resynthesized at around 80 minutes when grown in M2G (24). We synchronized wild-type cells and pulse-chased with [35S]methionine after either 10 minutes

(for the swarmer-to-stalked cell transition) or 85 minutes (for predivisional cells). CtrA was rapidly cleared during the swarmer-to-stalked cell transition, but remained completely stable in predivisional cells until at least 125 minutes post-synchrony, demonstrating that CtrA is protected from degradation by ClpXP in predivisional cells.

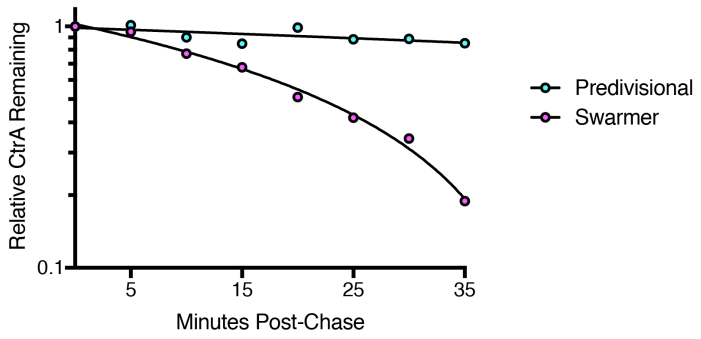

Figure 7: *de novo*-synthesized CtrA is not degraded in predivisional cells. Graphs showing the relative amount of [35S]-labeled CtrA remaining after pulse-chasing with [35S]methionine in either swarmer or predivisional cells. Cells were synchronized, released into M2G, and allowed to proceed through the cell cycle. [35S]methionine was added at either 10 minutes for swarmer cells, or 85 minutes for predivisional cells, and chased with unlabled methionine after 5 minutes. Samples were taken and immediately frozen at the indicated timepoints. CtrA was immunoprecipitated for each sample, run on polyacrylamide gels, and imaged using a phosphorimager. Data points were fitted with a line of best fit (N=1).

Recent Developments

The field encompassing CtrA proteolysis has seen significant advances in the years since this work was performed. Here, we will highlight the current literature regarding the interactions of the accessory factors with CtrA and ClpXP, the mechanism of action catalyzing CtrA degradation, and the subcellular localization of this hierachial adaptor-mediated proteolytic complex.

CtrA activity must be curbed during the swarmer-to-stalked cell transition and in the stalked compartment of late predivisional cells to permit the initiation of DNA replication (23). This is accomplished through the coordinated dephosphorylation and proteolysis of CtrA at the indicated cell cycle intervals. The mechanisms controlling CtrA phosphorylation are described in chapter 1. CtrA is degraded by the ClpXP protease via a hierarchial adaptor complex (28, 101) which is composed of three proteins: (i) the single-domain response regulator CpdR (16, 17), (ii) the tethering protein RcdA (31), and (iii) the hybrid response regulator-DGC PopA (32). CpdR is phosphorylated on Asp51 by the CckA-ChpT phosphorelay, but only the unphosphorylated form is competent for CtrA degradation (16, 17). PopA is inactive as a DGC, but binding of cdG to its allosteric "I-site" is required for its function as proteolytic adaptor (32). Efficient, timed degradation of CtrA *in vivo* absolutely requires the presence and activation of these three proteins, and while none is essential for viability, the omission of any single adaptor component prevents CtrA proteolysis *in vivo* (17, 31, 32).

Based on these *in vivo* findings, it was at first surprising that CtrA could be degraded by ClpXP with ATP *in vitro* in the absence of any other factors (171). The half-life of degradation was estimated at around five minutes, a rate consistent with its clearance during the SW-ST transition (24, 171). *In vitro* reconstitution experiments revealed that the adaptor proteins work together to stimulate CtrA proteolysis beyond the unassisted rate. Addition of unphosphorylated CpdR, RcdA, PopA, and cdG to reactions with ClpXP, CtrA, and ATP reduce the K_m of proteolysis 10-fold, while having a negligible effect on v_{max} (28). Absence of any component of the adaptor complex results in a failure to stimulate CtrA proteolysis beyond the basal rate, indicating a unique and essential role for each component.

Further studies have dissected the roles of individual proteins within the adaptor complex. Using ClpXP substrates that depend on CpdR for degradation, but not on RcdA or PopA, it was shown that CpdR binds directly to NTD_{ClpX} to prime the unfoldase for engagement with substrates (Fig. 2c) (27). Interaction with CpdR creates a unique ClpX recruitment interface upon which CpdR-dependent substrates or additional adaptors bind (27). Although CpdR does not interact independently with substrates, it may form part of the primed interface on ClpX where substrates are recognized (27, 101). This mechanism serves *in vivo* to limit the degradation of selected proteins to times when CpdR is dephosphorylated.

Priming of ClpX by CpdR is required for the subsequent binding of the adaptor component RcdA (101). All of the *Caulobacter* ClpXP substrates known to require RcdA also need CpdR, but only some substrates additionally require PopA (101). Similar to SspB, RcdA contains an N-terminal dimerization domain and a disordered C-terminal peptide (174). The N-terminal domain of RcdA is thought to bind directly to proteolytic substrates, though this awaits experimental confirmation. Studies in which the C-terminal peptides of SspB and RcdA were exchanged demonstrated that the C-terminus of RcdA interacts with ClpX in a CpdR-dependent manner (101). Both interactions are required for the degradation of RcdA-dependent substrates, suggesting that RcdA can work as a tether, analogous to the function of SspB in the degradation of ssrA-tagged substrates (Fig. 2d).

The final protein in the hierarchical adaptor complex is PopA, which contains two tandem receiver domains followed by a catalytically inactive DGC domain which binds cdG. The N-terminal receiver domain interacts directly with RcdA independent of cdG binding, but only cdG-bound PopA is competent to bind CtrA for delivery to ClpXP (Fig. 2d) (28, 190). The α1 helix of the CtrA receiver domain contains three amino acids that are critical for the interaction with PopA, but the region of PopA that recognizes CtrA has not been defined (28). Because CtrA is both an inhibitor of chromosome replication and an essential transcription factor, its proteolysis must be strictly regulated. The requirement for unphosphorylated CpdR and the cdG-dependency of the PopA-CtrA interaction together ensure that CtrA is only degraded *in vivo* prior to chromosome replication, when the CckA-ChpT pathway is in phosphatase mode and when cdG levels simultaneously rise (Fig. 2e).

Despite progress in understanding the adaptor complex mechanism, there is a persistent discontinuity between *in vitro* and *in vivo* studies of CtrA proteolysis. CtrA can be degraded *in vitro* by ClpXP and ATP without the addition of any other factors (171), and ClpXP is present throughout the *Caulobacter* cell cycle (30), yet pulse-chase assays indicate that CtrA is very

stable outside of the short window preceding chromosome replication (24). Why does unassisted ClpXP not proteolyze CtrA at other times during the cell cycle? One factor able to protect CtrA is the transcriptional co-regulatory protein SciP. SciP synthesis begins in late PD cells and accumulates to peak levels in SW cells, where it forms a ternary complex with CtrA and DNA at CtrA-binding sequences (183, 184). Most CtrA-activated genes are expressed during the predivisional stage of the cell cycle (21), and SciP prevents inappropriate expression of these genes in swarmer cells by blocking the recruitment of RNA polymerase (RNAP) to the ternary complex (95). Importantly, SciP increases the affinity of CtrA for its DNA binding sites, helping to protect CtrA from degradation by unassisted ClpXP *in vitro* (95).

Although SciP and DNA stabilize CtrA *in vitro*, their contribution to CtrA stability *in vivo* is unclear. The half-life of CtrA is increased when SciP is overexpressed (183, 184), but the stability of CtrA is unchanged in a Δ*sciP* mutant (183). Issues of stoichiometry also limit the number of CtrA molecules that could be protected within CtrA-SciP-DNA complexes. Each *Caulobacter* swarmer cell contains ~9,500 molecules of CtrA (182), but the chromosome has only ~100 CtrA-dependent promoters (21). Even if each promoter bound several CtrA monomers, most CtrA molecules should be excluded from the protective effect of the CtrA-SciP-DNA ternary complex. Finally, because SciP is absent from early predivsional cells (183, 184), a separate protective mechanism for CtrA would be needed at this stage of the cell cycle.

In addition to temporal changes in activity, the CtrA proteolytic complex also dynamically localizes to specific sites within the cell. CtrA, ClpXP, RcdA, CpdR, and PopA are each transiently located at the incipient stalked pole during the swarmer cell development and at the stalked pole in late predivsional cells (17, 31, 32, 99). The polar organizing factor PopZ, unphosphorylated CpdR, and cdG binding to PopA are all necessary for localization of the protease, adaptor complex, and substrate (17, 32, 191). It was originally hypothesized that co-localization of the components, as detected by fluorescence microscopy, was critical for CtrA degradation. However, the *in vitro* experiments outlined above showed that the adaptor proteins have mechanistic roles beyond substrate localization. Moreover, amino acid substitutions in RcdA were found that prevent its own polar accumulation and that of CtrA, but still support CtrA proteolysis at wild-type rates (174). It may be that proteases and adaptor complexes are located at particular positions chiefly to degrade substrates that are immobilized in large complexes, such as the chemoreceptor array found at the flagellar pole (192-194).

Chapter 3

An essential tyrosine phosphatase homolog is required for lipopolysaccharide biosynthesis in *Caulobacter crescentus*

3.1 Introduction

Gram-negative bacteria are enclosed in a three-layer envelope, composed of the inner or cytoplasmic membrane (IM), a thin layer of peptidoglycan (PG), and an outer membrane (OM). The OM is a protective barrier that is inherently less permeable than the IM to lipophilic compounds (195). This property is conferred by lipopolysaccharide (LPS), a molecule found exclusively in the outer leaflet of the OM. The canonical LPS structure, first described in *Escherichia coli*, consists of three segments: 1) lipid A, a hexa-acylated, phosphorylated glucosamine disaccharide; 2) a core oligosaccharide; and 3) a large polymeric polysaccharide (O-antigen). Phosphates at the 1- and 4'- positions of lipid A are bridged by divalent cations, such as Ca^{2+}, and contribute, along with the hydrophilic sugars and saturated acyl chains, to the barrier function of the OM (195).

LPS biosynthetic and export pathways are best characterized in *E. coli*. The lipid A moiety is synthesized at the cytoplasmic face of the IM via the Raetz pathway (Fig. 8a), comprising nine conserved enzymes (196). The core oligosaccharide is assembled upon lipid A, and the completed lipid A-core is flipped to the periplasmic face of the IM by the flippase MsbA. The O-antigen is synthesized independently upon the lipid carrier undecaprenol phosphate (Und-P) at the cytoplasmic face of the IM, producing oligomeric repeat units that are exported to the periplasm, polymerized to generate the O-antigen, and ligated to the core. The mature LPS (smooth LPS or S-LPS) is shuttled to the OM via the Lpt export system (197). The lipid A portion of LPS is widely considered an essential structural component of the OM, which makes the lipid A biosynthesis pathway an attractive target for antibiotic drug discovery (198).

Lipid A, historically known as endotoxin, is a potent stimulator of the innate immune system in mammals. The Toll-like receptor 4/myeloid differentiation factor 2 (TLR4/MD-2) complex detects the presence of lipid A during Gram-negative infections and triggers the release of proinflammatory cytokines (IL-6, TNF-α, and IL-1β) via the activation of NF-κB (199). In sufficient amounts, lipid A induces an unregulated, systemic inflammatory response that results in septic shock (200). As *E. coli* is used to produce approximately one third of approved protein therapeutics, a major hurdle in biopharmaceutical production is the removal of endotoxin from final products. Endotoxin removal methods can greatly increase manufacturing costs and often result in poor recovery or activity of the desired product (201).

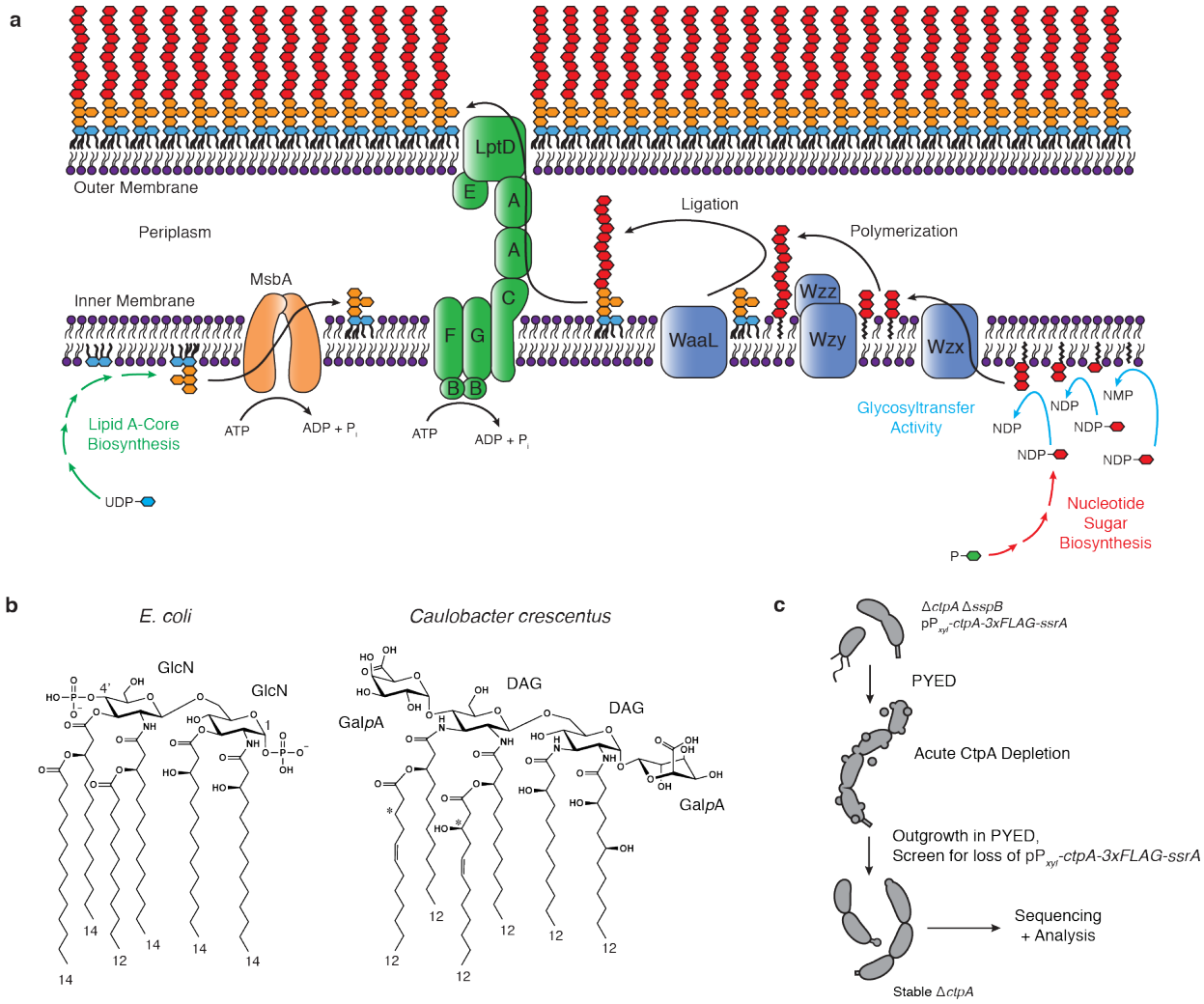

Figure 8: Lipopolysaccharide (LPS) biosynthesis, lipid A structures, and isolation of Δ*ctpA* suppressor mutants. a, Simplified LPS biosynthesis and export pathways elucidated in *E. coli* (196). O-antigen sugars: red hexagons; core sugars: orange hexagons; lipid A sugars: blue hexagons. Lipids of LPS and the O-antigen carrier undecaprenyl phosphate are bolded for clarity. Number of arrows does not necessarily indicate number of steps. **b**, The major lipid A species of *E. coli* and *Caulobacter* (202, 203). GlcN: glucosamine; DAG: 2,3-diamino-2,3-dideoxy-D-glucose; Gal*p*A: galactopyranuronic acid. Asterisks indicate two putative positions of a hydroxyl group. **c**, Depletion of CtpA results in OM integrity defects and cell chaining (204). Cells with mutations that suppress the lethality of CtpA removal can outgrow in depletion conditions, lose the *ctpA* covering plasmid, and become stable suppressor strains.

Efforts to eliminate lipid A from *E. coli* strains used in biopharmaceutical production have demonstrated that the intermediate molecule lipid IV_A is sufficient for viability, but only if the strain also has compensatory mutations that promote the flipping of this species across the IM (205, 206). Strains of *E. coli* completely devoid of lipid A have thus far been impossible to generate. However, not all bacteria with an OM produce lipid A (e.g. *Borrelia burgdorferi, Treponema pallidum*, and *Sphingomonas spp.*), and lipid A-deficient mutants of *Neisseria meningitidis*, *Moraxella catarrhalis*, and *Acinetobacter baumannii* have been recovered in

laboratory settings in the past two decades (207-211). It remains unclear why at least a minimal lipid A structure is essential in most Gram-negative bacteria but is dispensable in a limited number of species.

Caulobacter crescentus is a model alpha-proteobacterium used in studies of bacterial cell cycle regulation and cell organization (212). The *Caulobacter* surface is covered by a paracrystalline surface layer (S-layer) composed of the protein RsaA, which is linked to the OM via the O-antigen of LPS (213). Despite conservation of the Raetz pathway in most Gram-negative bacteria, significant variation exists in the lipid A structures of diverse organisms. The predominant *Caulobacter* lipid A species (202) varies from that of *E. coli* (214) (Fig. 8b), chiefly in that the 1- and 4′-phosphates are replaced by galactopyranuronic acid. While the genes responsible for phosphate removal (*lpxE* and *lpxF*) have been identified in other alpha-proteobacteria such as *Rhizobium etli* (215), homologs are absent from *Caulobacter* (216, 217); thus, it is unknown how *Caulobacter* completes LPS biosynthesis.

The tyrosine phosphatase homolog *ctpA* (for *Caulobacter* tyrosine phosphatase A) is essential for viability and has been implicated in cell envelope maintenance, but its molecular function remains unknown (204). Depletion of CtpA causes extensive OM blebbing, failure to resolve PG at the division site, and cell death. Here, we describe experiments showing that *ctpA* is required for lipid A biosynthesis. A screen for suppressors of *ctpA* essentiality recovered strains with null mutations in the O-antigen biosynthetic pathway or in the ferric uptake regulator *fur*. Mutations in *fur*, but not mutations that affect O-antigen synthesis, also permitted deletion of *lpxC*, which encodes an otherwise essential enzyme catalyzing the first committed step in lipid A biosynthesis. Δ*ctpA* and Δ*lpxC* strains containing suppressor mutations have significantly reduced or undetectable levels of lipid A, respectively. Limiting available iron in the growth medium phenocopies the *fur* mutation in allowing *Caulobacter* to survive in the absence of LpxC activity. These results reveal an unexpected connection between iron and lipid A essentiality in *Caulobacter* and suggest that lipid A may be conditionally essential for viability in other bacteria.

3.2 Methods

Growth conditions. Strains and plasmids used in this study are listed in Tables 3 and 4, respectively. All *Caulobacter crescentus* strains were derived from NA1000 (185). *Caulobacter* was grown in peptone-yeast extract medium (PYE) (218) at 30°C. Solid media were prepared using Fisher agar (BP1423). PYE was supplemented with 0.3% xylose (PYEX) or 0.2% dextrose (PYED) where indicated. When changing between inducing and non-inducing conditions, cells were first washed twice with PYE before being released into the opposite medium. Counter-selection using *sacB* was performed with 3% sucrose. 100 μM 2,2'-dipyridyl was added to culture medium to achieve low-iron conditions. Antibiotics added to PYE growth medium were used at the following concentrations (μg/mL) for liquid (L) or solid (S) medium: kanamycin, 5 (L), 25 (S); chloramphenicol, 1 (L/S); nalidixic acid, 20 (S); gentamycin, 25 (L), 5 (S); oxytetracycline, 1 (L), 2 (S); spectinomycin, 25 (L), 100 (S); hygromycin, 100 (L/S). *E. coli* was grown in Luria broth at 37°C, supplemented with antibiotics at the following concentrations

(μg/mL) for liquid (L) or solid (S) medium: kanamycin, 30 (L), 50 (S); chloramphenicol, 20 (L), 30 (S); gentamycin, 15 (L), 20 (S); tetracycline, 12 (L/S); spectinomycin, 50 (L/S); hygromycin, 100 (L/S). CHIR-090 was obtained from APExBIO.

Plasmid construction. Cultures of either *Caulobacter crescentus* NA1000 or plasmid-bearing *E. coli* Top10 cells were used as templates to amplify fragments for cloning with the Q5 High-Fidelity DNA Polymerase (New England Biolabs (NEB)). The correct fragments were isolated after agarose gel electrophoresis using the Zymoclean Gel DNA Recovery kit (Zymo Research). Unless otherwise indicated, restriction enzymes were obtained from NEB, ligations were performed using NEB T4 DNA ligase, and Gibson assembly was performed using NEB Gibson Assembly Master Mix. Plasmid constructs were confirmed by DNA sequencing. Plasmids and sequences are available upon request. Plasmid descriptions are listed in Table 4, and primer sequences used for plasmid construction are listed in Appendix Table 4.

pZIK133. The LpxC depletion vector was constructed by placing the *lpxC* coding region, C-terminally fused to a 3xFLAG tag (amino acid sequence: DYKDHDGDYKDHDIDYKDDDDK) followed by the *Caulobacter* ssrA tag (amino acid sequence: AANDNFAEEFAVAA), under control of the *xylX* promoter. The *xylX* promoter was amplified using the pJS14-PxylX and PxylX-lpxC R primers, and consisted of 432 bp upstream of the start codon (186). The PxylX-lpxC F and lpxC-3xFLAG R primers were used to amplify *lpxC*. The C-terminal fusion was amplified from pAB6 using the lpxC-3xFLAG F and ssrA-pJS14 primers. The final plasmid was assembled via Gibson cloning into a BamHI/EcoRI-digested pJS14 backbone.

pZIK134. For the *lpxC* knockout construct, flanking homology regions were amplified using the primers lpxC UpF and lpxC UpR for the 5'- region, and lpxC DownF and lpxC DownR for the 3'- region. The 5'- arm included a 5'- SpeI site and a 3'- EcoRI site, and the 3'- arm included a 5'- EcoRI site and a 3'- SphI site. These fragments were digested with the indicated enzymes and ligated into SpeI/SphI-digested pNPTS138. This intermediate plasmid was linearized with EcoRI, and the EcoRI-digested *tetAR* cassette from pKOC3 was inserted to make the final construct.

pZIK73 and *pZIK78*. For the *CCNA_01553* and *CCNA_00497* knockout constructs, flanking homology regions were amplified using the following primer pairs: pZIK73 5'- region (01553 UpF; 01553 UpR), pZIK73 3'- region (01553 DownF; 01553 DownR), pZIK78 5'- region (00497::hyg UpF; 00497::hyg UpR), pZIK78 3'- region (00497::hyg DownF; 00497::hyg DownR). For each construct, the 5'- arm included a 5'- SpeI site and a 3'- SmaI site, and the 3'- arm included a 5'- SmaI site and a 3'- EcoRI site. These fragments were digested with the indicated enzymes and ligated into SpeI/EcoRI-digested pNPTS138. The intermediate plasmids were linearized with SmaI, and the SmaI-digested *hyg* cassette from pHP45Ω-hyg was inserted to make the final constructs.

pZIK80, *pZIK81*, *pZIK82*, and *pZIK161*. For the *CCNA_03733*, *CCNA_01068*, *CCNA_01055*, and *CCNA_00055* knockout constructs, flanking homology regions were amplified using the following primer pairs: pZIK80 5'- region (03733::hyg UpF; 03733::hyg UpR), pZIK80 3'- region (03733::hyg DownF; 03733::hyg DownR), pZIK81 5'- region (01068::hyg UpF; 01068::hyg UpR), pZIK81 3'- region (01068::hyg DownF; 01068::hyg DownR), pZIK82 5'-

region (01055::hyg UpF; 01055::hyg UpR), pZIK82 3'- region (01055::hyg DownF; 01055::hyg DownR), pZIK161 5'- region (fur UpF; fur UpR), pZIK161 3'- region (fur DownF; fur DownR). Each 5'- arm included a 5'- SpeI site and a 3'- BamHI site, and each 3'- arm included a 5'- BamHI site and a 3'- EcoRI site. These fragments were digested with the indicated enzymes and ligated into SpeI/EcoRI-digested pNPTS138. The intermediate plasmids were linearized with BamHI, and the BamHI-digested hyg cassette from pHP45Ω-hyg was inserted to make the final constructs.

pZIK167. For the *mlaACDEF* knockout construct, flanking homology regions were amplified using the primers mla KO UpF and mla KO UpR for the 5'- region, and the primers mla KO DownF and mla KO DownR for the 3'- region. The 5'- arm included a 5'- SpeI site and a 3'- EcoRI site, and the 3'- arm included a 5'- EcoRI site and a 3'- MluI site. These fragments were digested with the indicated enzymes and ligated into SpeI/MluI-digested pNPTS138. This intermediate plasmid was linearized with EcoRI. The *aacC1* cassette from pVMCS-4 was amplified with added EcoRI sites using the aacC1 EcoRI F and aacC1 EcoRI R primers. This fragment was digested with EcoRI and ligated to the intermediate plasmid to make the final construct.

pZIK93, pZIK171, and pZIK179. For these overexpression vectors, *uppS*, *mlaACDEF*, or *murA* was placed under control of the xylX promoter on the high-copy plasmid pJS14. PCR fragments representing the *xylX* promoter and each coding region were inserted into BamHI/EcoRI-digested pJS14 using Gibson assembly. PCR fragments for Gibson assembly were amplified using the following primer pairs. pZIK93: P_{xylX} (pJS14-PxylX; PxylX-uppS R), *uppS* (PxylX-uppS F; uppS-pJS14). pZIK171: P_{xylX} (171 PxylX_fwd; 171 PxylX_rev), *mlaACDEF* (171 mla_operon_fwd; 171 mla_operon_rev). pZIK179: P_{xylX} (pJS14-PxylX; PxylX-murA R), *murA* (PxylX-murA F; murA-pJS14).

pZIK172-174. *CCNA_00497, CCNA_01553, or CCNA_03733* were placed under control of the *xylX* promoter on pXCERN-2, which integrates at the xylX promoter. The corresponding genes were initially cloned into pVCERN-2 before being moved into pXCERN-2. Genes were amplified with the following primer pairs: *CCNA_00497* (pVCERN-2 00497 F; pVCERN-2 00497 R), *CCNA_01553* (pVCERN-2 01553 F; pVCERN-2 01553 R), *CCNA_03733* (pVCERN-2 03733 F; pVCERN-2 03733 R). Primer sets replace the start codon with an NdeI site and add a SacI site after the stop codon. The corresponding gene fragment and pVCERN-2 were digested with NdeI and SacI and ligated together. An NdeI/MluI fragment was subsequently excised from each vector and moved to pXCERN-2 cut with the same enzymes.

pZIK175. *CCNA_00055* was placed under control of the *xylX* promoter on pXCERN-2, which integrates at the *xylX* promoter. *CCNA_00055* was initially cloned into pVCERN-2 before being moved into pXCERN-2. *CCNA_00055* was amplified using the Pvan-fur and fur-pVCERN primers, and this fragment was inserted into NdeI/SacI-digested pVCERN-2 via Gibson assembly. The NdeI/MluI fragment was subsequently excised and ligated into NdeI/MluI-digested pXCERN-2.

Strain construction. Plasmids were mobilized via triparental mating from *E. coli* Top10 donor cells to *Caulobacter* recipient cells using *E. coli* HB101 harboring pRK2013 (218). Counter-

selection against *E. coli* was performed using nalidixic acid. For Δ*ctpA* or Δ*lpxC* backgrounds, *Caulobacter* was electroporated with purified plasmid (219). For disruption of genes with antibiotic resistance cassettes on pNPTS138-derived suicide plasmids, cells that performed the first recombination event were grown to full density to allow the second recombination event to occur before being counter-selected on 3% sucrose. To generate stable strains lacking *ctpA* or *lpxC*, candidate suppressor genes were disrupted as above in the *ctpA* or *lpxC* depletion strain. These strains were grown in PYED without chloramphenicol to allow loss of the covering plasmid, and cells were streaked on PYED before being tested for chloramphenicol sensitivity. We were unable to knock out *ctpA* or *lpxC* directly in strains with deletions of candidate suppressor genes. All knockouts were confirmed via PCR.

Suppressor screen. KR3906 was grown to full density in PYEX. 300 μL of culture was transferred onto an open, sterile Petri dish and mutagenized in a UV Stratalinker 1800 (Stratagene) with 30,000 μJ of energy. Mutagenized cells were plated on PYED. Recovered colonies were passaged in liquid PYED overnight to allow loss of the covering plasmid, and samples were streaked onto PYED. Isolated colonies were screened for chloramphenicol sensitivity. Chlor^S isolates were grown in PYE and saved at -80°C in 10% dimethylsulfoxide (DMSO). Loss of *ctpA* was confirmed via PCR using the primers ctpA KO F and ctpA KO R, which anneal to the interior of the gene.

Illumina sequencing and variant analysis. Strains were grown to full density in PYE, and genomic DNA was extracted using the Quick-DNA Miniprep Kit (Genesee) or the DNeasy Blood & Tissue Kit (Qiagen). gDNA was submitted to the UC Berkeley Functional Genomics Laboratory, where libraries were prepared using a PCR-free protocol with multiplexing (http://qb3.berkeley.edu/gsl/). Samples were sequenced at the UC Berkeley Vincent J. Coates Genomics Sequencing Laboratory using a 300PE or 150PE MiSeq v3 run. Genomic sequencing data were analyzed for variants using the Galaxy platform at usegalaxy.org (220). Adapter sequences were removed using Cutadapt, and sequences were aligned to the NA1000 genome (216) using Bowtie2. FreeBayes was used to analyze the BAM files for variants. Variants with quality scores below 300 were discarded as noise.

Chemical sensitivity assays. Cultures were grown to mid-exponential phase (OD_{660} 0.2-0.5) in PYE, and an amount of cells equivalent to 250 μL of an $OD_{660} = 0.2$ culture was added to 4 mL of PYE swarm agar (0.3% w/v agar) pre-warmed to 42°C. Swarm agar containing bacteria was spread onto solid PYE and allowed to set for at least 10 minutes. Antibiotics or detergents were added to sterile 6 mm Whatman filter disks and allowed to dry in a fume hood for 10 minutes before discs were placed onto swarm agar surfaces. Plates were incubated upright at 30°C, and the diameter of the zone of clearing or haze was measured after 24 hours. The total amount of antibiotic or detergent added to each disk is as follows: kanamycin (100 μg), rifampicin (100 μg), vancomycin (1 mg), colistin (100 μg), polymyxin B (100 μg), CHIR-090 (100 μg), fosfomycin (50 μg), TWEEN 20 (10 μL of 10% solution), Triton X-100 (10 μL of 10% solution), sodium dodecyl sulfate (10 μL of 10% solution). Tests using CHIR-090 or fosfomycin used one quarter of the standard amount of cells to reduce growth haze and permit accurate measurement of the zone of clearing. For testing the sensitivity of strains overexpressing genes from pJS14, cells were grown in PYED/chloramphenicol and washed twice with PYE. Control cells were added to PYED swarm agar and plated immediately on PYED, while a parallel aliquot

was further grown in PYEX/chloramphenicol for 6 hours to permit gene overexpression before washing and plating in PYEX swarm agar. 100 μM 2,2'-dipyridyl was included in all media for testing the sensitivity of strains in low iron conditions.

Limulus amebocyte lysate (LAL) assay. The ToxinSensor Chromogenic LAL Endotoxin Assay kit (GenScript) was used to determine endotoxin units/mL of culture. Cells were grown to mid-exponential phase (OD_{660} 0.2-0.5), washed twice with non-pyrogenic LAL reagent water, and normalized in this water to OD_{660} = 0.1. Cell suspensions were serially diluted in non-pyrogenic water and analyzed according to manufacturer's instructions.

Growth assays. For growth curves of stable (non-depletion) strains, cells grown to OD_{660} 0.2-0.5 in PYE were released into PYE at OD_{660} = 0.02 and allowed to incubate with shaking at 30°C. At each indicated time, a sample was withdrawn for OD_{660} measurement and enumeration of CFU/ml on solid PYE medium. For cell viability assays during LpxC or CtpA depletion, cells were grown in PYEX with chloramphenicol to OD_{660} 0.2-0.5, washed twice in PYE, and normalized in PYE to OD_{660} = 0.1 in PYE. Cells were serially diluted 10-fold, and 5 μL of each dilution was spotted onto either PYEX or PYED, starting with the normalized suspension. Plates were imaged after 2.5 days using an Epson scanner. Strains overexpressing genes from pXCERN-2-derived vectors were treated similarly, except the cells were initially grown in PYED/kanamycin, and cells were plated onto either PYEX or PYED, both with kanamycin. All viability assays were performed in triplicate.

LPS extraction, Pro-Q Emerald 300 staining, and immunoblotting. LPS was extracted from overnight cultures using a hot aqueous-phenol technique adapted from Westpahl and Jann (221, 222). 1 mL of culture at OD_{660} = 0.75 was pelleted and resuspended in 200 μL 1x tricine buffer (2x = 200 mM Tris-HCl pH 6.8, 2% sodium dodecyl sulfate (SDS), 40% glycerol, 0.04% Coomassie G-250, 2% 2-mercaptoethanol (BME)). Suspensions were boiled for 15 minutes and allowed to cool to room temperature. 5 μL of 20 mg/mL Proteinase K (Thermo) was added to each sample before incubation at 55°C for three hours. Suspensions were mixed with 200 μL ice-cold Tris-saturated phenol, vortexed, and incubated at 65°C for 15 minutes before being cooled to room temperature. 1 mL diethyl ether was added to each sample before vortexing and spinning for 10 minutes in a table-top centrifuge at 16,000 x *g*. The bottom blue layer was removed to a fresh tube, and the extraction was repeated on the blue layer starting from the phenol step. 200 μL 2x tricine buffer was added to each sample before analysis on 16.5% Mini-PROTEAN Tris-Tricine gels (Bio-Rad). Gels were stained using Pro-Q Emerald 300 Lipopolysaccharide Gel Stain Kit (Molecular Probes; P20495) per manufacturer's instructions. For visualizing LPS species from whole-cell lysates, cells were normalized by OD_{660}, pelleted, and resuspended to 100 μL in 1x tricine buffer. Proteinase K (125 ng/μL) was added, and lysates were incubated overnight at 55°C. Samples were boiled for 5 minutes before being gel electrophoresis. Western blots were probed with α-S-LPS at a concentration of 1:20,000 (213).

Mass spectrometry experiments. Lipid A was extracted by the hot ammonium isobutyrate method (223). Mass spectrometry (MS) and tandem mass spectrometry (MS/MS) data were acquired on a Synapt G2 mass spectrometer (Waters Corp., Manchester, UK) equipped with electrospray ionization (ESI). To do so each sample was dissolved in $CHCl_3$:MeOH (v:v 2:1) and infused at a rate of 3 μL/min. All data were acquired in negative ion mode with sensitivity mode

engaged. MS/MS was carried out using trap collision-induced dissociation (CID). To optimize the signal-to-noise ratio, each tandem mass spectrum was obtained over a 5- to 10-minute period.

Differential interference contrast microscopy. Cells were immobilized on agarose pads (1% w/v in reverse osmosis-purified water). Images were taken using a Zeiss EC Plan-Neofluar 100x/1.3 Oil M27 objective on a Zeiss AxioImager M1 microscope with a Hamamatsu Digital CCD Camera (C8484-03G01). Images were acquired using iVision software and processed using ImageJ.

CryoEM imaging and tomographic processing. Cultures (5 mL) of KR4000, KR4102, KR4103, and KR3906 grown to OD_{660} 0.2-0.5 were centrifuged (4°C, 16,000 x *g*, 15 minutes), and cell pellets were resuspended in 50 μL PYE. For KR3906, cells grown in PYEX were washed twice with PYE, released into PYED at OD_{660} = 0.02, and incubated for 10 hours before harvest. 3 μL of cell suspension, mixed 1:1 with Fiducial markers (10-nm gold particles conjugated to Protein A; Aurion) was applied to glow-discharged quantifoil girds (R2/2) and frozen in liquid ethane using an automatic plunge freezing device (Vitrobot, FEI. 12˚C, 8-12s blot time, blot force 8, humidity 100%). Grids of KR4000 and KR4103 were imaged on a Jeol3100 cryoTEM operating at 300kV with in column omega energy filter and K2 direct electron camera. Grids of KR4102 and KR3906 were imaged on a Krios Cryo TEM (FEI) operating at 300kV with post column energy filter (Quantum, GATAN) and K2 direct electron camera. All data were collected with the automatic data collection program serialEM (224). Square overview images were acquired using a defocus of 80-100 microns at a nominal magnification of 3600-6500x (Krios) or 1200x (Jeol) using the polygon montage operation (specimen pixel size: 33-67Å). Beam intensity was set to $8e^-$/px/s over an empty hole and exposure times ranged from 2-5s depending on ice thickness. Bidirectional tomographic tilt series were collected from ±60° using a defocus of 6-8 μm and at a magnification which provided specimen pixel size of 4-7 Å. Total dose of the tilt series were kept between 60-90 $e^-/Å^2$. All tilt series images were collected in movie mode and the frames aligned using MotionCor2 (225). Aligned frames were compiled into stacks and processed using IMOD (226). Contrast of resulting tomograms was enhanced using a non-linear anisotropic diffusion filter (227) and manually segmented using the 3D visualization program AMIRA (ThermoFisher).

Table 3. List of strains used in this study

Strain Number	Description	Reference
KR4000	Wild-type Caulobacter NA1000	(185)
KR3180	NA1000 pJS14	This study
KR1499	Δ*sspB*::aadA	(204)
KR3877	Δ*CCNA_00497::hyg*	This study
KR4198	Δ*CCNA_00497::hyg* pJS14	This study
KR3871	Δ*CCNA_01553::hyg*	This study
KR4197	Δ*CCNA_01553::hyg* pJS14	This study
KR4076	Δ*fur::hyg*	This study
KR4199	Δ*fur::hyg* pJS14	This study
KR3953	Δ*CCNA_00497::hyg* Δ*sspB::aadA*	This study

KR4115	Δ*CCNA_01055::hyg* Δ*sspB::aadA*	This study
KR4116	Δ*CCNA_01068::hyg* Δ*sspB::aadA*	This study
KR3954	Δ*CCNA_01553::hyg* Δ*sspB::aadA*	This study
KR3955	Δ*CCNA_03733::hyg* Δ*sspB::aadA*	This study
KR4077	Δ*fur::hyg* Δ*sspB::aadA*	This study
KR4153	Δ*sspB::aadA* pXCERN-2	This study
KR4154	Δ*CCNA_00497::hyg* Δ*sspB::aadA* pXCERN-2	This study
KR4155	Δ*CCNA_01553::hyg* Δ*sspB::aadA* pXCERN-2	This study
KR4156	Δ*CCNA_03733::hyg* Δ*sspB::aadA* pXCERN-2	This study
KR4157	Δ*fur::hyg* Δ*sspB::aadA* pXCERN-2	This study
KR4158	Δ*CCNA_00497::hyg* Δ*sspB::aadA* pZIK172	This study
KR4159	Δ*CCNA_01553::hyg* Δ*sspB::aadA* pZIK173	This study
KR4160	Δ*CCNA_03733::hyg* Δ*sspB::aadA* pZIK174	This study
KR4161	Δ*fur::hyg* Δ*sspB::aadA* pZIK175	This study
KR3906	Δ*ctpA::tetAR* Δ*sspB::aadA* pAB6	(204)
KR4111	Δ*ctpA::tetAR* Δ*sspB::aadA* Δ*CCNA_00497::hyg* pAB6	This study
KR4112	Δ*ctpA::tetAR* Δ*sspB::aadA* Δ*CCNA_01553::hyg* pAB6	This study
KR4092	Δ*ctpA::tetAR* Δ*sspB::aadA* Δ*CCNA_03733::hyg* pAB6	This study
KR4090	Δ*ctpA::tetAR* Δ*sspB::aadA* Δ*fur::hyg* pAB6	This study
KR4007	Δ*lpxC::tetAR* Δ*sspB::aadA* pZIK133	This study
KR4008	Δ*lpxC::tetAR* Δ*sspB::aadA* Δ*CCNA_00497::hyg* pZIK133	This study
KR4223	Δ*lpxC::tetAR* Δ*CCNA_00497::hyg* pZIK133	This study
KR4009	Δ*lpxC::tetAR* Δ*sspB::aadA* Δ*CCNA_01553::hyg* pZIK133	This study
KR4010	Δ*lpxC::tetAR* Δ*sspB::aadA* Δ*CCNA_03733::hyg* pZIK133	This study
KR4091	Δ*lpxC::tetAR* Δ*sspB::aadA* Δ*fur::hyg* pZIK133	This study
KR4113	Δ*ctpA::tetAR* Δ*sspB::aadA* Δ*CCNA_00497::hyg*	This study
KR4114	Δ*ctpA::tetAR* Δ*sspB::aadA* Δ*CCNA_01553::hyg*	This study
KR4104	Δ*ctpA::tetAR* Δ*sspB::aadA* Δ*CCNA_03733::hyg*	This study
KR4102	Δ*ctpA::tetAR* Δ*sspB::aadA* Δ*fur::hyg*	This study
KR4103	Δ*lpxC::tetAR* Δ*sspB::aadA* Δ*fur::hyg*	This study
KR4176	Δ*ctpA::tetAR* Δ*sspB::aadA* Δ*fur::hyg* pZIK175	This study
KR4177	Δ*ctpA::tetAR* Δ*sspB::aadA* Δ*fur::hyg* pXCERN-2	This study
KR4178	Δ*lpxC::tetAR* Δ*sspB::aadA* Δ*fur::hyg* pZIK175	This study
KR4179	Δ*lpxC::tetAR* Δ*sspB::aadA* Δ*fur::hyg* pXCERN-2	This study
KR4180	Δ*ctpA::tetAR* Δ*sspB::aadA* Δ*CCNA_03733::hyg* pZIK174	This study
KR4181	Δ*ctpA::tetAR* Δ*sspB::aadA* Δ*CCNA_03733::hyg* pXCERN-2	This study
KR4182	Δ*ctpA::tetAR* Δ*sspB::aadA* Δ*CCNA_00497::hyg* pZIK172	This study
KR4183	Δ*ctpA::tetAR* Δ*sspB::aadA* Δ*CCNA_00497::hyg* pXCERN-2	This study

KR4148	Δ*lpxC::tetAR* Δ*sspB::aadA* Δ*fur::hyg* pZIK133	This study
KR4149	Δ*lpxC::tetAR* Δ*sspB::aadA* Δ*fur::hyg* pJS14	This study
KR4150	Δ*ctpA::tetAR* Δ*sspB::aadA* Δ*CCNA_03733::hyg* pAB6	This study
KR4151	Δ*ctpA::tetAR* Δ*sspB::aadA* Δ*CCNA_03733::hyg* pJS14	This study
KR4166	Δ*mlaACDEF::aacC1*	This study
KR4167	Δ*mlaACDEF::aacC1* Δ*sspB::aadA*	This study
KR4196	Δ*mlaACDEF::aacC1* Δ*sspB::aadA* Δ*fur::hyg*	This study
KR4119	NA1000 pZIK93	This study
KR4147	NA1000 pZIK171	This study
KR4170	NA1000 pZIK179	This study
KR4205	Δ*ctpA::tetAR* Δ*sspB::aadA* suppressor isolate #3	This study
KR4206	Δ*ctpA::tetAR* Δ*sspB::aadA* suppressor isolate #8	This study
KR4207	Δ*ctpA::tetAR* Δ*sspB::aadA* suppressor isolate #16	This study
KR4208	Δ*ctpA::tetAR* Δ*sspB::aadA* suppressor isolate #21	This study
KR4209	Δ*ctpA::tetAR* Δ*sspB::aadA* suppressor isolate #32	This study
KR4210	Δ*ctpA::tetAR* Δ*sspB::aadA* suppressor isolate #36	This study
KR4211	Δ*ctpA::tetAR* Δ*sspB::aadA* suppressor isolate #38	This study
KR4212	Δ*ctpA::tetAR* Δ*sspB::aadA* suppressor isolate #40	This study
KR4213	Δ*ctpA::tetAR* Δ*sspB::aadA* suppressor isolate #43	This study
KR4214	Δ*ctpA::tetAR* Δ*sspB::aadA* suppressor isolate #44	This study
KR4215	Δ*ctpA::tetAR* Δ*sspB::aadA* suppressor isolate #47	This study
KR4216	Δ*ctpA::tetAR* Δ*sspB::aadA* suppressor isolate #52	This study
KR4217	Δ*ctpA::tetAR* Δ*sspB::aadA* suppressor isolate #53	This study
KR4218	Δ*ctpA::tetAR* Δ*sspB::aadA* suppressor isolate #54	This study
KR4219	Δ*ctpA::tetAR* Δ*sspB::aadA* suppressor isolate #57	This study
KR4220	Δ*ctpA::tetAR* Δ*sspB::aadA* suppressor isolate #111	This study
KR4221	Δ*ctpA::tetAR* Δ*sspB::aadA* suppressor isolate #112	This study
KR4224	Δ*lpxC::tetAR* Δ*sspB::aadA* suppressor isolate #1	This study
KR4225	Δ*lpxC::tetAR* Δ*sspB::aadA* suppressor isolate #5	This study

Table 4. List of plasmids used in this study

Name	Description	Reference
pJS14	Broad host-range cloning vector; high copy; chlor^R; pBBR1MCS derivative with unique EcoRI site	(J. Skerker, unpublished)
pNPTS138	kan^R; sacB-containing integration vector	(M.R. Alley, unpublished)
pXCERN-2	For integration at P_{xylX}; encodes xylose-inducible *cerulean* that can be swapped for gene of interest; kan^R	(228)
pAB6	pJS14-P_{xylX}-*ctpA-3xFLAG-ssrA*	(204)
pZIK133	pJS14-P_{xylX}-*lpxC-3xFLAG-ssrA*	This study

pZIK172	pXCERN-2-P_{xylX}-*CCNA_00497*	This study
pZIK173	pXCERN-2-P_{xylX}-*CCNA_01553*	This study
pZIK174	pXCERN-2-P_{xylX}-*CCNA_03733*	This study
pZIK175	pXCERN-2-P_{xylX}-*CCNA_00055* (*fur*)	This study
pZIK93	pJS14-P_{xylX}-*CCNA_01996* (*uppS*)	This study
pZIK171	pJS14-P_{xylX}-*CCNA_03806-CCNA_03807-CCNA_03808-CCNA_03809-CCNA_03810* (*mlaACDEF*)	This study
pZIK179	pJS14-P_{xylX}-*CCNA_02435* (*murA*)	This study
pZIK78	pNPTS138-*CCNA_00497::hyg*; for replacing *CCNA_00497* with hygromycin resistance cassette	This study
pZIK82	pNPTS138-*CCNA_01055::hyg*; for replacing *CCNA_01055* with hygromycin resistance cassette	This study
pZIK81	pNPTS138-*CCNA_01068::hyg*; for replacing *CCNA_01068* with hygromycin resistance cassette	This study
pZIK73	pNPTS138-*CCNA_01553::hyg*; for replacing *CCNA_01553* with hygromycin resistance cassette	This study
pZIK80	pNPTS138-*CCNA_03733::hyg*; for replacing *CCNA_03733* with hygromycin resistance cassette	This study
pZIK161	pNPTS138-*CCNA_00055::hyg*; for replacing *fur* with hygromycin resistance cassette	This study
pZIK134	pNPTS138-*CCNA_02064::tetAR*; for replacing *lpxC* with tetracycline resistance cassette	This study
pZIK167	pNPTS138-*CCNA_03806-CCNA_03807-CCNA_03808-CCNA_03809-CCNA_03810::aacC1*; for replacing *mlaACDEF* with gentamycin resistance cassette	This study
pHP45Ω-hyg	For isolating *hyg* fragment; hyg^R; amp^R	(229)
pKOC3	Contains *tetAR* flanked by EcoRI sites; amp^R; tet^R	(230)
pVMCS-4	For amplification of *aacC1*; $gent^R$	(228)

3.3 Results

Suppressor mutations affecting fur or O-antigen biosynthesis permit the loss of ctpA

To investigate the function of *ctpA* in *Caulobacter* physiology, we used a CtpA depletion strain to select suppressors that could survive under non-permissive conditions. *ctpA* is expressed at very low levels in *Caulobacter* (231). Efficient expression and regulated depletion of CtpA were achieved by expressing *ctpA::3xFLAG::ssrA* from a xylose-driven promoter (186) on a high-copy plasmid in a Δ*ctpA* strain also lacking the proteolytic adaptor *sspB* (204). This depletion strain (KR3906), used as the parent in our suppressor analysis, exhibited division defects, significant OM blebbing, and ultimately death when grown in the absence of xylose (Fig 9) (204).

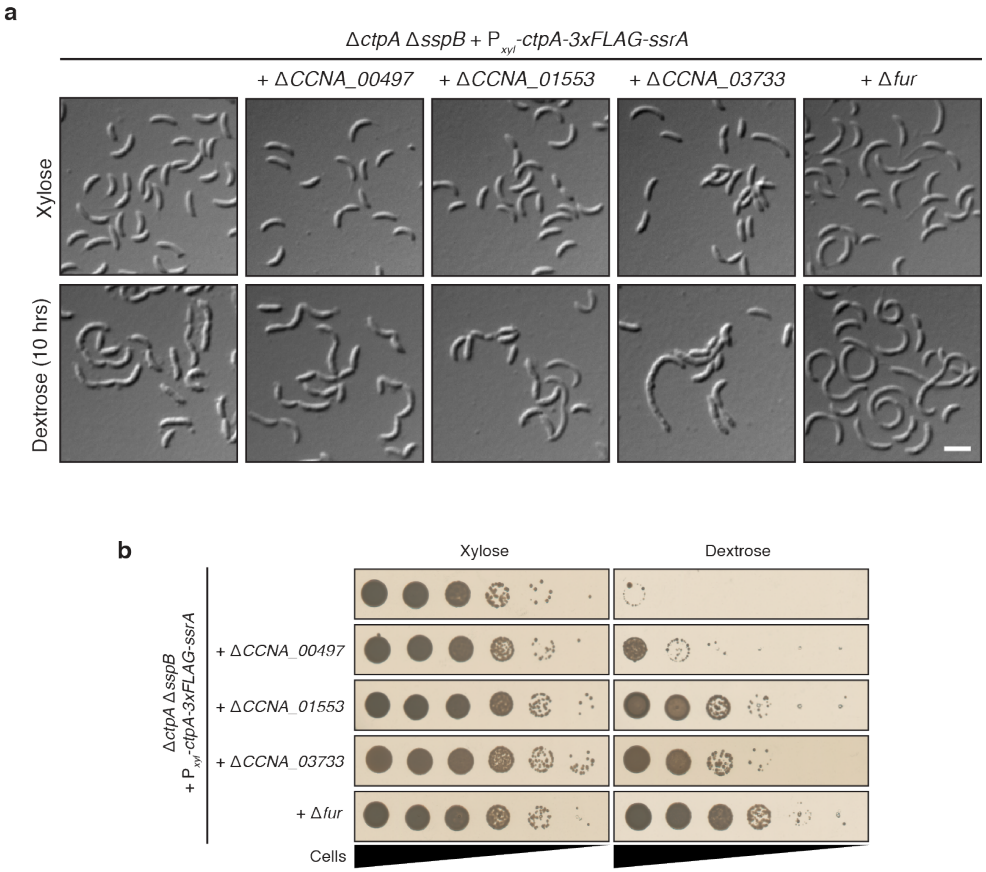

Figure 9: Null mutations in *fur* or O-antigen repeat unit biosynthetic genes improve adverse phenotypes of CtpA depletion. a, DIC images of the CtpA depletion strain KR3096 and four derivative depletion strains, each lacking the indicated putative Δ*ctpA* suppressor. Strains grown in PYEX were diluted back into PYEX (Xylose) or shifted to PYED (Dextrose) for 10 hours. Scale bar, 3 μm. **b**, The indicated strains cultured in PYEX were normalized to OD_{660} = 0.1, and ten-fold serial dilutions were plated on PYE under either inducing (Xylose) or non-inducing (Dextrose) conditions. Plates were incubated for 3 days and are representative of at least three independent trials.

We UV-mutagenized KR3906, plated survivors on solid medium lacking xylose but supplemented with dextrose (PYED) to deplete CtpA, and passaged any recovered colonies in PYED liquid medium to allow loss of the plasmid bearing *ctpA*. Isolates that had successfully lost the plasmid were identified via chloramphenicol sensitivity and the inability to PCR-amplify *ctpA* (Fig. 8c). Genome resequencing of 17 confirmed suppressors revealed 16 strains with mutations in nine genes predicted to participate in O-antigen biosynthesis, as well as two strains with mutations in the ferric uptake regulator *fur* (Appendix Table 2). Due to the frequent occurrence of frameshift or nonsense mutations, we began with the assumption that each mutation caused loss of function of the affected gene.

To confirm that specific null mutations suppress the lethality of *ΔctpA*, we took two experimental approaches. We first deleted each of four candidate suppressor genes in the CtpA depletion strain KR3906, while propagating the strains on xylose-containing medium (PYEX) to provide CtpA protein. To determine how each disruption affected cells during acute CtpA

depletion, we shifted each mutant onto liquid or solid PYED medium and observed cell morphology or viability (Fig. 9). In the second approach, we plated each mutant on PYED medium and screened viable colonies for loss of the *ctpA*-bearing plasmid as described above to acquire stable *ΔctpA ΔsspB* derivatives (Fig. 8c). We chose for deletion the following four candidate suppressors: (i) *CCNA_00497*, previously shown to be necessary for wild-type levels of S-LPS (232); (ii) *CCNA_01553*, annotated as a glycosyltransferase which initiates O-antigen synthesis upon Und-P (216); (iii) *CCNA_03733*, a homolog of *manC* involved in synthesizing the activated sugar GDP-D-mannose (233), which is incorporated into both the core oligosaccharide and O-antigen of *Caulobacter* S-LPS (234); and iv) *fur* (*CCNA_00055*).

Compared to CtpA depletion in the parent strain KR3906, acute depletion of CtpA in the Δ*fur* mutant caused much less OM blebbing, but still yielded filamentous cells indicative of a division defect (Fig. 9a). Surprisingly, neither phenotype appeared to be markedly improved when CtpA was depleted in the strains lacking *CCNA_00497*, *CCNA_01553*, or *CCNA_03733* (Fig. 9a). Despite these morphological defects, both Δ*fur* and individual mutations in predicted O-antigen synthesis genes significantly improved viability during depletion of CtpA on solid PYED medium (Fig. 9b).

In each stable *ΔctpA ΔsspB* mutant, the OM was smooth with minimal blebbing, but chains of cells were still prevalent in the *ΔCCNA_01553* and *Δfur* backgrounds (Fig. 10a). These reconstituted suppressor strains are morphologically similar to the original isolates containing point mutations in the same genes (Appendix Fig. 1). *ΔctpA ΔsspB Δ00497* and *ΔctpA ΔsspB Δ03733* have longer doubling times than their parallel *ctpA*$^{+}$ strains, but all derivatives are able to reach similar stationary phase densities in PYE medium (Fig. 10b, Appendix Fig. 2). As expected, restoring the expression of *fur*, *CCNA_00497*, or *CCNA_03733* using a xylose-inducible promoter reduced the viability of each corresponding stable *ΔctpA* strain (Fig. 10c). We were unable to address the effects of regulated *CCNA_01553* expression in the stable *ΔctpA* background because leaky expression from the uninduced *xylX* promoter was sufficient to produce CCNA_01553 and restore O-antigen production (Appendix Fig. 3). Together, these results confirm that null mutations affecting *fur* or O-antigen biosynthesis allow *Caulobacter* to survive in the absence of *ctpA*.

Since most of the O-antigen-related genes identified in our suppressor analysis have not previously been studied in *Caulobacter*, we deleted individual genes in the control strain lacking *sspB* (KR1499) to verify that they affect S-LPS production. Whole-cell lysates treated with proteinase K and probed with antibodies recognizing S-LPS showed that, as predicted, each mutant caused a partial or complete elimination of S-LPS (Fig. 11a), which appears as a single high-molecular-weight species (213). When the same lysates were stained with Pro-Q Emerald 300 to detect carbohydrates (Fig. 11a), the mutants contained varying amounts of S-LPS and of three low-molecular weight bands that may, by analogy with other bacteria, represent distinct species of lipid A +/- core oligosaccharide (235). This inference is supported by the band pattern in the strain lacking *CCNA_03733* (*manC*). The core oligosaccharide of *Caulobacter* LPS contains a single penultimate mannose residue (234); thus, the size difference observed in the largest lipid A-core band for Δ*CCNA_03733* (Fig. 11a, *) may arise from a reduced core oligosaccharide. Because the wide, intermediate band (Fig. 11a, **) is not altered in any of the mutants, we infer that it does not represent a species of S-LPS, but it currently remains

uncharacterized. Deletion of *fur* in the Δ*sspB* background did not affect the size or amount of S-LPS or any of the presumed lipid A +/- core species (Fig. 11a). Because S-LPS is present in this strain, we conclude that null mutations in *fur* suppress the lethality of Δ*ctpA* by a mechanism other than loss of O-antigen.

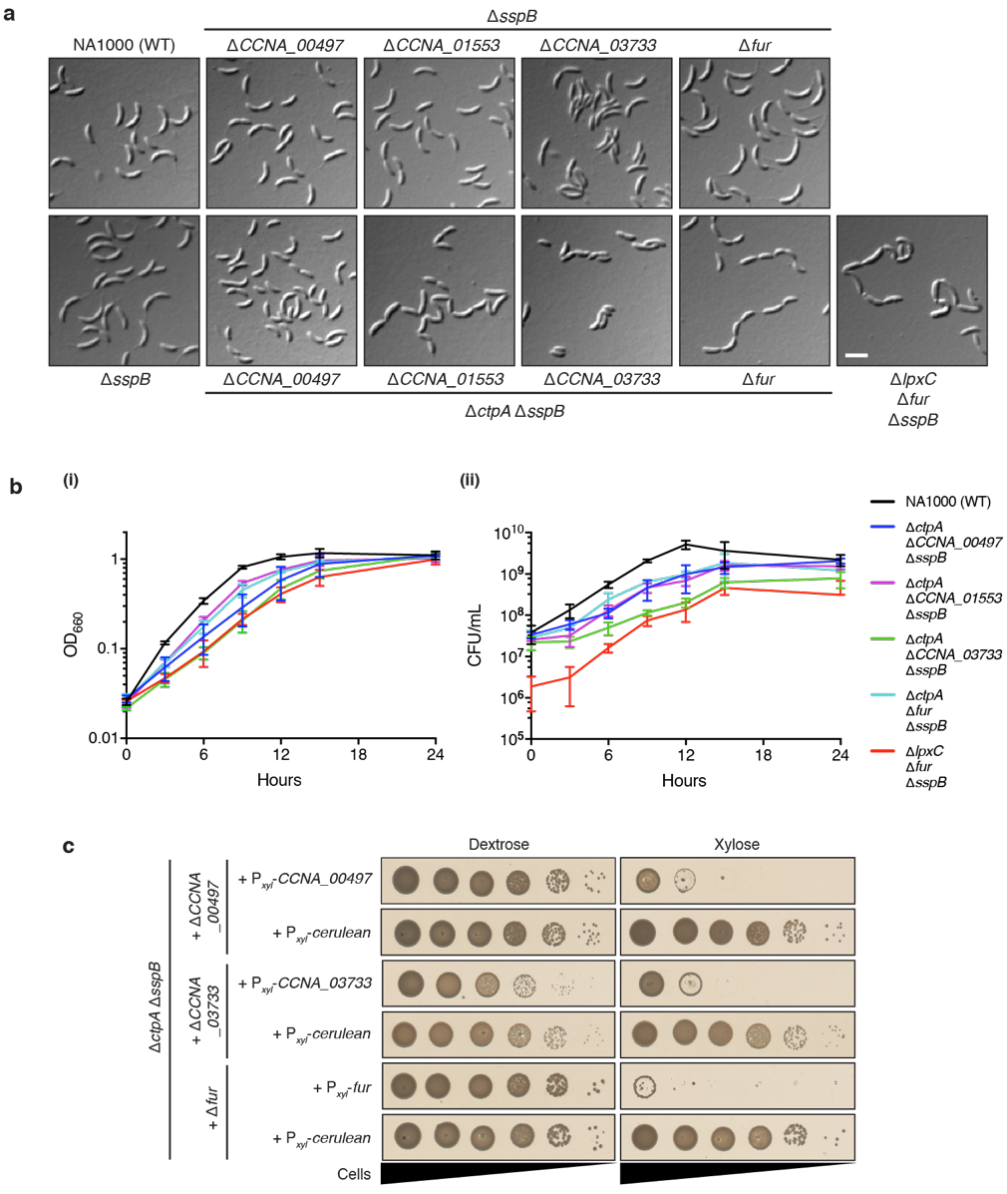

Figure 10: Expression of *fur* or O-antigen repeat unit biosynthetic genes is lethal in stable strains lacking *ctpA*. a, DIC images of the indicated strains grown in PYE. Stable Δ*ctpA* strains were isolated as single colonies from their respective depletion strains as described in the text. Scale bar, 3 μm. **b**, Growth curves of the indicated strains in PYE showing (i) OD_{660} and (ii) colony-forming units (CFU) per mL (mean ± s.d., N=3). Growth of strains with mutations only in suppressor genes and *sspB* did not deviate significantly from WT, and have been moved to the appendix for clarity (Supplementary Fig. 3). **c**, Viability assays of stable Δ*ctpA* Δ*sspB* mutants, each harboring a vactor for P_{xyl}-driven expression of either the respective suppressor gene or the *cerulean* gene as a control. Exponential-phase liquid cultures of each strain in PYED/kanamycin were normalized to OD_{660} = 0.1, and ten-fold serial dilutions were plated on PYE/kanamycin with either 0.2% dextrose or 0.3% xylose. Plates were incubated for 3 days and are representative of at least three independent trials.

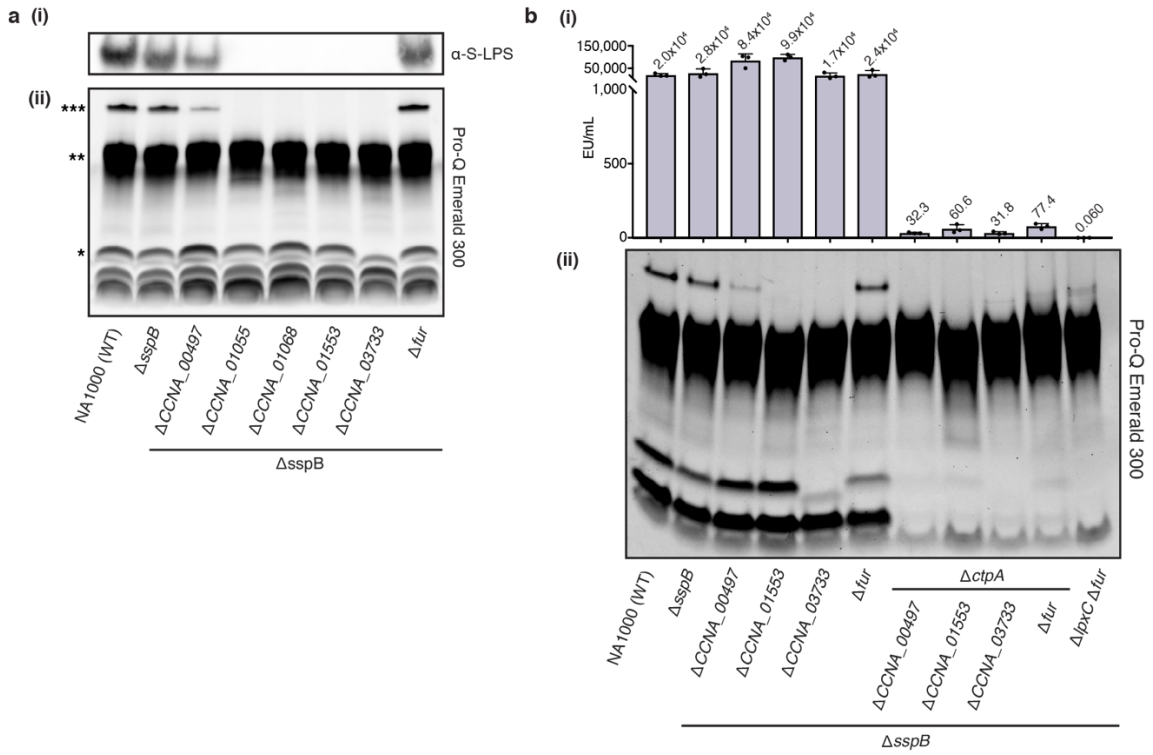

Figure 11: Strains lacking *ctpA* show a drastic reduction in lipid A levels. a, (i) α-S-LPS-probed immunoblot and (ii) Pro-Q Emerald 300-stained polyacrylamide gel of the same whole-cell lysates of the indicated strains. Samples were normalized by OD_{660}. *** = S-LPS, ** = putative uncharacterized carbohydrate, * = putative full-length lipid A-core moiety. Bands below * may represent various species of lipid A +/- core or other low-molecular weight carbohydrates. **b**, (i) Endotoxin units (EU) per mL of whole cells (OD_{660} = 0.1) of the strains indicated in (ii), quantified via LAL assay (mean ± s.d., N=3). Dots represent individual data points, and numeric values above bars represent mean values. (ii) PAGE and Pro-Q Emerald staining of hot aqueous-phenol LPS extracts of the indicated strains. Cultures were normalized by OD_{660} prior to extraction, and 3.75% of each extract was analyzed.

Cells lacking ctpA have dramatically reduced lipid A levels

The *ctpA* locus is transcribed divergently from an operon containing four genes involved in the late stages of lipid A-core biosynthesis and export (Fig. 12a). Like *ctpA*, these genes are also essential for *Caulobacter* viability (236). Neighboring loci in a divergent orientation may be co-regulated via overlapping promoter regions, and this arrangement is an excellent predictor shared function (237). Since CtpA depletion results in OM defects, and suppressor mutations were identified in O-antigen biosynthetic genes, we hypothesized that *ctpA* is required for some aspect of LPS biosynthesis or export.

We extracted LPS from stable mutants lacking *ctpA*, along with their *ctpA*$^+$ counterparts, and analyzed them by PAGE and Pro-Q Emerald 300 staining. As with the whole-cell lysates (Fig. 11a), full-length S-LPS was recovered from NA1000, Δ*sspB*, and Δ*fur* Δ*sspB*, while only smaller species were present in the three O-antigen mutants (Fig. 11b). Interestingly, the stable Δ*ctpA* Δ*sspB* strains lacking *CCNA_00497*, *CCNA_01553*, *CCNA_03733*, or *fur* were also deficient in the small species that could represent lipid A +/- core oligosaccharide. To determine

if the *ctpA* mutants actually contain reduced levels of lipid A, we used the Limulus Amebocyte Lysate (LAL) assay to detect this molecule in live *Caulobacter* strains. All *ΔctpA* mutants tested contained approximately 1,000-fold less lipid A than NA1000 or the corresponding *ctpA*$^+$ strains (Fig. 11b).

Mutations in fur permit loss of the essential LPS biosynthetic gene lpxC and lipid A

Since lipid A is considered an essential component of nearly all Gram-negative outer membranes, we were surprised to measure such a dramatic reduction in lipid A in the stable Δ*ctpA* mutants. These results prompted us to determine if mutations in *fur* or O-antigen synthesis could allow *Caulobacter* to eliminate a conserved enzyme of the Raetz pathway and lose lipid A entirely. LpxC catalyzes removal of the 2-acetyl group from acylated UDP-GlcNAc, the first committed step in lipid A synthesis in most bacteria (Fig. 12a) (203). The *lpxC* homolog *CCNA_02064* is essential for viability in wild-type *Caulobacter* (236). We constructed an LpxC depletion strain (KR4007) analogous to the CtpA depletion strain, using a plasmid-encoded *lpxC::3xFLAG::ssrA* fusion driven by the *xylX* promoter in a Δ*sspB* Δ*lpxC* background. We subsequently deleted *fur*, *CCNA_00497*, *CCNA_01553*, or *CCNA_03733* in this strain and examined the effects of acute LpxC depletion during growth in PYED. In the absence of any candidate suppressor mutations, LpxC depletion resulted in chains of cells with extensive membrane blebs (Fig. 12b). Cells lacking an O-antigen biosynthesis gene still showed membrane blebs and chaining when LpxC was depleted (Appendix Fig. 4). Cells lacking *fur* had fewer OM blebs upon LpxC depletion, but still frequently formed chains (Fig. 12b). These morphologies are generally similar to those seen during acute CtpA depletion, but unlike CtpA, only Δ*fur* allowed significant growth of the LpxC depletion strain on solid PYED medium (Fig. 12c).

When we attempted to isolate stable Δ*lpxC* mutants using the same outgrowth and screening process as for Δ*ctpA* (Fig. 8c), only the strain harboring the Δ*fur* mutation permitted complete loss of *lpxC*. We initially recovered two Δ*lpxC* isolates from the Δ*CCNA_00497* background, but genome resequencing revealed that these strains had acquired additional mutations in *fur* (Appendix Table 3). As in Δ*ctpA* Δ*fur* Δ*sspB*, the stable Δ*lpxC* Δ*fur* Δ*sspB* mutant still formed chains (Fig. 10a), and xylose-driven *fur* expression induced lethality in this background (Fig. 12d). According to the LAL assay, Δ*lpxC* Δ*fur* Δ*sspB* cells contained an amount of lipid A comparable to the reverse-osmosis purified water control (Fig. 11b), suggesting that lipid A is completely absent. LPS extracted from this strain lacked S-LPS, as well as all putative lipid A +/- core species (Fig. 11b). As with *ctpA*, plasmid-expressed *lpxC* complemented the deletion phenotype (Appendix Fig. 5). Because no lipid A was detected in Δ*lpxC* Δ*fur* Δ*sspB* by the LAL assay, we suggest that the Pro-Q Emerald-stained bands remaining in this strain are contaminants unrelated to LPS.

To confirm that *ctpA* and *lpxC* mutants contained little or no lipid A, we analyzed extracted lipid A species by mass spectrometry (Appendix Fig. 6). Expected masses consistent with the published *Caulobacter crescentus* lipid A structure were absent from both Δ*ctpA* Δ*fur* Δ*sspB* and Δ*lpxC* Δ*fur* Δ*sspB*. However, the control strains NA1000, Δ*sspB*, and Δ*fur* Δ*sspB* contained lipid A ions that were further characterized by tandem mass spectrometry. A

discussion of the structures derived by comparison to the previously reported *Caulobacter* lipid A structure may be found in Appendix Fig. 6.

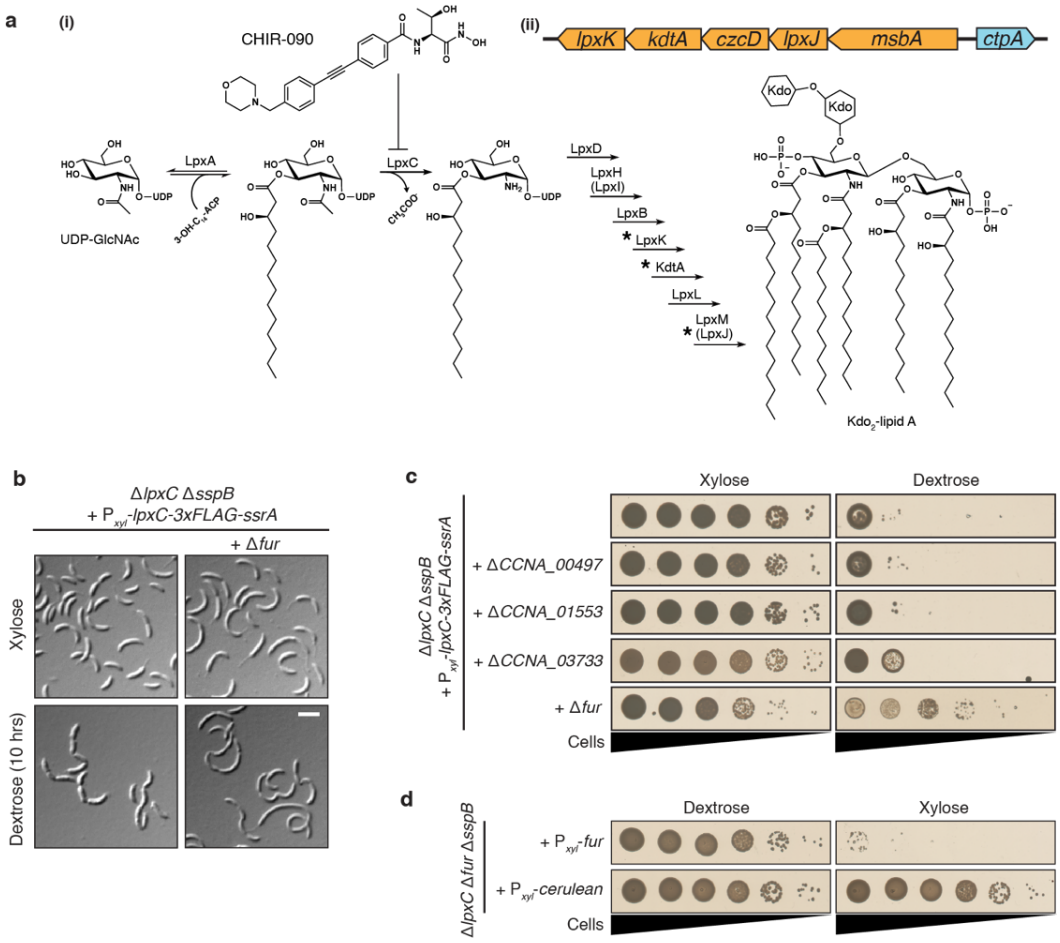

Figure 12: The early Raetz pathway enzyme LpxC is dispensable in *Caulobacter crescentus* lacking *fur*. a, (i) A simplified depiction of the Raetz pathway highlights the presence of three enzymes encoded by genes in an operon adjacent to *ctpA* in the NA1000 genome (ii). *Caulobacter* contains *lpxI* and *lpxJ* homologs at the indicated steps. CHIR-090 is an inhibitor of LpxC. (UDP-GlcNAc: uridine diphosphate N-acetylglucosamine; Kdo: 3-deoxy-D-manno-oct-2-ulosonic acid; ACP: acyl carrier protein). **b**, DIC images of Δ*lpxC* Δ*sspB* +/- Δ*fur* cells harboring the LpxC depletion vector pZIK133 grown in either PYEX or PYED for 10 hours. Scale bar, 3 μm. **c**, Viability assays of LpxC depletion strains, with or without mutations that suppressed ΔctpA, plated on either PYEX or PYED. **d**, Viability assays of stable Δ*lpxC* Δ*fur* Δ*sspB* harboring either a P_{xyl}-*fur* or a P_{xyl}-*cerulean* expression vector. Cells from both **c** and **d** were plated from 10-fold serially diluted suspensions normalized to OD_{660} = 0.1. Plates were incubated for 3 days and are representative of at least three independent trials. Plates in **d** included kanamycin to retain expression vectors.

Both lipophilic and large hydrophilic compounds are excluded from Gram-negative bacteria by lateral interactions between LPS molecules, and LPS defects are usually associated with increased chemical sensitivity (195). We employed disc diffusion assays to measure the sensitivity of LPS-deficient Δ*ctpA* and Δ*lpxC* cells to a variety of antibiotics and detergents (Fig. 13). While the *fur* or O-antigen mutations alone did not appreciably change the resistance

profiles compared to the wild-type strain (NA1000), strains lacking *ctpA* and *lpxC* had greater sensitivity to rifampicin, bacitracin, vancomycin, and all tested detergents. Sensitivity to colistin or polymyxin B was similar in all tested strains, consistent with the fact that wild-type *Caulobacter* lipid A lacks the 1- and 4'- phosphates required for colistin and polymyxin B binding (238, 239). Critically, the Δ*lpxC* and Δ*ctpA* mutants were more resistant than all other strains to CHIR-090, an inhibitor of LpxC (240), confirming that LpxC activity and lipid A are already greatly reduced or absent in these mutants (Fig. 13a, 15a).

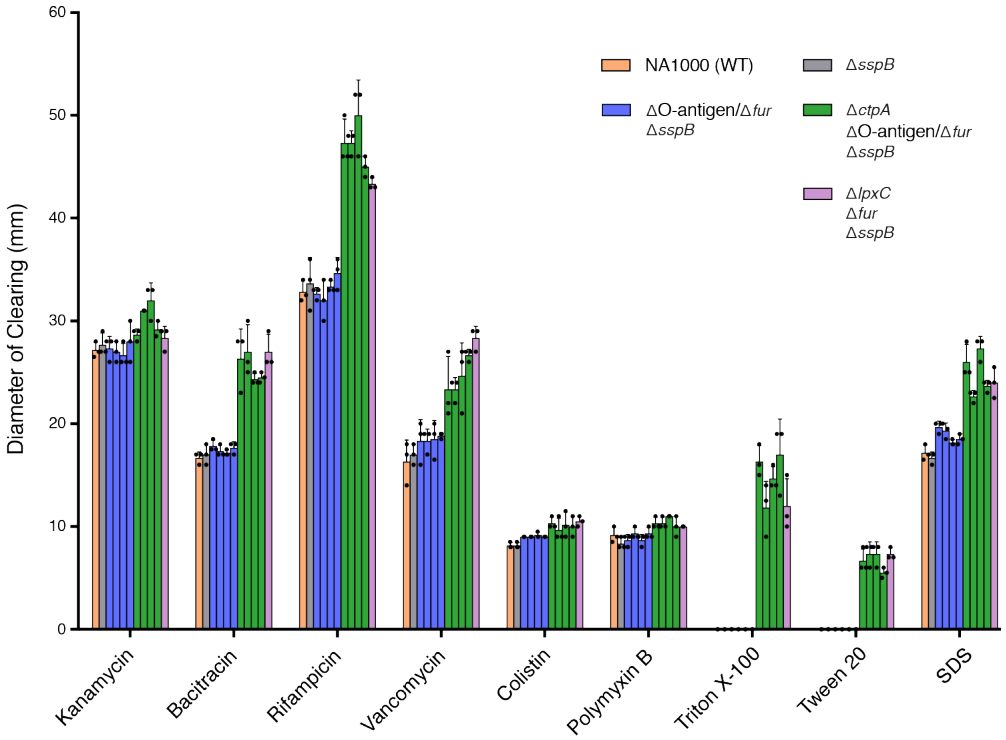

Figure 13: *lpxC* and *ctpA* mutants show increased sensitivity to antibiotics and detergents. Diameters of zones of clearing in disk diffusion assays for chemical sensitivity of stable Δ*ctpA* and Δ*lpxC* strains compared to their suppressor backgrounds (Δ*sspB* with ΔO-antigen or Δ*fur*) and to NA1000. Values reported are diameters of clearing minus the diameter of the disk (6 mm) (mean ± s.d., N=3). Dots indicate individual data points. Suppressor mutations present in strains repressed by blue or green bars are, from left to right, Δ*CCNA_00497*, Δ*CCNA_01553*, Δ*CCNA_03733*, Δ*fur*.

Caulobacter mutants with little or no lipid A produce a three-layer cell envelope

To assess how the loss of *ctpA* or *lpxC* affects cell envelope structure, we analyzed NA1000, Δ*ctpA* Δ*fur* Δ*sspB* and Δ*lpxC* Δ*fur* Δ*sspB* strains via electron cryotomography (Fig. 14). As expected, the S-layer is absent from both mutants due to the loss of its O-antigen attachment site (213). Despite drastic reductions in lipid A levels, the Δ*ctpA* Δ*fur* Δ*sspB* and Δ*lpxC* Δ*fur* Δ*sspB* mutants still elaborate a three-layer cell envelope, including an outer membrane (Fig. 14c, d). Although much less severe than during acute CtpA depletion (Fig. 14d), membrane blebs were often observed at the cell poles or division sites in Δ*ctpA* Δ*fur* Δ*sspB* and Δ*lpxC* Δ*fur* Δ*sspB* cells (Fig. 14c, d). Interestingly, a significant proportion of both the *ctpA* and

lpxC mutants exhibited defects in stalk structure or IM distortions at the pole or midcell (N = 100; Δ*ctpA* Δ*fur* Δ*sspB*: 61%; Δ*lpxC* Δ*fur* Δ*sspB*: 51%; NA1000: 4%). Images (Fig. 14b) of the CtpA depletion strain KR3906 grown for 12 hours in PYED reaffirm that blebs occur where the OM has detached from the underlying peptidoglycan (PG) and IM (204).

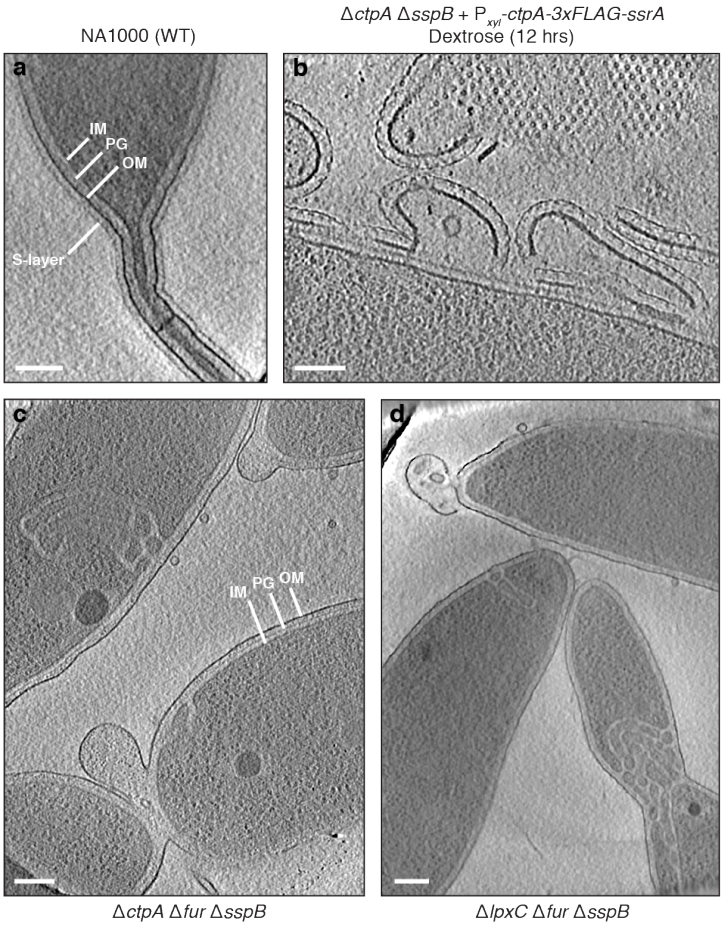

Figure 14: Stable mutants lacking *ctpA* or *lpxC* have a three-layer cell envelope but display polar or midcell membrane abnormalities. Electron cryotomography images of the indicated strains. **a**, *Caulobacter crescentus* NA1000 has three cell envelope layers: inner membrane (IM), peptidoglycan (PG), outer membrane (OM), surmounted by an S-layer. **b**, Depletion of CtpA from KR3906 during 12 hours of growth in PYED results in detachment of the OM and S-layer from the underlying PG. Stable strains of Δ*ctpA* Δ*fur* Δ*sspB* (**c**) and Δ*lpxC* Δ*fur* Δ*sspB* (**d**) have a three-layer envelope consisting of IM, PG, and OM. Polar or midcell IM defects or OM blebs are frequently observed for strains in **c** and **d**.

Mutations affecting O-antigen synthesis suppress ΔctpA lethality independent of Und-P sequestration

Und-P is used in both the O-antigen and PG biosynthetic pathways as a lipid carrier for precursor synthesis and transport to the periplasm (241, 242). Upon release of the precursor molecules, undecaprenyl pyrophosphate (Und-PP) is dephosphorylated and recycled back to the cytoplasmic face of the IM (243). Because O-antigen is ligated directly onto lipid A-core from

Und-P, the absence of lipid A may cause an accumulation of O-antigen-Und-P assemblies and a corresponding reduction in Und-P available for PG synthesis. In support of this theory, *E. coli* mutants producing an incomplete lipid A-core species unable to act as an acceptor for O-antigen have severe morphological defects that are reversed by mutations blocking O-antigen synthesis (244). The lipid A deficiency of Δ*ctpA* cells may lead to Und-P sequestration and death, which could be suppressed by mutations preventing O-antigen synthesis. We therefore asked if chemical inhibition of *Caulobacter* lipid A synthesis could be ameliorated by other genetic manipulations that increase the amount of Und-P available for PG biosynthesis.

We reasoned that, if inhibition of lipid A synthesis is harmful due to Und-P sequestration, increasing the pool of Und-P or increasing flux through the PG synthesis pathway should decrease *Caulobacter* sensitivity to the LpxC inhibitor CHIR-090 (244). We overexpressed *uppS*, encoding Und-P synthase (245), or *murA*, which catalyzes the first committed step of PG synthesis (246), in wild-type *Caulobacter* NA1000 and measured CHIR-090 sensitivity by the disk diffusion assay. In *E. coli*, overexpression of *uppS* or *murA* successfully alleviates morphological defects associated with sequestered Und-P (244). In *Caulobacter*, however, overexpression of *uppS* or *murA* did not render cells less sensitive to CHIR-090, unlike mutations in *fur* or O-antigen biosynthetic genes (Fig. 15a and Fig. 16a). To verify that gene overexpression was successful, we determined that the strain overexpressing *murA* had a dramatic increase in resistance to the MurA inhibitor fosfomycin (247) (Fig. 16b). These results are inconsistent with a mechanism whereby loss of O-antigen ameliorates severe reductions in lipid A levels by freeing sequestered Und-P.

Increased mla transcription in the Δfur mutant is not required to survive a block in lipid A synthesis

Proteins in the Mla (Maintenance of OM lipid asymmetry) pathway are believed to catalyze retrograde transport of phospholipids from the OM to the IM (248). Mutations in *mla* genes accumulate during laboratory evolution of lipid A-free *A. baumannii* strains and are associated with increased fitness (249). In the retrograde model of Mla function, it is advantageous to inhibit the removal of phospholipids from the outer leaflet of the OM when no lipid A is available (249). However, a recent study has challenged this model by showing that *A. baumannii mla* mutants accumulate newly synthesized phospholipids in the IM, consistent with the Mla system transporting phospholipids in an anterograde manner toward the OM (250).

Since the *Caulobacter* Δ*lpxC* Δ*fur* Δ*sspB* mutant produces an OM in the absence of detectable lipid A, we hypothesize that it constructs a symmetric phospholipid bilayer. In *Caulobacter*, transcription of the *mlaACDEF* operon is directly or indirectly inhibited by Fur and by iron availability (251, 252). If the Mla system performs anterograde phospholipid transport, then deletion of *fur* could suppress the lethality of Δ*lpxC* and Δ*ctpA* by increasing *mla* transcription and providing additional phospholipids for OM construction in the absence of lipid A. We therefore asked if the *mla* operon is required in Δ*fur* cells to compensate for chemical inhibition of lipid A synthesis. We disrupted the *mla* operon in NA1000, Δ*sspB*, and Δ*fur* Δ*sspB* cells and compared their sensitivity to CHIR-090 with the corresponding *mla*$^+$ strains. The CHIR-090 resistances of Δ*mlaACDEF* strains were unchanged relative to their *mla*$^+$ counterparts (Fig. 15a).

Importantly, the Δ*fur* Δ*sspB* Δ*mlaACDEF* mutant maintained high resistance to CHIR-090, indicating that upregulation of *mla* transcription is not required to survive a block in lipid A synthesis. In fact, *mla* overexpression increased the sensitivity of *Caulobacter* to CHIR-090 (Fig. 16a).

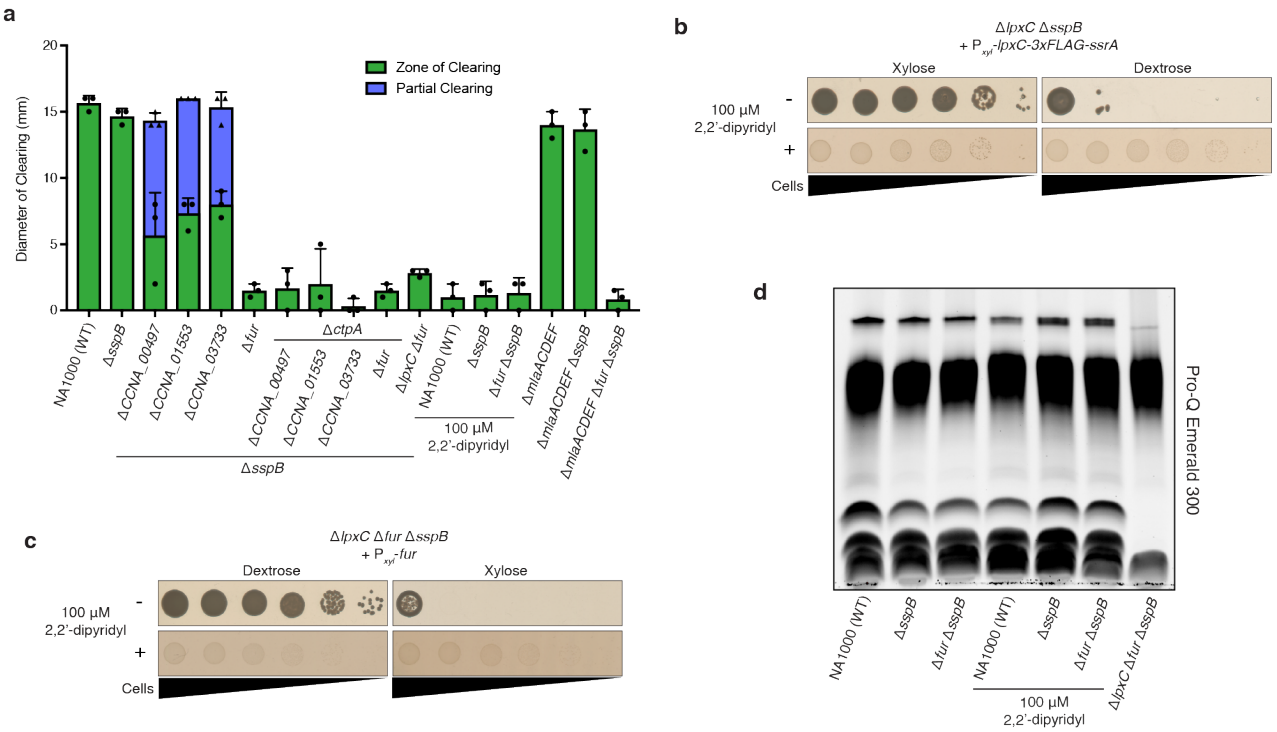

Figure 15: Iron limitation is sufficient to render LPS non-essential via a mechanism that does not require the *mla* operon. a, CHIR-090 sensitivity measured by disk diffusion assay. Values reported are the diameter of clearing minus the diameter of the disk (6 mm) (mean ± s.d., N=3). Partial clearing indicates the outer diameter of a ring of intermediate growth between the cleared area and the area of uninhibited lawn growth. Dots and triangles indicate individual measurements of cleared and partially cleared zones, respectively. The DMSO solvent control did not inhibit growth of any strain. **b**, Viability of the LpxC depletion strain growth in inducing (xylose) or depleting (dextrose) conditions, in the presence or absence of 100 μM 2,2'-dipyridyl. **c**, Viability of the stable Δ*lpxC* Δ*fur* Δ*sspB* strain harboring a P_{xyl}-*fur* plasmid, grown in noninducing (dextrose) or inducing (xylose) conditions, in the presence or absence of 100 μM 2,2'-dipyridyl. Cells in both **b** and **c** were plated from 10-fold serially diluted suspensions normalized to OD_{660} = 0.1 on PYEX or PYED. Plates were incubated for 3 days and are representative of at least three independent trials. Plates in **c** included kanamycin to retain the expression vector. Iron limitation slowed *Caulobacter* growth in all conditions, but preserved the viability of strains lacking only LpxC. **d**, Pro-Q Emerald-stained polyacrylamide gel of Proteinase K-treated whole-cell lysates of the indicated strains grown overnight in the presence or absence of 100 μM 2,2'-dipyridyl. Samples were normalized by OD_{660}.

Iron limitation supports viability in the absence of lipid A

Since Fur requires bound Fe^{2+} for activity (253), iron limitation may mimic the phenotypes of a Δ*fur* mutant, including the ability to render LPS nonessential in wild-type *Caulobacter*. Culturing NA1000 with the iron chelator 2,2'-dipyridyl conferred resistance to CHIR-090 equivalent to that of the Δ*fur* mutant (Fig. 15a). Neither depleting LpxC in *fur*$^+$ cells nor inducing *fur* in Δ*lpxC* Δ*fur* Δ*sspB* cells caused a reduction in viability in the presence of

2,2'-dipyridyl (Fig. 15b, c). The NA1000, Δ*sspB*, and Δ*fur* Δ*sspB* strains cultured in 2,2'-dipyridyl retained all predicted LPS and lipid A +/- core species (Fig. 15d). Therefore, low iron availability does not induce the loss of lipid A, but is sufficient to maintain *Caulobacter* viability when lipid A is eliminated by chemical or genetic means.

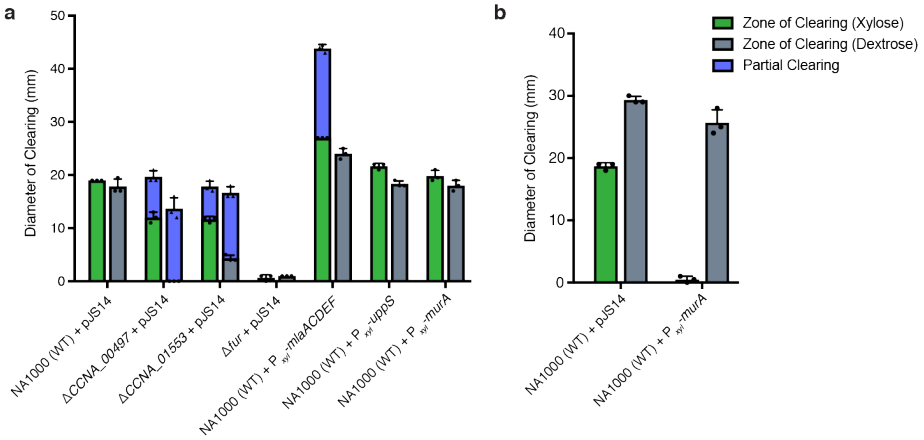

Figure 16: Overexpression of *mlaACDEF*, *uppS*, or *murA* does not suppress the lethality of LPS loss. a, CHIR-090 or **b**, fosfomycin sensitivity of strains overexpressing *mlaACDEF*, *uppS*, or *murA* measured by disk diffusion assay. Cells were grown in PYED/chloramphenicol for 6 hours before sensitivity was assayed. Values reported are the diameter for clearing minus the diameter of the disk (6 mm) (mean ± s.d., N=3). Partial clearing indicates the outer diameter of a ring of intermediate growth between the cleared area and the area of uninhibited lawn growth. Dots and triangles indicate individual measurements of cleared and partially clearned zones, respectively.

3.4 Discussion

Caulobacter crescentus is only the fourth LPS-bearing Gram-negative bacterium, and the first non-pathogen, demonstrated to survive in the absence of lipid A. Viability of Δ*lpxC* mutants required elimination of the iron-responsive transcription factor Fur or growth in iron-limited medium. While *fur* mutations and iron limitation have not been connected with the ability of *N. meningitidis*, *M. catarrhalis*, or *A. baumannii* to lose lipid A, they have been linked to OM homeostasis in *Haemophilus influenzae*, *Vibrio cholerae*, and *E. coli*, where they stimulate the formation of OM vesicles (254). In these bacteria, Fur directly or indirectly stimulates *mla* transcription, and loss of function mutations in *mla* genes or in *fur* are sufficient to upregulate OM vesicle production (254). In light of these studies and of the increased fitness conferred by *mla* mutations upon the *A. baumannii lpxA* mutant, we investigated the connection between Fur, the Mla system, and lipid A loss in *Caulobacter*.

Our initial screen for suppressors of Δ*ctpA* lethality retrieved no mutations in *mla* genes, and deletion of the *mla* operon neither increased nor decreased the susceptibility of a wild-type strain to the LpxC inhibitor CHIR-090. These results argue that inactivation of the Mla system is insufficient to allow *Caulobacter* to survive drastic reductions in lipid A content. In contrast to *H. influenzae*, *V. cholerae*, and *E. coli*, Fur and iron restriction repress expression of the *mla* operon in *Caulobacter* (251, 252). We therefore tested the hypothesis that upregulation of *mla*

transcription is the mechanism by which *fur* mutants survive inhibition of lipid A synthesis. We found that the Mla system is not necessary for Δ*fur* cells to resist the effects of the LpxC inhibitor CHIR-090, and increased *mla* expression makes *Caulobacter* less resistant to the drug. Together, these results argue that *fur* deletion renders *ctpA* or *lpxC* inessential for viability by a mechanism unrelated to the regulation of *mla* transcription. Additionally, deletion of *fur* alone does not eliminate the O-antigen, so mutations in *fur* and in O-antigen synthesis genes appear to allow the loss of CtpA in different ways. Because we isolated no Δ*ctpA*-mutations in genes within the Fur regulon, we suggest that upregulation of one or more genes normally repressed by Fur is responsible for the ability to lose *ctpA*, *lpxC*, and lipid A.

It is not immediately apparent how the elimination of the O-antigen segment of LPS could permit the loss of *ctpA* and a drastic reduction in the amount of lipid A per cell. One hypothesis was that a reduction in the number of lipid A-core acceptor sites for O-antigen sequestered Und-P within O-antigen-Und-P assemblies and made it unavailable for PG synthesis. Blocking O-antigen synthesis would thereby release Und-P for use in other essential pathways. We initially found this explanation unlikely because of the variety of Δ*ctpA*-suppressing mutations we isolated in the O-antigen synthesis pathway. Suppressors were identified not only in genes predicted to transfer the first activated sugar onto Und-P, but also in genes predicted to elongate O-antigen assemblies already in progress (Appendix Table 2). Late interruptions in O-antigen synthesis would be expected to yield incomplete O-antigen-Und-P assemblies, rather than releasing Und-P. In agreement with this inference, we found that genetic manipulations shown to ameliorate Und-P sequestration in *E. coli* were unable to improve *Caulobacter* resistance to CHIR-090. Instead, we hypothesize that the reduced size or amount of O-antigen on the cell surface increases the likelihood that a cell undergoing *ctpA* depletion can transition from an LPS-based OM to one containing primarily phospholipids, perhaps by changing the ability of LPS to intermix laterally with phospholipids in the outer leaflet of the OM (255, 256).

Although CtpA is essential for wild-type levels of lipid A and LPS, its precise molecular function remains to be determined. Because Δ*ctpA* mutants contain residual levels of lipid A, we favor the hypothesis that CtpA has a regulatory role rather than catalyzing a step in lipid A synthesis. However, we cannot rule out a catalytic role because, while the Raetz pathway is conserved in *Caulobacter*, the enzymes responsible for structural differences between *Caulobacter* and *E. coli* lipid A have not been identified. Alternatively, CtpA could be involved in another cellular process that, when perturbed, indirectly inhibits LPS production.

No single theme has emerged to explain either the widespread essentiality of lipid A or the capacity of individual species to survive in its absence. Hypotheses to explain the essential nature of lipid A include its chemical barrier function, the detrimental activation of stress responses when it is depleted, the perturbation of outer membrane protein function in the absence of lipid A, and the accumulation of toxic intermediates when lipid A biosynthesis is interrupted (257). Toxic intermediates do prevent the loss of later steps of the Raetz pathway in *A. baumannii* (258), but this doesn't explain the inability of most bacteria to lose early-acting genes in lipid A synthesis, such as *lpxC*. Studies of *A. baumannii* clinical isolates revealed that some strains are prevented from losing lipid A by the glycosyltransferase activity of penicillin-binding protein 1A (259), but the precise mechanism linking these pathways is unclear. In contrast, we recovered no Δ*ctpA* or Δ*lpxC* suppressors in genes associated with PG synthesis. Capsular

polysaccharides were once thought to compensate for the absence of lipid A in *N. meningitidis* mutants (260), but non-capsulated strains capable of losing lipid A were subsequently identified (261). Now, however, there is no model to explain why lipid A-deficient mutants cannot be isolated in the closely related, non-capsulated species *N. gonorrhoeae*. Studies describing transcriptional adaptations in lipid A-deficient strains of *A. baumannii* have consistently observed increases in the expression of lipoproteins and the Lol pathway for lipoprotein transport to the OM (259, 262). One hypothesis based on these results is that excess surface lipoproteins compensate for the absence of lipid A in *A. baumannii lpxA* or *lpxC* mutants (259), but it is not yet known if upregulation of lipoprotein production and transport are required for *A. baumannii* to lose lipid A.

The ability of iron limitation to render lipid A dispensable in *Caulobacter* raises the possibility that lipid A could be conditionally essential in a wider range of bacteria than previously thought. Bacteria and hosts compete for iron as an important nutrient, and the human innate immune response limits iron availability to pathogens through mechanisms such as reducing iron absorption in the intestine and sequestering it in ferritin complexes (263). If, as in *Caulobacter*, a pathogenic species can lose lipid A in an iron-limited host environment, this could reduce the effectiveness of antibiotics that target lipid A synthesis. While lipid A-deficient strains of *A. baumannii* are less virulent than their wild-type counterparts (264), mutations that improve their fitness have been isolated during relatively short periods of laboratory evolution (249). Certain pathogens may therefore be able to undergo transitory loss of lipid A while employing compensatory mechanisms to retain cellular integrity. Further studies in *Caulobacter*, and the isolation of additional lipid A-free Gram-negative species, will contribute to our understanding of the mechanisms and limits of lipid A essentiality in diverse bacteria.

References

1. Kirkpatrick CL & Viollier PH (2012) Decoding caulobacter development. *FEMS Microbiol.Rev*. 36: 193-205.
2. Zschiedrich CP, Keidel V & Szurmant H (2016) Molecular mechanisms of two-component signal transduction. *J.Mol.Biol*. 428: 3752-3775.
3. Gao R & Stock AM (2010) Molecular strategies for phosphorylation-mediated regulation of response regulator activity. *Curr. Opin. Microbiol*. 13: 160-167.
4. Bourret RB (2010) Receiver domain structure and function in response regulator proteins. *Curr. Opin. Microbiol*. 13: 142-149.
5. Silversmith RE (2010) Auxiliary phosphatases in two-component signal transduction. *Curr. Opin. Microbiol*. 13: 177-183.
6. Huynh TN & Stewart V (2011) Negative control in two-component signal transduction by transmitter phosphatase activity. *Mol.Microbiol*. 82: 275-286.
7. Jenal U, Reinders A & Lori C (2017) Cyclic di-GMP: Second messenger extraordinaire. *Nat. Rev. Microbiol*. 15: 271-284.
8. Chou SH & Galperin MY (2016) Diversity of cyclic di-GMP-binding proteins and mechanisms. *J. Bacteriol*. 198: 32-46.
9. Dubey BN, *et al* (2016) Cyclic di-GMP mediates a histidine kinase/phosphatase switch by noncovalent domain cross-linking. *Sci.Adv*. 2: e1600823.
10. Mann TH, Childers WS, Blair JA, Eckart MR & Shapiro L (2016) A cell cycle kinase with tandem sensory PAS domains integrates cell fate cues. *Nat.Commun*. 7: 11454.
11. Wheeler RT & Shapiro L (1999) Differential localization of two histidine kinases controlling bacterial cell differentiation. *Mol Cell* 4: 683-694.
12. Hecht GB, Lane T, Ohta N, Sommer JM & Newton A (1995) PMC394470; an essential single domain response regulator required for normal cell division and differentiation in caulobacter crescentus. *Embo J*. 14: 3915-3924.
13. Matroule J-, Lam H, Burnette DT & Jacobs-Wagner C (2004) Cytokinesis monitoring during development: Rapid pole-to-pole shuttling of a signaling protein by localized kinase and phosphatase in caulobacter. *Cell* 118: 579-590.
14. Quon KC, Marczynski GT & Shapiro L (1996) Cell cycle control by an essential bacterial two-component signal transduction protein. *Cell* 84: 83-93.
15. Jacobs C, Domian IJ, Maddock JR & Shapiro L (1999) Cell cycle-dependent polar localization of an essential bacterial histidine kinase that controls DNA replication and cell division. *Cell* 97: 111-120.
16. Biondi EG, *et al* (2006) Regulation of the bacterial cell cycle by an integrated genetic circuit. *Nature* 444: 899-904.
17. Iniesta AA, McGrath PT, Reisenauer A, McAdams HH & Shapiro L (2006) A phospho-signaling pathway controls the localization and activity of a protease complex critical for bacterial cell cycle progression. *Proc.Natl.Acad.Sci.USA* 103: 10935-10940.
18. Chen YE, Tsokos CG, Biondi EG, Perchuk BS & Laub MT (2009) Dynamics of two phosphorelays controlling cell cycle progression in caulobacter crescentus. *J. Bacteriol*. 191: 7417-7429.
19. Iniesta AA, Hillson NJ & Shapiro L (2010) Cell pole-specific activation of a critical bacterial cell cycle kinase. *Proc.Natl.Acad.Sci.USA* 107: 7012-7017.

20. Chen YE, *et al* (2011) Spatial gradient of protein phosphorylation underlies replicative asymmetry in a bacterium. *Proc.Natl.Acad.Sci.USA* 108: 1052-1057.
21. Laub MT, Chen SL, Shapiro L & McAdams HH (2002) Genes direcly controlled by CtrA, a master regulator of the caulobacter cell cycle. *Proc.Natl.Acad.Sci.USA* 99: 4632-4637.
22. Laub MT, McAdams HH, Feldblyum T, Fraser CM & Shapiro L (2000) Global analysis of the genetic network controlling a bacterial cell cycle. *Science* 290: 2144-2148.
23. Quon KC, Yang B, Domian IJ, Shapiro L & Marczynski GT (1998) Negative control of bacterial DNA replication by a cell cycle regulatory protein that binds at the chromosome origin. *Proc.Natl.Acad.Sci.USA* 95: 120-125.
24. Domian IJ, Quon KC & Shapiro L (1997) Cell type-specific phosphorylation and proteolysis of a transcriptional regulator controls the G1-to-S transition in a bacterial cell cycle. *Cell* 90: 415-424.
25. Jacobs C, Ausmees N, Cordwell SJ, Shapiro L & Laub MT (2003) Functions of the CckA histidine kinase in caulobacter cell cycle control. *Mol.Microbiol*. 47: 1279-1290.
26. Rood KL, Clark NE, Stoddard PR, Garman SC & Chien P (2012) Adaptor-dependent degradation of a cell-cycle regulator uses a unique substrate architecture. *Structure* 20: 1223-1232.
27. Lau J, Hernandez-Alicea L, Vass RH & Chien P (2015) A phosphosignaling adaptor primes the AAA+ protease ClpXP to drive cell cycle-regulated proteolysis. *Mol.Cell* 59: 104-116.
28. Smith SC, *et al* (2014) Cell cycle-dependent adaptor complex for ClpXP-mediated proteolysis directly integrates phosphorylation and second messenger signals. *Proc.Natl.Acad.Sci.USA* 111: 14299-14234.
29. Jacobs C, Hung D & Shapiro L (2001) Dynamic localization of a cytoplasmic signal transduction response regulator controls morphogenesis during the caulobacter cell cycle. *Proc.Natl.Acad.Sci.USA* 98: 4095-4100.
30. Jenal U & Fuchs T (1998) An essential protease involved in bacterial cell-cycle control. *Embo J*. 17: 5658-5669.
31. McGrath PT, Iniesta AA, Ryan KR, Shapiro L & McAdams HH (2006) A dynamically localized protease complex and a polar specificity factor control a cell cycle master regulator. *Cell* 124: 535-547.
32. Duerig A, *et al* (2009) Second messenger-mediated spatiotemporal control of protein degradation regulates bacterial cell cycle progression. *Genes Dev*. 23: 93-104.
33. Hung D & Shapiro L (2002) A signal transduction protein cues proteolytic events critical to caulobacter cell cycle progression. *Proc.Natl.Acad.Sci.USA* 99: 13160-13165.
34. Tsokos CG, Perchuk BS & Laub MT (2011) A dynamic complex of signaling proteins uses polar localization to regulate cell-fate asymmetry in caulobacter crescentus. *Dev.Cell* 20: 329-341.
35. Paul R, *et al* (2008) Allosteric regulation of histidine kinases by their cognate response regulator determines cell fate. *Cell* 133: 452-461.
36. Ebersbach G, Briegel A, Jensen GJ & Jacobs-Wagner C (2008) A self-associating protein critical for chromosome attachment, division, and polar organization in caulobacter. *Cell* 134: 956-968.
37. Radhakrishnan SK, Thanbichler M & Viollier PH (2008) The dynamic interplay between a cell fate determinant and a lysozyme homolog drives the asymmetric division cycle of caulobacter crescentus. *Genes Dev*. 22: 212-225.

38. Perez AM, *et al* (2017) A localized complex of two protein oligomers controls the orientation of cell polarity. *mBio* 8
39. Childers WS, *et al* (2014) Cell fate regulation governed by a repurposed bacterial histidine kinase. *PLoS Biol*. 12: e1001979.
40. Wu J, Ohta N, Zhao J- & Newton A (1999) PMC23901; A novel bacterial tyrosine kinase essential for cell division and differentiation. *Proc.Natl.Acad.Sci.USA* 96: 13068-13073.
41. Reisinger SJ, Huntwork S, Viollier PH & Ryan KR (2007) DivL performs critical cell cycle functions in caulobacter crescentus independent of kinase activity. *J. Bacteriol*. 189: 8308-8320.
42. Pierce DL, *et al* (2006) Mutations in DivL and CckA rescue a divJ null mutant of caulobacter crescentus by reducing the activity of CtrA. *J. Bacteriol*. 188: 2473-2482.
43. Christen M, *et al* (2010) Asymmetrical distribution of the second messenger c-di-GMP upon bacterial cell division. *Science* 328: 1295-1297.
44. Abel S, *et al* (2013) Bi-modal distribution of the second messenger c-di-GMP controls cell fate and asymmetry during the caulobacter cell cycle. *PLoS Genet*. 9: e1003744.
45. Paul R, *et al* (2004) Cell cycle-dependent dynamic localization of a bacterial response regulator with a novel di-guanylate cyclase output domain. *Genes Dev*. 18(6): 715-727.
46. Paul R, *et al* (2007) Activation of the diguanylate cyclase PleD by phosphorylation-mediated dimerization. *J.Biol.Chem*. 282: 29170-29177.
47. Abel S, *et al* (2011) Regulatory cohesion of cell cycle and cell differentiation through interlinked phosphorylation and second messenger networks. *Mol.Cell* 43: 550-560.
48. Lori C, *et al* (2015) Cyclic di-GMP acts as a cell cycle oscillator to drive chromosome replication. *Nature* 523: 236-239.
49. Petters T, *et al* (2012) The orphan histidine protein kinase SgmT is a c-di-GMP receptor and regulates composition of the extracellular matrix together with the orphan DNA binding response regulator DigR in myxococcus xanthus. *Mol.Microbiol*. 84: 147-165.
50. Poindexter JS (1964) Biological properties and classification of the caulobacter group. *Bacteriol.Rev*. 28: 231-295.
51. Shapiro L & Maizel JV, J. (1973) PMC251651; synthesis and structure of caulobacter crescentus flagella. *J. Bacteriol*. 113: 478-485.
52. Smit J & Agabian N (1982) Caulobacter crescentus pili: Analysis of production during development. *Dev.Biol*. 89: 237-247.
53. Bodenmiller D, Toh E & Brun YV (2004) PMC344395; development of surface adhesion in caulobacter crescentus. *J. Bacteriol*. 186: 1438-1447.
54. Levi A & Jenal U (2006) Holdfast formation in motile swarmer cells optimizes surface attachment during caulobacter crescentus development. *J. Bacteriol*. 188: 5315-5318.
55. Nesper J, Reinders A, Glatter T, Schmidt A & Jenal U (2012) A novel capture compound for the identification and analysis of cyclic di-GMP binding proteins. *J. Proteomics* 75: 4874-4878.
56. Hug I, Deshpande S, Sprecher KS, Pfohl T & Jenal U (2017) Second messenger-mediated tactile response by a bacterial rotary motor. *Science* 358: 531-534.
57. Nesper J, *et al* (2017) Cyclic di-GMP differentially tunes a bacterial flagellar motor through a novel class of CheY-like regulators. *eLife* 6: e28842.
58. Sprecher KS, *et al* (2017) Cohesive properties of the caulobacter crescentus holdfast adhesin are regulated by a novel c-di-GMP effector protein. *mBio* 8: 294.

59. Davis NJ, *et al* (2013) De- and repolarization mechanism of flagellar morphogenesis during a bacterial cell cycle. *Genes Dev*. 27: 2049-2062.
60. Sommer JM & Newton A (1989) PMC209601; turning off flagellum rotation requires the pleiotropic gene pleD: pleA, pleC, and pleD define two morphogenic pathways in caulobacter crescentus. *J. Bacteriol*. 171(1): 401.
61. Christen M, *et al* (2007) DgrA is a member of a new family of cyclic diguanosine monophosphate receptors and controls flagellar motor function in caulobacter crescentus. *Proc.Natl.Acad.Sci.USA* 104: 4112-4117.
62. Aldridge P & Jenal U (1999) Cell cycle-dependent degradation of a flagellar motor component requires a novel-type response regulator. *Mol.Microbiol*. 32(2): 379-391.
63. Grunenfelder B, *et al* (2004) Identification of the protease and the turnover signal responsible for cell cycle-dependent degradation of the caulobacter FliF motor protein. *J. Bacteriol*. 186: 4960-4971.
64. Li G, *et al* (2012) Surface contact stimulates the just-in-time deployment of bacterial adhesins. *Mol.Microbiol*. 83: 41-51.
65. Maddock JR & Shapiro L (1993) Polar localization of the chemoreceptor complex in the escherichia coli cell. *Science* 259: 1717-1723.
66. Tropini C & Huang KC (2012) Interplay between the localization and kinetics of phosphorylation in flagellar pole development of the bacterium caulobacter crescentus. *PLoS Comp.Biol*. 8: e1002602.
67. Subramanian K, Paul MR & Tyson JJ (2015) Dynamical localization of DivL, and PleC in the asymmetric division cycle of caulobacter crescentus: A theoretical investigation of alternative models. *PLoS Comp.Biol*. 11: e1004348.
68. Sciochetti SA, Ohta N & Newton A (2005) The role of polar localization in the function of an essential caulobacter crescentus tyrosine kinase. *Mol.Microbiol*. 56: 1467-1480.
69. Angelastro PS, Sliusarenko O & Jacobs-Wagner C (2010) Polar localization of the CckA histidine kinase and cell cycle periodicity of the essential master regulator CtrA in caulobacter. *J. Bacteriol*. 192: 539-552.
70. Sanselicio S, Berge M, Theraulaz L, Radhakrishnan SK & Viollier PH (2015) Topological control of the caulobacter cell cycle circuitry by a polarized single-domain PAS protein. *Nat.Commun*. 6: 7005.
71. Barchinger SE & Ades SE (2013) Regulated proteolysis: Control of the escherichia coli s(E)-dependent cell envelope stress response. *Subcell.Biochem*. 66: 129-160.
72. Moliere N & Turgay K (2013) General and regulatory proteolysis in bacillus subtilis. *Subcell.Biochem*. 66: 73-103.
73. Janssen BD & Hayes CS (2012) The tmRNA ribosome-rescue system. *Adv.Protein Chem.Struct.Biol*. 86: 151-191.
74. Gur E (2013) The lon AAA+ protease. *Subcell.Biochem*. 66: 35-51.
75. Olivares AO, Baker TA & Sauer RT (2016) Mechanistic insights into bacterial AAA+ proteases and protein-remodelling machines. *Nat. Rev. Microbiol*. 14: 33-44.
76. Wang J, Hartling JA & Flanagan JM (1997) The structure of ClpP at 2.3 A resolution suggests a model for ATP-dependent proteolysis. *Cell* 91: 447-456.
77. Grimaud R, Kessel M, Beuron F, Steven AC & Maurizi MR (1998) Enzymatic and structural similarities between the escherichia coli ATP-dependent proteases, ClpXP and ClpAP. *J.Biol.Chem*. 273: 12476-12481.

78. Tu GF, Reid GE, Zhang JG, Moritz RL & Simpson RJ (1995) C-terminal extension of truncated recombinant proteins in escherichia coli with a 10Sa RNA decapeptide. *J.Biol.Chem.* 270: 9322-9326.
79. Keiler KC, Waller PR & Sauer RT (1996) Role of a peptide tagging system in degradation of proteins synthesized from damaged messenger RNA. *Science* 271: 990-993.
80. Gottesman S, Roche E, Zhou Y & Sauer RT (1998) The ClpXP and ClpAP proteases degrade proteins with carboxy-terminal peptide tails added by the SsrA-tagging system. *Genes Dev.* 12: 1338-1347.
81. Levchenko I, Seidel M, Sauer RT & Baker TA (2000) A specificity-enhancing factor for the ClpXP degradation machine. *Science* 289: 2354-2356.
82. Flynn JM, *et al* (2001) Overlapping recognition determinants within the ssrA degradation tag allow modulation of proteolysis. *Proc.Natl.Acad.Sci.USA* 98: 10584-10589.
83. Farrell CM, Baker TA & Sauer RT (2007) Altered specificity of a AAA+ protease. *Mol.Cell* 25: 161-166.
84. Martin A, Baker TA & Sauer RT (2008) Diverse pore loops of the AAA+ ClpX machine mediate unassisted and adaptor-dependent recognition of ssrA-tagged substrates. *Mol.Cell* 29: 441-450.
85. Wah DA, Levchenko I, Baker TA & Sauer RT (2002) Characterization of a specificity factor for an AAA+ ATPase: Assembly of SspB dimers with ssrA-tagged proteins and the ClpX hexamer. *Chem.Biol.* 9: 1237-1245.
86. Dougan DA, Weber-Ban E & Bukau B (2003) Targeted delivery of an ssrA-tagged substrate by the adaptor protein SspB to its cognate AAA+ protein ClpX. *Mol.Cell* 12: 373-380.
87. Levchenko I, Grant RA, Wah DA, Sauer RT & Baker TA (2003) Structure of a delivery protein for an AAA+ protease in complex with a peptide degradation tag. *Mol.Cell* 12: 365-372.
88. Wah DA, *et al* (2003) Flexible linkers leash the substrate binding domain of SspB to a peptide module that stabilizes delivery complexes with the AAA+ ClpXP protease. *Mol.Cell* 12: 355-363.
89. Flynn JM, Levchenko I, Sauer RT & Baker TA (2004) Modulating substrate choice: The SspB adaptor delivers a regulator of the extracytoplasmic-stress response to the AAA+ protease ClpXP for degradation. *Genes Dev.* 18: 2292-2301.
90. Studemann A, *et al* (2003) Sequential recognition of two distinct sites in sigma(S) by the proteolytic targeting factor RssB and ClpX. *Embo J.* 22: 4111-4120.
91. Nierman WC, *et al* (2001) Complete genome sequence of caulobacter crescentus. *Proc.Natl.Acad.Sci.USA* 98(7): 441.
92. Lupas A, Flanagan JM, Tamura T & Baumeister W (1997) Self-compartmentalizing proteases. *Trends Biochem.Sci.* 22: 399-404.
93. Katayama-Fujimura Y, Gottesman S & Maurizi MR (1987) A multiple-component, ATP-dependent protease from escherichia coli. *J.Biol.Chem.* 262: 4477-4485.
94. Wojtkowiak D, Georgopoulos C & Zylicz M (1993) Isolation and characterization of ClpX, a new ATP-dependent specificity component of the clp protease of escherichia coli. *J.Biol.Chem.* 268: 22609-22617.
95. Gora KG, *et al* (2013) Regulated proteolysis of a transcription factor complex is critical to cell cycle progression in caulobacter crescentus. *Mol.Microbiol.* 87: 1277-1289.

96. Williams B, Bhat N, Chien P & Shapiro L (2014) ClpXP and ClpAP proteolytic activity on divisome substrates is differentially regulated following the caulobacter asymmetric cell division. *Mol.Microbiol.* 93: 853-866.
97. Wright R, Stephens C, Zweiger G, Shapiro L & Alley MR (1996) Caulobacter lon protease has a critical role in cell-cycle control of DNA methylation. *Genes Dev.* 10: 1532-1542.
98. Gorbatuyk B & Marczynski GT (2001) Physiological consequences of blocked caulobacter crescentus dnaA expression, an essential DNA replication gene. *Mol.Microbiol.* 40: 485-497.
99. Ryan KR, Judd EM & Shapiro L (2002) The CtrA response regulator essential for caulobacter crescentus cell-cycle progression requires a bipartite degradation signal for temporally controlled proteolysis. *J.Mol.Biol.* 324: 443-455.
100. Taylor JA, Ouimet M-, Wargachuk R & Marczynski GT (2011) The caulobacter crescentus chromosome replication origin evolved two classes of weak DnaA binding sites. *Mol.Microbiol.* 82: 312-326.
101. Joshi KK, Berge M, Radhakrishnan SK, Viollier PH & Chien P (2015) An adaptor hierarchy regulates proteolysis during a bacterial cell cycle. *Cell* 163: 419-431.
102. Christen M, Christen B, Folcher M, Schauerte A & Jenal U (2005) Identification and characterization of a cyclic di-GMP-specific phosphodiesterase and its allosteric control by GTP. *J.Biol.Chem.* 280: 30829-30837.
103. Bleichert S, Botchan MR & Berger JM (2017) Mechanisms for initiating cellular DNA replication. *Science* 355: eaah6317.
104. Katayama T, Kasho K & Kawakami H (2017) The DnaA cycle in escherichia coli: Activation, function, and inactivation of the initiator protein. *Front.Microbiol* 8: 2496.
105. Marczynski GT (1999) Chromosome methylation and measurement of faithful, once and only once per cell cycle chromosome replication in caulobacter crescentus. *J. Bacteriol.* 181(7): 1984-1993.
106. Collier J & Shapiro L (2009) Feedback control of DnaA-mediated replication initiation by replisome-associated HdaA protein in caulobacter. *J. Bacteriol.* 191: 5706-5716.
107. Jonas K, Chen YE & Laub MT (2011) Modularity of the bacterial cell cycle enables independent spatial and temporal control of DNA replication. *Curr.Biol.* 21: 1092-1101.
108. Fernandez-Fernandez C, Grosse K, Sourjik V & Collier J (2013) The b-sliding clamp directs the localization of HdaA to the replisome in caulobacter crescentus. *Microbiology* 159: 2237-2248.
109. Wargachuk R & Marczynski GT (2015) The caulobacter crescentus homolog of DnaA (HdaA) also regulates the proteolysis of the replication initiator protein DnaA. *J. Bacteriol.* 197: 3521-3532.
110. Collier J, Murray SR & Shapiro L (2006) DnaA couples DNA replication and the expression of two cell cycle master regulators. *Embo J.* 25: 346-356.
111. Gorbatuyk B & Marczynski GT (2005) Regulated degradation of chromosome replication proteins DnaA and CtrA in caulobacter crescentus. *Mol.Microbiol.* 55: 1233-1245.
112. Jonas K, Liu J, Chien P & Laub MT (2013) Proteotoxic stress induces a cell-cycle arrest by stimulating lon to degrade the replication initiator DnaA. *Cell* 154: 623-636.
113. Tsilibaris V, Maenhaut-Michel G & Van Melderen L (2006) Biological roles of the lon ATP-dependent protease. *Res.Microbiol.* 157: 701-713.
114. Liu J, Francis LI, Jonas K, Laub MT & Chien P (2016) ClpAP is an auxiliary protease for DnaA degradation in caulobacter crescentus. *Mol.Microbiol.* 102: 1075-1085.

115. Stephens C, Reisenauer A, Wright R & Shapiro L (1996) A cell cycle-regulated bacterial DNA methyltransferase is essential for viability. *Proc.Natl.Acad.Sci.USA* 93: 1210-1214.
116. Zweiger G, Marczynski GT & Shapiro L (1994) A caulobacter DNA methyltransferase that functions only in the predivisional cell. *J.Mol.Biol*. 235: 472-485.
117. Mohapatra SS, Fioravanti A & Biondi EG (2014) DNA methylation in caulobacter and other alphaproteobacteria during cell cycle progession. *Trends Microbiol*. 22: 528-535.
118. Haakonsen DL, Yuan AH & Laub MT (2015) The bacterial cell cycle regulator GcrA is a s70 cofactor that drives gene expression from a subset of methylated promoters. *Genes Dev*. 29: 2272-2286.
119. Collier J, McAdams HH & Shapiro L (2007) A DNA methylation ratchet governs progression through a bacterial cell cycle. *Proc.Natl.Acad.Sci.USA* 104: 17111-17116.
120. Radhakrishnan SK, Pritchard S & Viollier PH (2010) Coupling prokaryotic cell fate and division control with a bifunctional and oscillating oxidoreductase homolog. *Dev.Cell* 18: 90-101.
121. Beaufay F, *et al* (2015) A NAD-dependent glutamate dehydrogenase coordinates metabolism with cell division in caulobacter crescentus. *Embo J*. 34: 1786-1800.
122. Kelly AJ, Sackett MJ, Din N, Quardokus EM & Brun YV (1998) Cell cycle-dependent transcriptional and proteolytic regulation of FtsZ in caulobacter. *Genes Dev*. 12: 880-893.
123. Martin ME, Trimble MJ & Brun YV (2004) Cell cycle-dependent abundance, stability and localization of FtsA and FtsQ in caulobacter crescentus. *Mol.Microbiol*. 54: 60-74.
124. Wang Y, Jones BD & Brun YV (2001) A set of ftsZ mutants blocked at different stages of cell division in caulobacter. *Mol.Microbiol*. 40: 347-360.
125. Bouveret E & Battesti A (2011) in eds Storz G & Hengge R (ASM Press, Washington, DC), pp 231-250.
126. Battesti A & Bouveret E (2006) Acyl carrier protein/SpoT interaction, the switch linking SpoT-dependent stress response to fatty acid metabolism. *Mol.Microbiol*. 62: 1048-1063.
127. Haseltine WA & Block R (1973) Synthesis of guanosine tetra- and pentaphosphate requires the presence of a codon-specific uncharged transfer ribonucleic acid in the acceptor site of ribosomes. *Proc.Natl.Acad.Sci.USA* 70: 1564-1568.
128. Xiao H, *et al* (1991) Residual guanosine 3',5'-bispyrophosphate synthetic activity of relA null mutants can be eliminated by spoT null mutations. *J.Biol.Chem*. 266: 5980-5990.
129. Seyfzadeh M, Keener J & Nomura M (1993) spoT-dependent accumulation of guanosine tetraphosphate in response to fatty acid starvation in escherichia coli. *Proc.Natl.Acad.Sci.USA* 90: 11004-11008.
130. Vinella D, Albrecht c, Cashel M & D'Ari R (2005) Iron limitation induces SpoT-dependent accumulation of ppGpp in escherichia coli. *Mol.Microbiol*. 56: 958-970.
131. Haugen SP, Ross W & Gourse RL (2008) Advances in bacterial promoter recognition and its control by factors that do not bind DNA. *Nat. Rev. Microbiol*. 6: 507-519.
132. Chiaramello AE & Zyskind JW (1990) Coupling of DNA replication to growth rate in escherichia coli: A possible role for guanosine tetraphosphate. *J. Bacteriol*. 172: 2013-2019.
133. Lesley JA & Shapiro L (2008) SpoT regulates DnaA stability and initiation of DNA replication in carbon-starved caulobacter crescentus. *J. Bacteriol*. 190: 6867-6880.
134. England JC, Perchuk BS, Laub MT & Gober JW (2010) Global regulation of gene expression and cell differentiation in caulobacter crescentus in response to nutrient availability. *J. Bacteriol*. 192: 819-833.

135. Ronneau S, Petit K, De Bolle X & Hallez R (2016) Phosphotransferase-dependent accumulation of (p)ppGpp in response to glutamine deprivation in caulobacter crescentus. *Nat.Commun*. 7: 11423.
136. Boutte CC, Henry JT & Crosson S (2012) ppGpp and polyphosphate modulate cell cycle progression in caulobacter crescentus. *J. Bacteriol*. 194: 28-35.
137. Boutte CC & Crosson S (2011) The complex logic of stringent response regulation in caulobacter crescentus: Starvation signalling in an oligotrophic environment. *Mol.Microbiol*. 80: 695-714.
138. Gonzalez D & Collier J (2014) Effects of (p)ppGpp on the progression of the cell cycle of caulobacter crescentus. *J. Bacteriol*. 196: 2514-2525.
139. Stott KV, *et al* (2015) (P)ppGpp modulates cell size and the initiation of DNA replication in caulobacter crescentus in response to a block in lipid biosynthesis. *Microbiology* 161: 553-564.
140. Reitzer L (2003) Nitrogen assimilation and global regulation in escherichia coli. *Annu Rev Microbiol* 57(1): 155-176.
141. Ely B (1991) Genetics of caulobacter crescentus. *Meth Enzymol* 204: 372-384.
142. Deutscher J, *et al* (2014) The bacterial phosphoeholpyruvate:Carbohydrate phosphotransferase system: Regulation by protein phosphorylation and phosphorylation-dependent protein-protein interactions. *Microbiol.Mol.Biol.Rev*. 78: 231-256.
143. Goodwin RA & Gage DJ (2014) Biochemical characterization of a nitrogen-type phosphotransferase system reveals that enzyme EI(ntr) integrates carbon and nitrogen signaling in sinorhizobium meliloti. *J. Bacteriol*. 196: 1901-1907.
144. Sanselicio S & Viollier PH (2015) Convergence of alarmone and cell cycle signaling from trans-encoded sensory domains. *mBio* 6: 1415.
145. Fioravanti A, *et al* (2013) DNA binding of the cell cycle transcriptional regulator GcrA depends on N6-adenosine methylation in caulobacter crescentus and other alphaproteobacteria. *PLoS Genet*. 9: e1003541.
146. Holtzendorff J, *et al* (2004) Oscillating global regulators control the genetic circuit driving a bacterial cell cycle. *Science* 304: 983-987.
147. Ross W, Vrentas CE, Sanchez-Vazquez P, Gaal T & Gourse RL (2013) The magic spot: A ppGpp binding site on E. coli RNA polymerase responsible for regulation of transcription initiation. *Mol.Cell* 50: 420-429.
148. Ross W, *et al* (2016) ppGpp binding to a site at the RNAP-DskA interface accounts for its dramatic effects on transcription initiation during the stringent response. *Mol.Cell* 62: 811-823.
149. Leslie DJ, *et al* (2015) Nutritional control of DNA replication initiation through the proteolysis and regulated translation of DnaA. *PLoS Genet*. 11: e1005342.
150. Storz G & Spiro S (2011) in eds Storz G & Hengge R (ASM Press, Washington, D.C.), pp 157-173.
151. Sporer AJ, Kahl LJ, Price-Whelan A & Dietrich LEP (2017) Redox-based regulation of bacterial development and behavior. *Annu. Rev. Biochem*. 86: 777-797.
152. Hanson GT, *et al* (2004) Investigating mitochondrial redox potential with redox-sensitive green fluorescent protein indicators. *J.Biol.Chem*. 279: 13044-13053.
153. Bhaskar A, *et al* (2014) Reengineering redox sensitive GFP to measure mycothiol redox potential of mycobacterium tuberculosis during infection. *PLoS Pathog*. 10: e1003902.

154. Narayanan S, Janakiraman B, Kumar L & Radhakrishnan SK (2015) A cell cycle-controlled redox switch regulates the topoisomerase IV activity. *Genes Dev*. 29: 1175-1187.
155. Espeli O, Levine C, Hassing H & Marians KJ (2003) Temporal regulation of topoisomerase IV activity in E. coli. *Mol.Cell* 11: 189-201.
156. Badrinarayanan A, Le TBK & Laub MT (2015) Bacterial chromosome organization and segregation. *Annu Rev Cell Dev Biol* 31: 171-199.
157. Miñambres B, Olivera ER, Jensen RA & Luengo JM (2000) A new class of glutamate dehydrogenases (GDH): BIOCHEMICAL AND GENETIC CHARACTERIZATION OF THE FIRST MEMBER, THE AMP-REQUIRING NAD-SPECIFIC GDH OF STREPTOMYCES CLAVULIGERUS. *Journal of Biological Chemistry* 275(50): 39529-39542.
158. Lindenberg S, Klauck G, Pesavento C, Klauck E & Hengge R (2013) The EAL domain protein YciR acts as a trigger enzyme in a c-di-GMP signalling cascade in E. coli biofilm control. *Embo J*. 32: 2001-2014.
159. Dahlstrom KM, Giglio KM, Sondermann H & O'Toole GA (2016) The inhibitory site of a diguanylate cyclase is a necessary element for interaction and signaling with an effector protein. *J. Bacteriol*. 198: 1595-1603.
160. Battesti A & Gottesman S (2013) Roles of adaptor proteins in regulation of bacterial proteolysis. *Curr. Opin. Microbiol*. 16: 140-147.
161. Bassermann F, Eichner R & Pagano M (2014) The ubiquitin proteasome system — implications for cell cycle control and the targeted treatment of cancer. *Biochimica Et Biophysica Acta (BBA) - Molecular Cell Research* 1843(1): 150-162.
162. Poindexter JS (1981) The caulobacters: Ubiquitous unusual bacteria. *Microbiol Rev* 45(1): 123-179.
163. Joshi KK & Chien P (2016) Regulated proteolysis in bacteria: Caulobacter. *Annu Rev Genet* 50(1): 423-445.
164. Ausmees N, Kuhn JR & Jacobs-Wagner C (2003) The bacterial cytoskeleton: An intermediate filament-like function in cell shape. *Cell* 115: 705-713.
165. Cabeen MT, *et al* (2009) Bacterial cell curvature through mechanical control of cell growth. *Embo J* 28(9): 1208-1219.
166. Persat A, Stone HA & Gitai Z (2014) The curved shape of caulobacter crescentus enhances surface colonization in flow. *Nat.Commun*. 5: 3824.
167. Fiebig A, *et al* (2014) A cell cycle and nutritional checkpoint controlling bacterial surface adhesion. *PLOS Genetics* 10(1): e1004101.
168. Tsokos CG & Laub MT (2012) Polarity and cell fate asymmetry in caulobacter crescentus. *Curr. Opin. Microbiol*. 15: 744-750.
169. Jenal U (2009) The role of proteolysis in the caulobacter crescentus cell cycle and development. *Res.Microbiol*. 160: 687-695.
170. Frandi A & Collier J (2019) Multilayered control of chromosome replication in *caulobacter crescentus*. *Biochem Soc Trans* 47(1): 187-196.
171. Chien P, Perchuk BS, Laub MT, Sauer RT & Baker TA (2007) Direct and adaptor-mediated substrate recognition by an essential AAA+ protease. *Proc.Natl.Acad.Sci.USA* 104: 6590-6595.
172. Chan C, *et al* (2004) Structural basis of activity and allosteric control of diguanylate cyclase. *Proc Natl Acad Sci U S A* 101(49): 17084-17089.

173. Christen B, *et al* (2006) Allosteric control of cyclic di-GMP signaling. *Journal of Biological Chemistry* 281(42): 32015-32024.
174. Taylor JA, Wilbur JD, Smith SC & Ryan KR (2009) Mutations that alter RcdA surface residues decouple protein localization and CtrA proteolysis in caulobacter crescentus. *J.Mol.Biol*. 394: 46-60.
175. Baker TA & Sauer RT (2012) ClpXP, an ATP-powered unfolding and protein-degradation machine. *Biochim. Biophys. Acta* 1823: 15-28.
176. Sauer RT & Baker TA (2011) AAA+ proteases: ATP-fueled machines of protein destruction. *Annu Rev Biochem* 80(1): 587-612.
177. Siddiqui SM, Sauer RT & Baker TA (2004) Role of the processing pore of the ClpX AAA+ ATPase in the recognition and engagement of specific protein substrates. *Genes & Development* 18(4): 369-374.
178. Martin A, Baker TA & Sauer RT (2008) Protein unfolding by a AAA+ protease is dependent on ATP-hydrolysis rates and substrate energy landscapes. *Nature Structural &Amp; Molecular Biology* 15: 139.
179. Martin A, Baker TA & Sauer RT (2008) Pore loops of the AAA+ ClpX machine grip substrates to drive translocation and unfolding. *Nature Structural &Amp; Molecular Biology* 15: 1147.
180. Glynn SE, Martin A, Nager AR, Baker TA & Sauer RT (2009) Structures of asymmetric ClpX hexamers reveal nucleotide-dependent motions in a AAA+ protein-unfolding machine. *Cell* 139(4): 744-756.
181. Wojtyra UA, Thibault G, Tuite A & Houry WA (2003) The N-terminal zinc binding domain of ClpX is a dimerization domain that modulates the chaperone function. *Journal of Biological Chemistry* 278(49): 48981-48990.
182. Judd EM, Ryan KR, Moerner WE, Shapiro L & McAdams HH (2003) Fluorescence bleaching reveals asymmetric compartment formation prior to cell division in caulobacter. *Proc.Natl.Acad.Sci.USA* 100: 8235-8240.
183. Gora KG, *et al* (2010) A cell-type-specific protein-protein interaction modulates transcriptional activity of a master regulator in caulobacter crescentus. *Mol.Cell* 39: 45-467.
184. Tan MH, Kozdon JB, Shen X, Shapiro L & McAdams HH (2010) An essential transcription factor, SciP, enhances robustness of caulobacter cell cycle regulation. *Proc.Natl.Acad.Sci.USA* 107: 18985-18990.
185. Evinger M & Agabian N (1977) Envelope-associated nucleoid from caulobacter crescentus stalked and swarmer cells. *J. Bacteriol*. 132: 294-301.
186. Meisenzahl AC, Shapiro L & Jenal U (1997) Isolation and characterization of a xylose-dependent promoter from caulobacter crescentus. *J. Bacteriol*. 179: 592-600.
187. Lessard JC (2013) Growth media for E. coli. *Meth Enzymol* 533: 181-189.
188. Roberts RC, *et al* (1996) Identification of a caulobacter crescentus operon encoding hcrA, involved in negatively regulating heat-inducible transcription, and the chaperone gene grpE. *J. Bacteriol*. 178: 1829-1841.
189. Madhusudan, *et al* (1996) Crystal structure of a phosphatase-resistant mutant of sporulation response regulator Spo0F from bacillus subtilis. *Structure* 4: 679-690.
190. Ozaki S, *et al* (2014) Activation and polar sequestration of PopA, a c-di-GMP effector protein involved in caulobacter crescentus cell cycle control. *Mol.Microbiol*. 94: 580-594.

191. Holmes JA, *et al* (2016) Caulobacter PopZ forms an intrinsically disordered hub in organizig bacterial cell poles. *Proc.Natl.Acad.Sci.USA* 113: 12490-12495.
192. Alley MR (2001) The highly conserved domain of the caulobacter McpA chemoreceptor is required for its polar localization. *Mol.Microbiol*. 40: 1335-1343.
193. Tsai JW & Alley MR (2001) Proteolysis of the caulobacter McpA chemoreceptor is cell cycle regulated by a ClpX-dependent pathway. *J. Bacteriol*. 183: 5001-5007.
194. Briegel A, *et al* (2008) Location and architecture of the caulobacter crescentus chemoreceptor array. *Mol.Microbiol*. 69: 30-41.
195. Nikaido H (2003) Molecular basis of bacterial outer membrane permeability revisited. *Microbiol. Mol. Biol. Rev*. 67: 593-656.
196. Whitfield C & Trent MS (2014) Biosynthesis and export of bacterial lipopolysaccharides. *Annu. Rev. Biochem*. 83: 99-128.
197. Hicks G & Jia Z (2018) Structural basis for the lipopolysaccharide export activity of the bacterial lipopolysaccharide transport system. *Int. J. Mol. Sci*. 19: E2680.
198. Zhou P & Zhao J (2017) Structure, inhibition, and regulation of essential lipid A enzymes. *Biochim. Biophys. Acta Mol. Cell. Biol. Lipids* 1862: 1424-1438.
199. Scott AJ, Oyler BL, Goodlett DR & Ernst RK (2017) Lipid A modifications in extreme conditions and identification of unique modifying enzymes to define the toll-like receptor 4 structure-activity relationship. *Biochem. Biophys. Acta* 1862: 1439-1450.
200. Van Amersfoort ES, Van Berkel TJ & Kuiper J (2003) Receptors, mediators, and mechanisms involved in bacterial sepsis and septic shock. *Clin. Microbiol. Rev*. 16: 379-414.
201. Saraswat M, *et al* (2013) Preparative purification of recombinant proteins: Current status and future trends. *Biomed. Res. Int*. 2013: 312709.
202. Smit J, *et al* (2008) Structure of a novel lipid A obtained from the lipopolysaccharide of *caulobacter crescentus*. *Innate Immun*. 14: 25-37.
203. Raetz CR & Whitfield C (2002) Lipopolysaccharide endotoxins. *Annu. Rev. Biochem*. 71: 635-700.
204. Shapland EB, Reisinger SJ, Bajwa AK & Ryan KR (2011) An essential tyrosine phosphatase homolog regulates cell separation, outer membrane integrity, and morphology in caulobacter crescentus. *J. Bacteriol*. 193: 4361-4370.
205. Meredith TC, Aggarwal P, Mamat U, Lindner B & Woodard RW (2006) Redefining the requisite lipopolysaccharide structure in *escherichia coli*. *ACS Chem. Biol*. 1: 33-42.
206. Mamat U, *et al* (2008) Single amino acid substitutions in either YhjD or MsbA confer viability to 3-deoxy-D-*manno*-oct-2-ulosonic acid-depleted *escherichia coli*. *Mol. Microbiol*. 67: 633-648.
207. Steeghs L, *et al* (1998) Meningitis bacterium is viable without endotoxin. *Nature* 392: 449-450.
208. Peng D, Hong W, Choudhury BP, Carlson RW & Gu X- (2005) *Moraxella cararrhalis* bacterium without endotoxin, a potential vaccine candidate. *Infect. Immun*. 73: 7569-7577.
209. Moffatt JH, *et al* (2010) Colistin resistance in *acinetobacter baumannii* is mediated by complete loss of lipopolysaccharide production. *Antimicrob. Agents Chemother*. 54: 4971-4977.

210. Porcella SF & Schwan TG (2001) *Borrelia burgdorferi* and *treponema pallidum*: A comparison of functional genomics, environmental adaptations, and pathogenic mechanisms. *J. Clin. Invest*. 107: 651-656.
211. Kawahara K, *et al* (1991) Chemical structure of glycosphingolipids isolated from *sphingomonas paucimobilis*. *FEBS Lett*. 292: 107-110.
212. Lasker K, Mann TH & Shapiro L (2016) An intracellular compass spatially coordinates cell cycle modules in *caulobacter crescentus* . *Curr. Opin. Microbiol*. 33: 131-139.
213. Walker SG, Karunaratne DN, Ravenscroft N & Smit J (1994) Characterization of mutants of *caulobactyer crescentus* defective in surface attachment of the paracrystalline surface layer. *J. Bacteriol*. 176: 6313-6323.
214. Qureshi N, *et al* (1988) Complete structural determination of lipopolysaccharide obtained from deep rough mutant of *escherichia coli*. purification by high performance liquid chromatography and direct analysis by plasma desorption mass spectrometry. *J. Biol. Chem*. 263: 11971-11976.
215. Ingram BO, Sohlenkamp C, Geiger O & Raetz CR (2010) Altered lipid A structures and polymyxin hypersensitivity of *rhizobium etli* mutants lacking the LpxE and LpxF phosphatases. *Biochem. Biophys. Acta* 180: 593-604.
216. Marks ME, *et al* (2010) The genetic basis of laboratory adaptation in caulobacter crescentus. *J. Bacteriol*. 192: 3678-3688.
217. Ely B & Scott LE (2014) Correction of the *caulobacter crescentus* NA1000 genome annotation. *PLoS One* 9: e91668.
218. Figurski DH & Helinski DR (1979) Replication of an origin-containing derivative of plasmid RK2 dependent on a plasmid function provided in *trans*. *Proc. Natl. Acad. Sci. USA* 76: 1648-1652.
219. Gilchrist A & Smit J (1991) Transformation of freshwater and marine caulobacters by electroporation. *J. Bacteriol*. 173: 921-925.
220. Afgan E, *et al* (2016) The galaxy platform for accessible, reproducible and collaborative biomedical analyses: 2016 update. *Nucleic Acids Res*. 44: W10.
221. Davis MRJ & Goldberg JB (2012) Purification and visualization of lipopolysaccharide from gram-negative bacteria by hot aqueous-phenol extraction. *J. Vis. Exp*. : 3916.
222. Westphal O & Jann K (1965) Bacterial lipopolysaccharides. *Methods Carbohydr. Chem*. 5: 83.
223. Leung LM, *et al* (2017) Identification of the ESKAPE pathogens by mass spectrometric analysis of microbial membrane glycolypids7: 6403.
224. Mastonarde DN (2005) Automated electron microscope tomography using robust prediction of specimen movements. *J. Struct. Biol*. 152: 36-51.
225. Zheng SQ, *et al* (2017) MonionCor2: Anisotropic correction of bean-induced motion for improved cryo-electron microscopy. *Nat. Methods* 14: 331-332.
226. Kremer JR, Mastonarde DN & McIntosh JR (1996) Computer visualization of three-dimensional image data using IMOD. *J. Struct. Biol*. 116: 71-76.
227. Frangakis AS & Hegerl R (2001) Noise reduction in electron tomographic reconstructions using nonlinear anisotropic diffusion. *J. Struct. Biol*. 135: 239-250.
228. Thanbichler M, Iniesta AA & Shapiro L (2007) A comprehensive set of plasmids for vanillate- and xylose-inducible gene expression in caulobacter crescentus. *Nucleic Acids Res*. 35: e137.

229. Blondelet-Rouault MH, Weiser J, Lebrihi A, Branny P & Pernodet JL (1997) Antibiotic resistance gene cassettes derived from the omega interposon for use in *E. coli* and *streptomyces*. *Gene* 190: 315-317.
230. Skerker JM, Prasol MS, Perchuk BS, Biondi EG & Laub MT (2005) Two-component signal transduction pathways regulating growth and cell cycle progresion in a bacterium: A systems-level analysis. *PLoS Biol*. 3: e334.
231. Schrader JM, *et al* (2014) The coding and noncoding architecture of the caulobacter crescentus genome. *PLoS Genet*. 10: e10044463.
232. Cabeen MT, *et al* (2010) Mutations in the lipopolysaccharide biosynthesis pathway interfer with crescentin-mediated cell curvature in *caulobacter crescentus*. *J. Bacteriol*. 192: 3368-3378.
233. Samuel G & Reeves P (2003) Biosynthesis of O-antigens: Genes and pathways involved in nucleotide sugar precursor synthesis and O-antigen assembly. *Carboyhdr. Res*. 338: 2503-2519.
234. Jones MD, Vinogradov E, Nomellini JF & Smit J (2015) The core and O-polysaccharide structure of the *caulobacter crescentus* lipopolysaccharide. *Carbohydr.Res*. 402: 111-117.
235. Marolda CL, Lahiry P, Vines E, Salidas S & Valvano MA (2006) Micromethods for the characterization of lipid A-core and O-antigen lipopolysaccharide. *Methods Mol. Biol*. 347: 237-252.
236. Christen B, *et al* (2011) The essential genome of a bacterium. *Mol.Syst.Biol*. 7: 528.
237. Korbel JO, Jensen LJ, von Mering C & Bork P (2004) Analysis of genomic context: Prediction of functional associations from conserved bidirectionally transcribed gene pairs. *Nat. Biotechnol*. 22: 911-917.
238. Miller AK, *et al* (2011) PhoQ mutations promote lipid A modification and polymyxin resistance of *pseudomonas aeruginosa* found in colistin-treated cystic fibrosis patients. *Antimicrob. Agents Chemother*. 55: 5761-5769.
239. Beceiro A, *et al* (2011) Phosphoethanolamine modification of lipid A in colistin-resistant variants of *acinetobacter baumannii* mediated by the *pmrAB* two-component regulatory system. *Antimicrob. Agents Chemother*. 55: 3370-3379.
240. McClerren AL, *et al* (2005) A slow, tight-binding inhibitor of the zinc-dependent deacetylase LpxC of lipid A biosynthesis with antibiotic activity comparable to ciprofloxacin. *Biochemistry* 44: 16574-16583.
241. Higashi Y, Strominger JL & Sweeley CC (1967) Structure of a lipid intermediate in cell wall peptidoglycan synthesis: A derivative of a C55 isoprenoid alcohol. *Proc. Natl. Acad. Sci. USA* 57: 1878-1884.
242. Wright A, Dankert M, Fennessey P & Robbins PW (1967) Characterization of a polyisoprenoid compound functional in O-antigen biosynthesis. *Proc. Natl. Acad. Sci. USA* 57: 1798-1803.
243. Manat G, *et al* (2014) Deciphering the metabolism of undeprenyl-phosphate: The bacterial cell-wall unit carrier at the membrane frontier. *Microb. Drub Resist*. 20: 199-214.
244. Jorgenson MA & Young KD (2016) Interrupting biosynthesis of O-antigen or the lipopolysaccharide core produces morphological defects in *escherichia coli* by sequestering undecaprenyl phosphate. *J. Bacteriol*. 198: 3070-3079.

245. Apfel CM, Takacs B, Fountoulakis M, Stieger M & Keck W (1999) Use of genomics to identify bacterial undecaprenyl pyrophosphate synthetase: Cloning, expression, and characterization of the essential *uppS* gene. *J. Bacteriol.* 181: 483-492.
246. Marquardt JL, Siegele DA, Kolter R & Walsh CT (1992) Cloning and sequencing of *escherichia coli murZ* and purification of its product, a UDP-N-acetylglucosamine enolpyruvyl transferase. *J. Bacteriol.* 174: 5748-5752.
247. Kahan FM, Kahan JS, Cassidy PJ & Kropp H (1974) The mechanism of action of fosfomycin (phosphonomycin). *Ann. N. Y. Acad. Sci.* 235: 364-386.
248. Malinverni JC & Silhavy TJ (2009) An ABC transport system that maintains lipid asymmetry in the gram-negative outer membrane. *Proc. Natl. Acad. Sci. USA* 106: 8009-8014.
249. Powers MJ & Trent MS (2018) Phospholipid retention in the absence of asymmetry strengthens the outer membrane permeability barrier to last-resort antibiotics. *Proc. Natl. Acad. Sci. USA* 115: E8527.
250. Kamischke C, *et al* (2019) The *acinetobacter baumannii* mla system and glycerophospholipid transport to the outer membrane. *eLife* 8: e40171.
251. da Silva Neto, J. F., Lourenco RF & Marques MV (2013) Global transcriptional response of *caulobacter crescentus* to iron availability. *BMC Genomics* 14: 549.
252. Leaden L, *et al* (2018) Iron deficiency generates oxidative stress and activation of the SOS response in *caulobacter crescentus*. *Front. Microbiol.* 9: 2014.
253. Bagg A & Neilands JB (1987) Ferric uptake regulation protein acts as a repressor, employing iron (II) as a cofactor to bind the operator of an iron transport operon in *escherichia coli*. *Biochemistry* 26: 5471-5477.
254. Roier S, *et al* (2015) A novel mechanism for the biogensis of outer membrane vesicles in gram-negative bacteria7: 10515.
255. Takeuchi Y & Nikaido H (1981) Persistence of segregated phospholipid domains in phospholipid-lipopolysaccharide mixed bilayers: Studies with spin-labeled phospholipids. *Biochemistry* 20: 523-529.
256. Kubiak J, Brewer J, Hansen S & Bagatolli LA (2011) Lipid lateral organization on giant unilamellar vesicles containing lipopolysaccharides. *Biophys. J.* 100: 978-986.
257. Zhang G, Meredity TC & Kahne D (2013) On the essentiality of lipopolysaccharide to gram-negative bacteria. *Curr. Opin. Microbiol.* 16: 779-785.
258. Wei JR, *et al* (2017) LpxK is essential for growth of *acinetobacter baumannii* ATCC 19606: Relationship to toxic accumulation of lipid A pathway intermediates. *mSphere* 2: 199.
259. Boll JM, *et al* (2016) A penicillin-binding protein inhibits selection of colistin-resistant, lipooligosaccharide-deficient *acinetobacter baumannii*. *Proc. Natl. Acad. Sci. USA* 113: E6237.
260. Steeghs L, *et al* (2001) Outer membrane composition of a lipopolysaccharide-deficient *neisseria meningitidis* mutant. *Embo J.* 20: 6937-6945.
261. Bos MP & Tommassen J (2005) Viability of a capsule- and lipopolysaccharide-deficient mutant of *neisseria meningitidis*. *Infect. Immun.* 73: 6194-6197.
262. Henry R, *et al* (2015) The transcriptomic response of *acinetobacter baumannii* to colistin and diripenem alone and in combination in an *in vitro* pharmacokinetics/pharmacodynamics model. *J. Antimicrob. Chermother.* 70: 1303-1313.

263. Cassat JE & Skaar EP (2013) Iron in infection and immunity. *Cell Host Microbe* 13: 509-519.
264. Carretero-Ledesma M, *et al* (2018) Phenotypic changes associated with colistin resistance due to lipopolysaccharide loss in *acinetobacter baumannii*. *Virulence* 9: 930-942.
265. Yoon SH, *et al* (2012) Surface acoustic wave nebulization facilitating lipid mass spectrometric analysis. *Anal. Chem.* 84: 6530-6537.
266. Chan S & Reinhold VN (1994) Detailed structural characterization of lipid A: Electrospray ionization coupled with tandem mass spectrometry. *Anal. Biochem.* 218: 63-73.

Appendix

Appendix Table 1. Species and National Center for Biotechnology Information genome accession numbers associated with the CtrA receiver domain sequences.

Species	Accession Numbers
Rhizobium etli CFN 42	NC_007761.1
Agrobacterium tumefaciens LBA2413	CP007225.1
Sinorhizobium meliloti SM11	CP001830.1
Mesorhizobium loti MAFF303099	BA000012.4
Brucella melitensis biovar Abortus 2308	NC_007618.1
Stappia aggregata, renamed Labrenzia aggregata IAM 12614	AAUW00000000.1
Bradyrhizobium japonicum USDA 6	NC_017249.1
Nitrobacter winogradskyi Nb-255	CP000115.1
Rhodopseudomonas palustris BisB5	CP000283.1
Azorhizobium caulinodans ORS 571	NC_009937.1
Xanthobacter autotrophicus Py2	CP000781.1
Methylobacterium extorquens HTCC2597	AAMO01000004.1
Roseobacter litoralis Och 149	CP002623.1
Roseovarius sp. 217	AAMV01000001.1
Rhodobacter sphaeroides 2.4.1	CP000143.2
Sagittula stellata E-37	AAYA01000004.1
Dinoroseobacter shibae DL12 = DSM16493	CP000830.1
Sulfitobacter sp. EE-36	AALV01000002.1
Loktanella vestfoldensis SKA53	AAMS01000005.1
Jannaschia sp. CCS1	NC_007802.1
Sphingomonas wittichii RW1	NC_009511.1
Paracoccus denitrificans PD1222	NC_008687.1

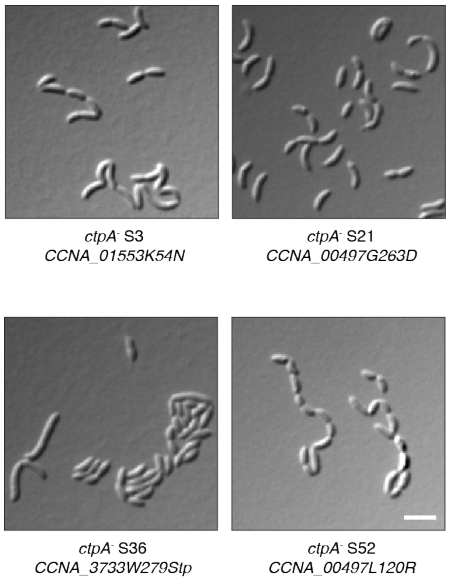

Appendix Figure 1: Isolates from the Δ*ctpA* suppressor screen show variations in morphology. DIC images of suppressor isolates confirmed to have lost the *ctpA* covering plasmid from the parent KR3906. Putative suppressor mutations identified by whole-genome resequencing are indicated. Scale bar, 3 μm.

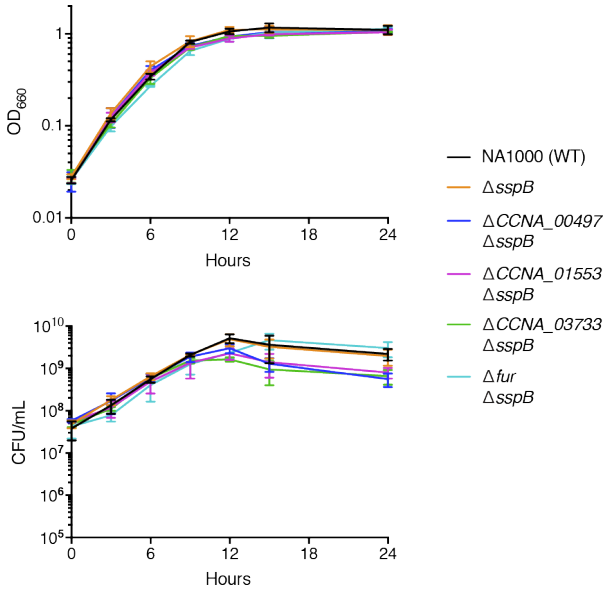

Appendix Figure 2: Δ*sspB* strains containing suppressor knockout mutations have growth characteristics comparable to wild-type strain NA1000. Growth curves showing OD_{660} and colony-forming units (CFU) per mL of the indicated strains grown in PYE (mean ± s.d., N=3).

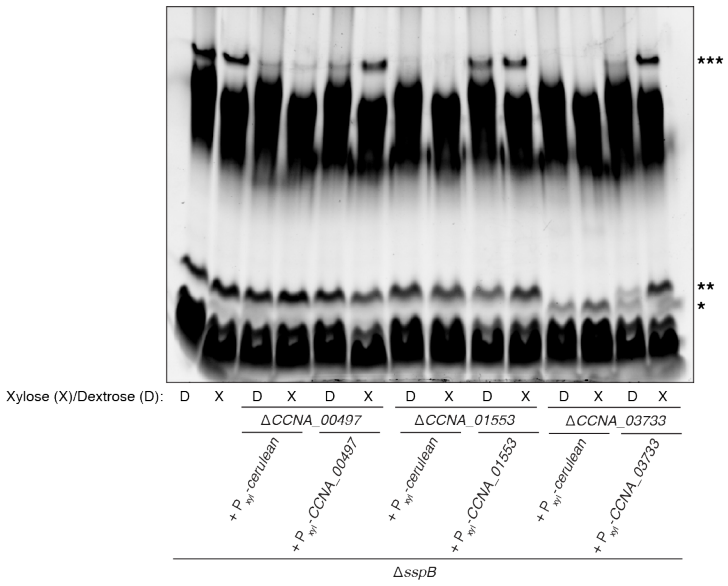

Appendix Figure 3: Complementation of O-antigen biosynthesis using plasmid-borne genes driven by a xylose-inducible promoter. Pro-Q Emerald-stained polyacrylamide gel of Proteinase K-treated whole-cell lysates of the indicated strains grown in either PYED or PYEX. Samples were normalized by OD_{660}. *** = S-LPS. ** = putative complete lipid A-core species. * = putative incomplete lipid A-core species in strains deficient in *manC* activity (*CCNA_03733*).

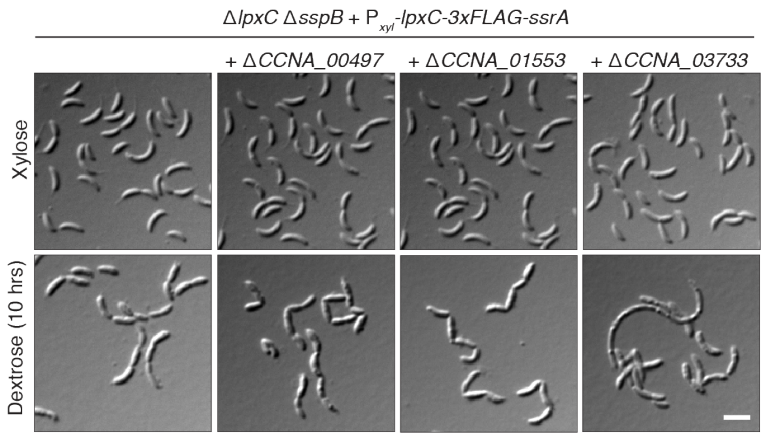

Appendix Figure 4: Disruption of O-antigen biosynthesis does not ameliorate the morphological effects of LpxC depletion. DIC images of the indicated strains grown in inducing (xylose) or depleting (dextrose) conditions for 10 hours. Scale bar, 3 μm.

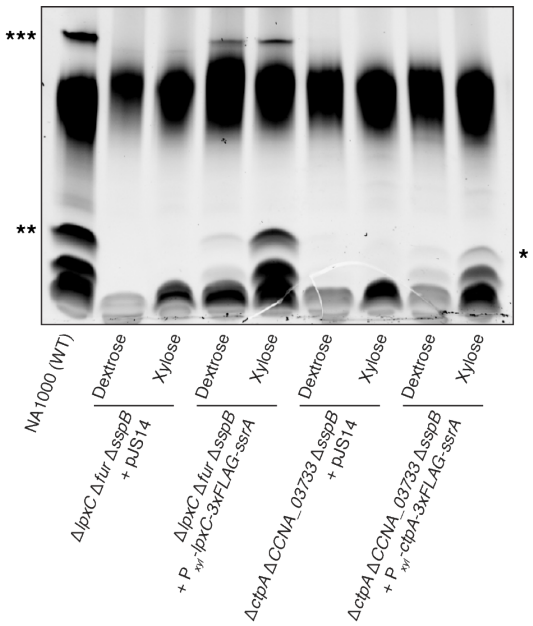

Appendix Figure 5: Lipid A production defects in *lpxC* and *ctpA* mutants can be complemented with the respective expression vector. Pro-Q Emerald-stained polyacrylamide gel of Proteinase K-treated whole-cell lysates of the indicated strains. Cells were grown in PYED with antibiotic before being washed 2x with PYE and released into either PYEX or PYED, both with antibiotic. Cultures were allowed to grow for 6 hours before harvesting. Samples were normalized by OD_{660}. NA1000 grown in PYE is included for reference. We interpret the appearance of S-LPS (***) and small amounts of lipid A +/- core (**) in Δ*lpxC* Δ*sspB* Δ*fur* + P_{xyl}-*lpxC-3xFLAG-ssrA* grown in PYED to mean that leaky expression of LpxC in dextrose is sufficient to drive some LPS production. For *ctpA* complementation, the full-length S-LPS is not restored and the lipid A-core species is reduced in size (*) because the strain still lacks *CCNA_03733*, which is needed for mannose incorporation into core polysaccharide and O-antigen.

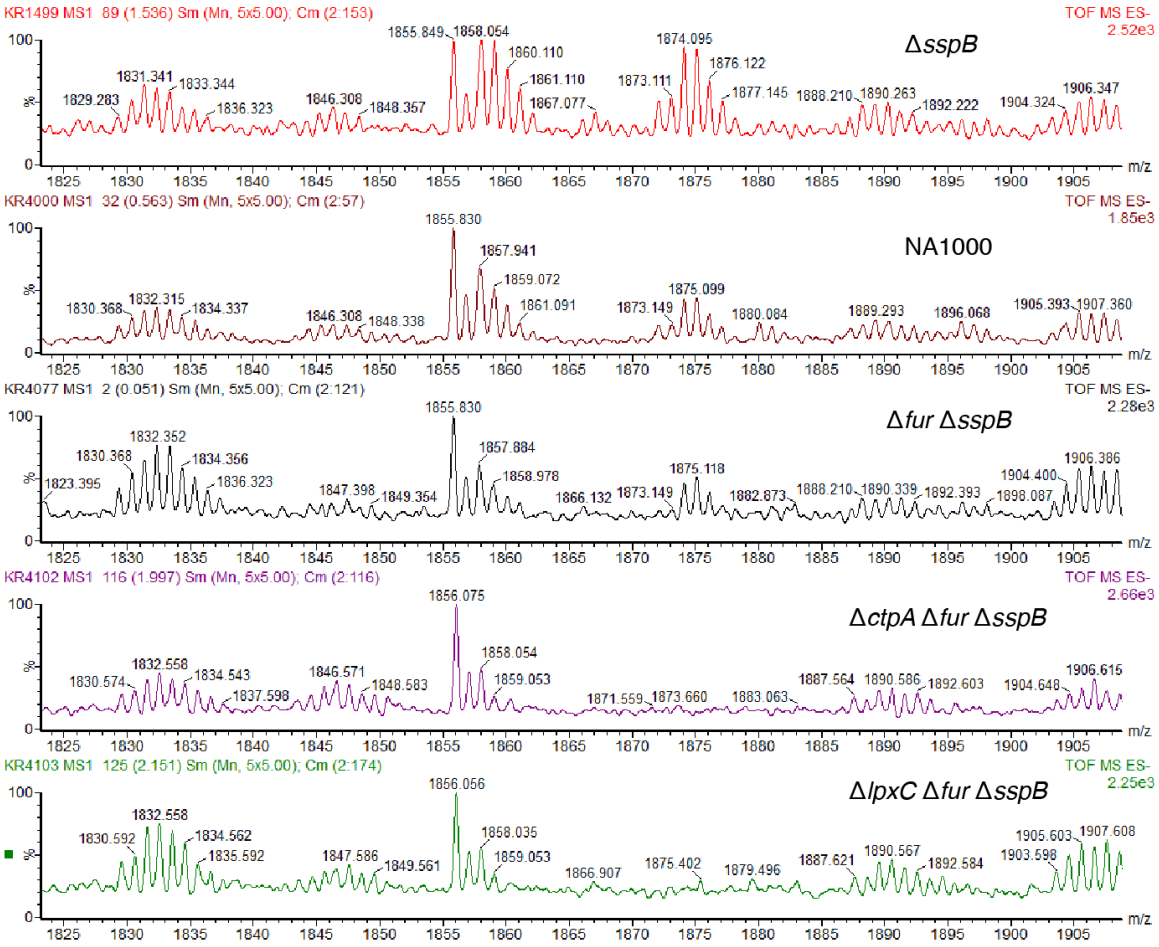

Appendix Figure 6a. Electrospray ionization mass spectrometry (ESI-MS) data of *Caulobacter* extracts. ESI-MS data for lipid extracts from the indicated strains. Both Δ*ctpA* Δ*fur* Δ*sspB* and Δ*lpxC* Δ*fur* Δ*sspB* lack the ion at *m/z* 1874, which is the reported *m/z* value for *Caulobacter* lipid A in negative ion mode as $[M\text{-}H]^{-1}$ (202). All extracts contain ions from *m/z* 1856 to 1860. In Δ*sspB*, NA1000 and Δ*fur* Δ*sspB*, but not in Δ*ctpA* Δ*fur* Δ*sspB* or Δ*lpxC* Δ*fur* Δ*sspB*, ESI-tandem mass spectrometry (ESI-MS/MS) identified an ion at *m/z* 1858 that represents a dehydroxylated form of 1874. The ion at *m/z* 1856 present in all samples was subjected to ESI-MS/MS and produced a fragmentation pattern unlike lipid A leading to the conclusion that this is a chemical contaminant of unknown origin and composition. Further adding to the conclusion that *m/z* 1858 is not lipid A in Δ*ctpA* Δ*fur* Δ*sspB* or Δ*lpxC* Δ*fur* Δ*sspB* is that theoretical chemical composition analysis produced isotopic distributions for *m/z* 1874 and *m/z* 1858 in Δ*sspB*, NA1000 and Δ*fur* Δ*sspB*, but not in Δ*ctpA* Δ*fur* Δ*sspB* or Δ*lpxC* Δ*fur* Δ*sspB*, that resemble the isotopic distribution for lipid A.

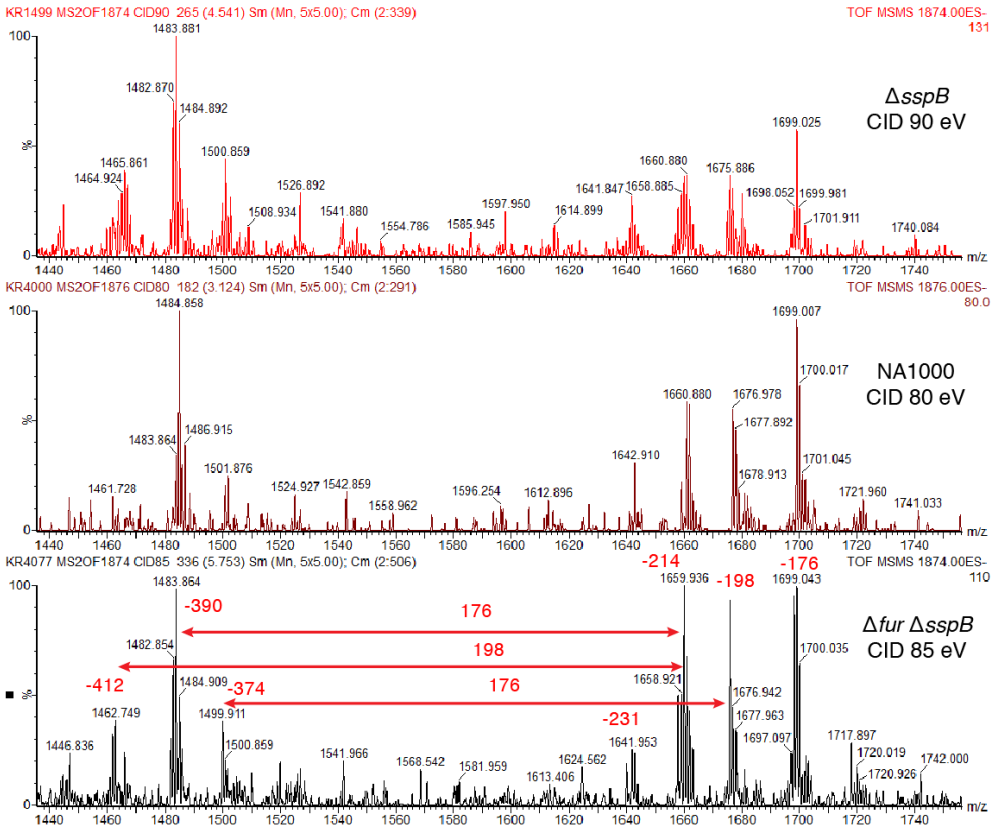

Appendix Fig. 6b. Tandem mass spectrometry data for *Caulobacter* strains containing lipid A at *m/z 1874*. Tandem mass spectra for the indicated strains are shown at collision energies of approximately 85 electron volts. Notably, all three produce the same type of fragmentation pattern. Ions at 1858 (data not shown) and *m/z* 1874 were fragmented and compared with the previously reported structure (202). We interpret the fragment ions as follows: -176 is a loss of galactopyranuronic acid; -198 and -214 are related to 2'b (12:1, 3OH) and 3'b (12:1) fatty acid losses; -412, -390, and -374 are combined losses of (-214 and -198), (-214 and -176) and (-198 and -176), respectively; -215 and -231 are from 2 (12:0) and 3 (12:0, 3OH) fatty acid losses, respectively, that are lower than -198 and -214; and -215 is in the ion envelope of -214. It is known that fatty acyls in the O'-branch and O positions are more labile during collision-induced dissociation than those in the N'-branch and N positions (265, 266).

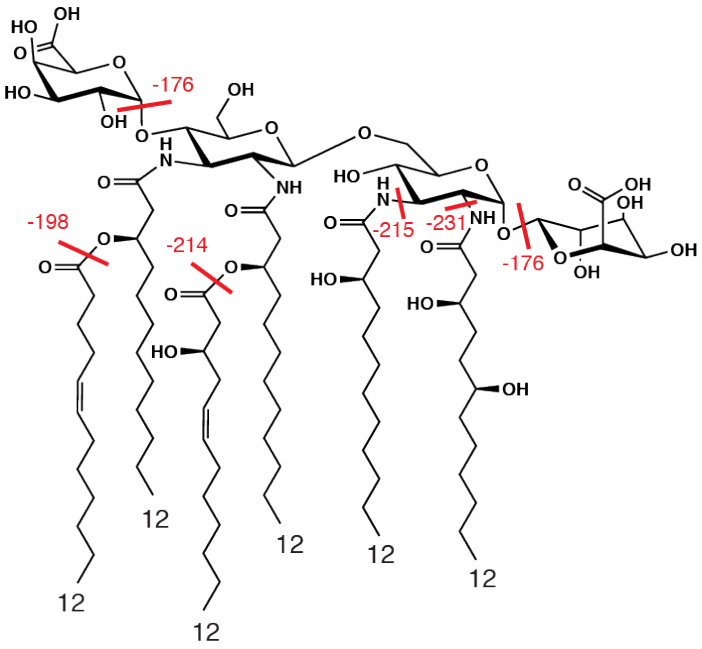

Appendix Figure 6c. Lipid A structure derived from MS and MS/MS analysis. Structure derived by tandem MS and comparison to previously reported structure (202) . Observed fragment ions in Appendix Figure 6b denoted in red.

Appendix Table 2. Single-nucleotide polymorphisms and indels in Δ*ctpA* suppressors

Strain	Position of Sequence	Gene	Annotation	Base Change	Amino Acid Substitution
Δ*ctpA* S3	1668695	CCNA_01553	Undecaprenyl-phosphate beta-N-acetyl-D-fucosaminephosphotransferase	G>T	K54N
	2383967	CCNA_02235	SGNH hydrolase family protein	G>A	G109D
Δ*ctpA* S8	3492550	CCNA_03316	UDP-N-acetylglucosamine 4,6-dehydratase/UDP-D-quinovosamine 4-dehydrogenase	AG>ATG	E487Frameshift
Δ*ctpA* S16	58496	CCNA_00055	Ferric uptake regulation protein	A>T	L38Q
Δ*ctpA* S21	515085	CCNA_00497	Putative rhamnosyl transferase	G>A	G263D
	1378399	CCNA_01250	FecCD-family transporter protein	GCC>GC	A340Frameshift
Δ*ctpA* S32	1157376	CCNA_01056*	Methyltransferase	A>AG	S31Framshift
	2164248	CCNA_02016	nuoMNADH-quinone oxidoreductase chain M	C>T	M7I
	2949436	CCNA_02792	TonB-dependent outer membrane receptor	A>G	S516G
Δ*ctpA* S36	3901011	CCNA_03733	Mannose-1-phosphate guanylyltransferase	C>T	W279Stop
Δ*ctpA* S38	726779	CCNA_00669	Glycosyltransferase family 99 protein WbsX	CTG>CG	Q476Frameshift
Δ*ctpA* S40	378822	CCNA_00362	Zinc uptake regulation protein	A>T	C156S
	2868272	-	-	G>C	-
	3913883	CCNA_03744	dTDP-glucose 4,6-dehydratase	T>A	I269F
Δ*ctpA* S43	1377138	CCNA_01249	ABC-transporter substrate binding protein	C>T	A169V
	1668861	CCNA_01553	Undecaprenyl-phosphate beta-N-acetyl-D-fucosaminephosphotransferase	CC>GA	P110E
	2976030	CCNA_02820	TadG-family protein	C>T	Silent
Δ*ctpA* S44	727833	CCNA_00669	Glycosyltransferase family 99 protein WbsX	A>C	L125R
Δ*ctpA* S47	537654	CCNA_00524	Conserved hypothetical cytosolic protein	A>AG	L369Frameshift
	1173251	CCNA_01068	Glycosyltransferase	GCC>GC	R293Frameshift
Δ*ctpA* S52	514656	CCNA_00497	Putative rhamnosyl transferase	T>G	L120R
	810384	CCNA_00752	3-hydroxybutyryl-CoA dehydrogenase	T>A	Stop>Y
	3797776	-	-	T>C	-
Δ*ctpA* S53	58379	CCNA_00055	Ferric uptake regulation protein	G>T	S77Stop
	1778110	CCNA_01656	Endonuclease/exonuclease/phosphatase family protein	A>C	L4R
	3900664	CCNA_03733	Mannose-1-phosphate guanylyltransferase	G>A	Q395Stop
Δ*ctpA* S54	1377127	CCNA_01249	ABC-transporter substrate binding protein	CGG>CG	G166Frameshift

	3492771	CCNA_03316	UDP-N-acetylglucosamine 4,6-dehydratase/UDP-D-quinovosamine 4-dehydrogenase	G>A	E561K
Δ*ctpA* S57	1492703	CCNA_01378	Protein-L-isoaspartate O-methyltransferase	G>GC	G59Frameshift
	2487074	CCNA_02347	Phosphomannomutase/phosphoglucomutase	G>A	G266D
Δ*ctpA* S111	295119	CCNA_00283	2,3,4,5-tetrahydropyridine-2,6-dicarboxylate N-succinyltransferase	A>T	L284Q
	1173965	CCNA_01068	Glycosyltransferase	TGC>T	R55Frameshift
Δ*ctpA* S112	311705	CCNA_00297	Two-component response regulator	C>T	W64Stop
	315570	CCNA_00301	Phosphotransferase family protein	T>G	I319S
	2487307	CCNA_02347	Phosphomannomutase/phosphoglucomutase	G>A	E344K
	3569520	CCNA_03399	Flavin prenyltransferase UbiX	C>T	A159T

Single-nucleotide polymorphisms and indels in ΔctpA suppressors. In addition to the indicated mutations, each strain is also Δ*ctpA* Δ*sspB*. Sequence positions refer to the genome of Caulobacter crescentus NA1000 (NC_011916.1). The prefix for each gene number is CCNA. Shaded rows represent mutations hypothesized to suppress the lethality of Δ*ctpA*. Asterisk, *CCNA_01056* frameshift most likely suppresses through a polar effect on the downstream gene *CCNA_01055*.

Appendix Table 3. Single-nucleotide polymorphisms and indels identified in Δ*lpxC* suppressors

Strain	Position of Sequence	Gene	Annotation	Base Change	Amino Acid Substitution
Δ*lpxC* S1	58446	CCNA_00055	Ferric uptake regulation protein	A>T	Y55N
	4000704	CCNA_03835	3-oxoacyl-(Acyl-carrier-protein) synthase	C>T	G396S
Δ*lpxC* S5	58436	CCNA_00055	Ferric uptake regulation protein	A>T	V58E

In addition to the indicated mutations, each strain is also Δ*lpxC* Δ*sspB*. Sequence positions refer to the genome of Caulobacter crescentus NA1000 (NC_011916.1). The prefix for each gene number is CCNA. Shaded rows represent mutations hypothesized to suppress the lethality of Δ*lpxC*.

Appendix Table 4. Primers used in Chapter 3

Name	Sequence (5'-3')
pJS14-PxylX	AGAACTAGTGGATCCTCACATGGTCTCGAA
PxylX-lpxC R	ACCCGAAGCCGACACGGCGTCGTCTCCCCA
PxylX-lpxC F	TGGGGAGACGACGCCGTGTCGGCTTCGGGT
lpxC-3xFLAG R	GTAGTCCATGGATCCAACCGCTTCTGCAAG
lpxC-3xFLAG F	CTTGCAGAAGCGGTTGGATCCATGGACTAC
ssrA-pJS14	CTTGATATCGAATTCTCACGCAGCGACGGC
pVCERN-2 00497 F	ACGCATATGAACAGCATTCTCCCG
pVCERN-2 00497 R	CCGGAGCTCCTAGATCGGCCGGCC
pVCERN-2 01553 F	ACGCATATGAAGCGTATGTTTGAT
pVCERN-2 01553 R	CCGGAGCTCCTAACGGGTGACGCC
pVCERN-2 03733 F	ACGCATATGGCTGCGATCTATCCG
pVCERN-2 03733 R	CCGGAGCTCTCAACGCGGCTTCGT
Pvan-fur	GAGGAAACGCATATGGATCGACTCGAAAAG
fur-pVCERN	AATTCTCCGGAGCTCTTACTCCTCCAGCGG
PxylX-uppS R	GGTGGTCGCCGGCATGGCGTCGTCTCCCCA
PxylX-uppS F	TGGGGAGACGACGCCATGCCGGCGACCACC
uppS-pJS14	CTTGATATCGAATTCTTAGCCGGCGACGGC
171 PxylX_fwd	cgctctagaactagtggatcctcaCATGGTCTCGAACAGGGC
171 PxylX_rev	ggcgccatGGCGTCGTCTCCCCAAAAC
171 mla_operon_fwd	acgacgccATGGCGCCTATGAGAAGC
171 mla_operon_rev	cgataagcttgatatcgaattcTCAGTGGGTCTCAGAGATC
PxylX-murA R	GGCGATGCGATCCATGGCGTCGTCTCCCCA
PxylX-murA F	TGGGGAGACGACGCCATGGATCGCATCGCC
murA-pJS14	CTTGATATCGAATTCTTACAGTTCCGCCTC
00497::hyg UpF	CTCACTAGTAGGACGACGCCCATA
00497::hyg UpR	ATCCCCGGGGGCAAGGGTCGAGAC
00497::hyg DownF	ATCCCCGGGCGCCCGCTGCTGTGG
00497::hyg DownR	AGCGAATTCACCGAGGATTTGGTT
01055::hyg UpF	CTCACTAGTGCTGGCGCTGGAAGA
01055::hyg UpR	ACCGGATCCTTGAGCGCCATGGGC
01055::hyg DownF	ACCGGATCCGATGGACGAGCGCAG
01055::hyg DownR	AGCGAATTCTACGATGACGAGTCG
01068::hyg UpF	CTCACTAGTGCGCGAGGACACCGT
01068::hyg UpR	ACCGGATCCGACGCCTGGGTGGCG
01068::hyg DownF	ACCGGATCCCAGGCGGCGCCATAT
01068::hyg DownR	AGCGAATTCTTGACCTGCTTGAGC
01553 UpF	AAAACTAGTATCGAGCAGGGCGTC

01553 UpR	GGCCCCGGGATCAAACATACGCTT
01553 DownF	ATCCCCGGGCCGGTGCTGACCGCA
01553 DownR	AAAGAATTCTATGCCGCCAAGCT
03733::hyg UpF	CTCACTAGTGACGCTGGCCCTTGT
03733::hyg UpR	ACCGGATCCGAAGGCGTGATCGAG
03733::hyg DownF	ACCGGATCCGCCGCCACACAGGAT
03733::hyg DownR	AGCGAATTCATGCTCAAGGACCTC
fur UpF	CTCACTAGTAAGAGGGTGACCTCG
fur UpR	ACCGGATCCGAGCTCTACGGGATG
fur DownF	ACCGGATCCTTCGATACAGGCCTT
fur DownR	AGCGAATTCTATATGCAGGCCTTC
lpxC UpF	CTCACTAGTTCAGATAGGCTTCGA
lpxC UpR	CATGAATTCCTCAATAACGCCGTG
lpxC DownF	CTTGAATTCCGTGTGCTGAAAATA
lpxC DownR	GACGCATGCTGGCCGCAAGCCGCG
mla KO UpF	CTCACTAGTGGGCGGTCTTCAGGT
mla KO UpR	CGGGAATTCGCGGATGCTCCTGCT
mla KO DownF	CGGGAATTCCCCTATGTGCGCCAG
mla KO DownR	GAGACGCGTGGCGCGCCGGTCGTT
aacC1 EcoRI F	CGCGAATTCgaattgacataagcc
aacC1 EcoRI R	GGGGAATTCgaattggccgcggcg
ctpA KO F	GAAGAAGCGCGGGATCAAGA
ctpA KO R	GTTGCCATGCTTGATGTGCA